UNIVERSITAT POLITÈCNICA DE VALÈNCIA

# UNIVERSITAT POLITÈCNICA DE VALÈNCIA

## School of Industrial Engineering

## Architecture optimization of fuel cell light commercial vehicles in terms of performance and environmental impact

End of Degree Project

Bachelor's Degree in Industrial Engineering

AUTHOR: Sáez Mallea, Ismael

Tutor: Novella Rosa, Ricardo

Cotutor: López Juárez, Marcos

ACADEMIC YEAR: 2022/2023

# ARCHITECTURE OPTIMIZATION OF FUEL CELL LIGHT COMMERCIAL VEHICLES IN TERMS OF PERFORMANCE AND ENVIRONMENTAL IMPACT

Ismael Sáez Mallea

# ACKNOWLEDGMENTS

*To my family, for their unconditional love.*

*To my friends, for their companionship and support.*

*To Marcos and Ricardo, for their guidance and mentorship.*

# ABSTRACT

In today's world, where decarbonizing transportation is key to achieve environmental sustainability, fuel cell vehicles have gained interest due their potential to reduce carbon emissions. This Bachelor's Thesis targets the optimization of the components of fuel cell light commercial vehicles with the objective of maximizing performance and minimizing environmental impact. To achieve this, a series of simulations are launched in GT-Suite and MATLAB, varying the vehicle fuel cell stack maximum power, battery energy content and hydrogen tank capacity. Energy management strategies are adjusted in order to achieve maximum range for each studied architecture, comparing the typical charge-sustaining-charge-depleting modes with blended control. Finally, a life cycle assessment (LCA) methodology is performed to evaluate the environmental footprint of the considered architectures and to understand their potential to reduce emissions against equivalent battery or internal combustion engine vehicles. After analyzing the results, it is concluded that performance is optimized when the vehicle counts with a large hydrogen tank, a large battery, and a medium-to-large fuel cell stack, while also including a blended energy management strategy. As for its environmental impact, the ideal size of the components is of a small battery and a medium-to-large fuel cell stack, showing potential of producing fewer emissions than battery or diesel-engine light commercial vehicles.

**Keywords:** hydrogen, light commercial vehicle, fuel cell vehicle, life cycle assessment, sizing, driving cycle.

# RESUMEN

En el mundo actual, donde la descarbonización del transporte es clave para alcanzar la sostenibilidad ambiental, los vehículos de pila de combustible han ganado interés debido a su potencial para reducir las emisiones de carbono. Este Trabajo Fin de Grado busca optimizar los componentes de un vehículo comercial ligero de pila de combustible con el objetivo de maximizar sus prestaciones y minimizar el impacto ambiental. Para ello, una serie de simulaciones son lanzadas en GT-Suite y MATLAB, variando la potencia máxima de la pila de combustible del vehículo, el contenido energético de su batería y la capacidad de su tanque de hidrógeno. Estrategias de gestión energética son variadas para alcanzar la máxima autonomía posible para cada una de las arquitecturas estudiadas, comparando los modos típicos de mantenimiento y consumo de carga con modos de control combinado. Finalmente, se realiza una metodología de análisis del ciclo de vida (LCA) para evaluar la huella ambiental de las arquitecturas consideradas y para comprender el potencial de reducción de emisiones comparado con vehículos equivalentes de batería o de motor de combustión interna. Tras analizar los resultados, se concluye que las prestaciones se optimizan cuando el vehículo cuenta con un tanque de hidrógeno grande, una batería grande, y una pila de combustible de tamaño medio-grande, además de una estrategia de control energético combinado. En lo que corresponde a su impacto ambiental, el tamaño ideal de los componentes es de una batería pequeña y de una pila de combustible de tamaño medio-grande, mostrando potencial de producir menos emisiones que vehículos comerciales ligeros de batería o motor diésel.

**Palabras clave:** hidrógeno, vehículo comercial ligero, vehículo de pila de combustible, análisis de ciclo de vida, dimensionado, ciclo de conducción.

# RESUM

En el món de hui, on la descarbonització del transport és clau per a aconseguir la sostenibilitat ambiental, els vehicles de pila de combustible han guanyat interès degut al seu potencial per a reduir les emissions de carboni. Aquest Treball Fi de Grau busca optimitzar els components d'un vehicle comercial lleuger de pila de combustible amb l'objectiu de maximitzar les seues prestacions i minimitzar l'impacte ambiental. Per a això, una sèrie de simulacions són llançades en GT-Suite i MATLAB, variant la potència màxima de la pila de combustible del vehicle, el contingut energètic de la seua bateria i la capacitat del seu tanc d'hidrogen. Estratègies de gestió energètica són variades per a aconseguir la màxima autonomia possible per a cadascuna de les arquitectures estudiades, comparant les estratègies típiques de manteniment i consum de càrrega amb estratègies de control combinat. Finalment, es realitza una metodologia d'anàlisi del cicle de vida (LCA) per a avaluar la petjada ambiental de les arquitectures considerades i per a comprendre el potencial de reducció d'emissions comparat amb vehicles equivalents de bateria o de motor de combustió interna. Després d'analitzar els resultats, es conclou que les prestacions s'optimitzen quan el vehicle compta amb un tanc d'hidrogen gran, una bateria gran, i una pila de combustible de grandària mitjana-gran, a més d'una estratègia de control energètic combinat. En el que correspon al seu impacte ambiental, la grandària ideal dels components és d'una bateria petita i d'una pila de combustible de grandària mitjana-gran, mostrant potencial de produir menys emissions que vehicles comercials lleugers de bateria o motor dièsel.

**Paraules clau:** hidrogen, vehicle comercial lleuger, vehicle de pila de combustible, anàlisi de cicle de vida, dimensionament, cicle de conducció**.**

# INDEX

**DOCUMENTS INDEX**


Document I: Memory ..... 1

Document II: Budget ..... 76

Document III: Annex ..... 81


**MEMORY INDEX**


1. Introduction ..... 3
    1.1. Context ..... 3
    1.2. Literature review ..... 3
        1.2.1. Hydrogen ..... 3
        1.2.2. Fuel cell vehicles ..... 4
        1.2.3. Life cycle assessment ..... 8
2. Objectives ..... 10
3. Methodology ..... 11
    3.1. Fuel cell vehicle model ..... 12
        3.1.1. Vehicle model description ..... 12
        3.1.2. Energy management strategy ..... 13
        3.1.3. Sizing ..... 14
    3.2. Optimization process ..... 15
        3.2.1. Driving cycle ..... 15
        3.2.2. Charge Depleting and charge sustaining simulations ..... 16
        3.2.3. Charge Blended mode ..... 17
    3.3. Life cycle assessment parameters ..... 18
        3.3.1. Scope and scenario ..... 18
        3.3.3. System boundaries ..... 19
        3.3.3. Impact categories ..... 19

3.3.4. Life cycle inventory ..... 20
3.3.5. Vehicle market analysis ..... 25
4. Results ..... 28
4.1. Components sizing results for standard CD + CS strategies ..... 28
4.1.1. Vehicle mass and payload ..... 28
4.1.2. Charge Depleting mode ..... 28
4.1.3. Charge Sustaining mode ..... 30
4.1.4. Charge Depleting and Charge Sustaining mode ..... 34
4.2. System optimization results ..... 37
4.3. Life cycle assessment ..... 46
4.3.1. Fuel production cycle ..... 46
4.3.3. Vehicle manufacturing cycle ..... 53
4.3.3. Operation cycle ..... 56
4.3.4. Complete life cycle ..... 57
4.3.5. Vehicles comparison ..... 60
5. Conclusions ..... 68
6. Future work ..... 70
References ..... 72

**BUDGET INDEX**

1. Introduction ..... 77
2. Time distribution ..... 77
3. Labour costs ..... 78
4. Equipment costs ..... 79
5. Total costs ..... 80

# FIGURE AND TABLE INDEX

**CHAPTER 1**


Figure 1.1: Fuel Cell Scheme ..... 5

Figure 1.2: Share of LCVs in Europe in 2021 ..... 8


**CHAPTER 3**


Figure 3.1: Methodology Flow Diagram ..... 11

Figure 3.2: Fuel Cell System Outline ..... 12

Figure 3.3: WLTC 3b Driving Cycle ..... 15

Figure 3.4: Electricity Production Emissions for every Estimated Scenario..... 18

Figure 3.5: LCA Boundaries ..... 19

Figures 3.6: Natural Gas Consumption in Europe..... 21

Figure 3.7: STEPS Gas Demand in Europe..... 21

Figure 3.8: SDS Gas Demand in Europe ..... 21

Figure 3.9: $H_2$ Demand in Europe..... 23

Figure 3.10: Water Electrolysis Dominant $H_2$ Production Scenario ..... 23

Figure 3.11: SMR Dominant for Ambitious $H_2$ Production Scenario..... 24

Figure 3.12: SMR Dominant for Business-as-Usual $H_2$ Production Scenario ..... 24


**CHAPTER 4**


Figure 4.1: Evolution of Battery SoC during CD Mode..... 29

Figure 4.2: Variation of CD Range when changing the Battery Capacity..... 29

Figure 4.3: CD Battery Consumption for each Architecture ..... 30

Figure 4.4: Evolution of the Battery SoC throughout a WLTC 3b Cycle..... 31

Figure 4.5: $H_2$ Consumption throughout a WLTC 3b Cycle ..... 31

Figure 4.6: CS Range for each Architecture ..... 32

Figure 4.7: Comparison of Current Density for Vehicles with different FC Stack Power. 33

Figure 4.8: $H_2$ Consumption in CS Mode for each Architecture..... 33

Figure 4.9: Evolution of Overall Range for every Architecture ..... 34

Figure 4.10: Total Energy Consumption for each Architecture, including Electricity and $H_2$ ..... 35

Figure 4.11: Percentage of Distance covered in CS Mode for all the Architectures..... 35

Figure 4.12: Range and Payload Comparison for all Architectures ..... 37

Figure 4.13: Evolution of the Battery SoC throughout a WLTC 3b Cycle in CB Mode ..... 37

Figure 4.14: Evolution of $H_2$ Consumption throughout a WLTC 3b Cycle in CB Mode..... 38

Figure 4.15: $H_2$ Consumption Comparison of different Energy Management Strategies for a Vehicle with 60 kW FC Stack Power, 40 kWh Battery Capacity and 5 kg of $H_2$ in its tank ..... 39

Figures 4.16: SoC Discharge and Range Comparison for all studied Architectures..... 40

Figure 4.17: Range Distribution for all Energy Management Strategies ..... 41

Figure 4.18: Battery Discharge and Consumption Comparison for all Architectures in CB mode ..... 42

Figure 4.19: Variation in $H_2$ Consumption when changing Battery Capacity..... 42

Figure 4.20: Range for all Architectures ..... 44

Figure 4.21: Consumption for all Architectures..... 44

Figures 4.22: Range for different Energy Management Strategies ..... 45

Figures 4.23: Consumption for different Energy Management Strategies..... 45

Figure 4.24: Electricity Production Well-to-Tank Emissions for all Scenarios ..... 47

Figure 4.25: Electricity Production Emissions per Lifetime for all the Scenarios..... 48

Figure 4.26: $H_2$ Well-to-Tank Emissions Comparison for different $H_2$ Production Trends ..... 49

Figure 4.27: $H_2$ Well-to-Tank Emissions Comparison for different NG Trends..... 50

Figure 4.28: $H_2$ Well-to-Tank Emissions Comparison for different $H_2$ Compression Strategies ..... 50

Figure 4.29: $H_2$ Well-to-Tank Emissions per Life..... 51

Figure 4.30: Energy Well-to-Tank Emissions per Life..... 52

Figure 4.31: Energy Well-to-Tank Emissions per Life in EU-2020 Scenario ..... 52

Figure 4.32: Energy Well-to-Tank Emissions per Life in EU-2050 Scenario ..... 53

Figure 4.33: Vehicle Manufacturing Emissions for all Architectures ..... 54

Figure 4.34: Segmented Vehicle Components Manufacturing Emissions in EU-2020 Scenario..... 55

Figure 4.35: Segmented Vehicle Components Manufacturing Emissions in EU-2050 Scenario..... 55

Figure 4.36: Tank-to-Wheel Emissions for all Architectures ..... 56
Figure 4.37: Life Cycle Emissions for all Architectures ..... 57
Figure 4.38: Life Cycle Emissions Segmentation in EU-2020 Scenario ..... 58
Figure 4.39: Life Cycle Emissions Segmentation in EU-2050 Scenario ..... 59
Figure 4.40: WLTC class 2 Driving Cycle ..... 60
Figure 4.41: Battery SoC Evolution in the BEV for both WLTC Cycles ..... 61
Figure 4.42: Payload and Range Comparison for all Vehicles ..... 62
Figure 4.43: Well-to-Tank Emissions for all Vehicles ..... 63
Figure 4.44: Vehicle Manufacturing Emissions for all Vehicles ..... 63
Figure 4.45: Vehicle Operation Emissions for all Vehicles ..... 64
Figure 4.46: Life Cycle Emissions for all Vehicles ..... 65
Figure 4.47: Segmented Life Cycle Emissions for all Vehicles in EU-2020 Scenario ..... 66
Figure 4.48: Segmented Life Cycle Emissions for all Vehicles in EU-2050 Scenario ..... 66
Figure 4.49: Payload and Emissions Comparison for all Vehicles in 2020 and 2050 ..... 67

**TABLES**

Table 1: Data for Vehicle Mass Calculations ..... 15
Table 2: Charge-Blended Simulation Strategies ..... 17
Table 3: $H_2$ and Electricity Production Emissions per Year and Pathway ..... 22
Table 4: Electrical Renault Master Characteristics ..... 26
Table 5: Diesel Renault Master Characteristics ..... 26
Table 6: Diesel Production Emissions ..... 27
Table 7: Range Evolution in CB Mode for all studied Architectures ..... 41
Table 8: Consumption Evolution in CB Mode for all Architectures ..... 43
Table 9: Electricity consumed to power different FCV Architectures ..... 47
Table 10: Vehicle Components Emissions Share in each Architecture ..... 56
Table 11: Change in GHG Emissions for all Architectures between 2020 and 2050 ..... 58
Table 12: Emissions Changes from a 80 kW – 60 kWh Architecture ..... 59
Table 13: Characteristics of all Vehicles ..... 61
Table 14: Simulation Time Distribution ..... 77
Table 15: Total Time Distribution ..... 78
Table 16: Labour Costs Distribution ..... 78
Table 17: Licences and Equipment Costs ..... 79

Table 18: Summary of the total Cost of the Project ..... 80

Table 19: European Union Sustainable Development Goals ..... 82

# SYMBOLS AND NOMENCLATURE

| | |
|---|---|
| ADR | Assembly, Disposal and Recycling |
| BoP | Body of Plant |
| BEV | Battery Electric Vehicle |
| CCS | Carbon Capture and Storage |
| $CH_4$ | Methane |
| CO | Carbon Monoxide |
| $CO_2$ | Carbon Dioxide |
| DoE | Department of Energy |
| $e^-$ | Electron |
| EMS | Energy Management Strategy |
| ETS | Energy Trends Reports |
| EV | Electriv Vehicle |
| FC | Fuel Cell |
| FCREx | Fuel Cell Range Extender |
| FCS | Fuel Cell System |
| FCV | Fuel Cell Vehicle |
| GHG | Greenhouse Gas |
| GWP | Global Warming Potential |
| HDV | Heavy Duty Vehicle |
| $H^+$ | Proton |
| $H_2$ | Hydrogen |

| | |
|---|---|
| $H_2O$ | Water |
| IEA | International Energy Agency |
| ICE | Internal Combustion Engine |
| ICEV | Internal Combustion Engine Vehicle |
| LCA | Life Cycle Assessment |
| LCI | Life Cycle Inventory |
| LCIA | Life Cycle Impact Assessment |
| LCV | Light Commercial Vehicle |
| LDV | Light Duty Vehicle |
| NI | Normal Improvement |
| OC | Optimal Control |
| $O_2$ | Oxygen |
| PEM | Proton Exchange Membrane |
| PMP | Pontryagin's Minimum Principle |
| Pt | Platinum |
| SDS | Sustainable Development Scenario |
| SI | Significant Improvement |
| SMR | Steam Methane Reforming |
| SoC | State of Charge |
| STEPS | Stated Policies Scenario |
| WLTP | Worldwide Harmonized Light Vehicles Test Procedure |

# DOCUMENT I:

# MEMORY

# MEMORY INDEX

1. Introduction ..... 3
1.1. Context ..... 3
1.2. Literature review ..... 3
1.2.1. Hydrogen ..... 3
1.2.2. Fuel cell vehicles ..... 4
1.2.3. Life cycle assessment ..... 8
2. Objectives ..... 10
3. Methodology ..... 11
3.1. Fuel cell vehicle model ..... 12
3.1.1. Vehicle model description ..... 12
3.1.2. Energy management strategy ..... 13
3.1.3. Sizing ..... 14
3.2. Optimization process ..... 15
3.2.1. Driving cycle ..... 15
3.2.2. Charge Depleting and charge sustaining simulations ..... 16
3.2.3. Charge Blended mode ..... 17
3.3. Life cycle assessment parameters ..... 18
3.3.1. Scope and scenario ..... 18
3.3.3. System boundaries ..... 19
3.3.3. Impact categories ..... 19
3.3.4. Life cycle inventory ..... 20
3.3.5. Vehicle market analysis ..... 25
4. Results ..... 28
4.1. Components sizing results for standard CD + CS strategies ..... 28
4.1.1. Vehicle mass and payload ..... 28
4.1.2. Charge Depleting mode ..... 28
4.1.3. Charge Sustaining mode ..... 30

4.1.4. Charge Depleting and Charge Sustaining mode ..... 34
4.2. System optimization results ..... 37
4.3. Life cycle assessment ..... 46
4.3.1. Fuel production cycle ..... 46
4.3.3. Vehicle manufacturing cycle ..... 53
4.3.3. Operation cycle ..... 56
4.3.4. Complete life cycle ..... 57
4.3.5. Vehicles comparison ..... 60
5. Conclusions ..... 68
6. Future work ..... 70
References ..... 72

# CHAPTER 1: INTRODUCTION

## 1.1. CONTEXT

Pollution and global warming are currently two of the main concerns of our society. Last year, 36.8 Gt of carbon dioxide equivalent ($CO_2$ eq.) were emitted worldwide, the most in history [1]. This value, alongside the expected rise in population, is expected to keep incrementing in the near future. From the total greenhouse gas (GHG) emissions in 2022, it is estimated that 7.98 Gt (21.7%) were associated with transport, which relies mainly on carbon-based fuels such as diesel and gasoline. Today, there are more than 285 million vehicles in the European Union (EU), a number that also grows every year. If the EU net-zero objective is to be accomplished by 2050, a drastic change must be made in the transportation sector by finding new ways of powering vehicles without relying on con GHG emitting fuels [2].

Because of this, hydrogen ($H_2$) has emerged as one of the possible solutions to the environmental problem. This fuel, which does not produce GHGs during its operation, promises to cover a large part of the energy demand in Europe and help achieve the net-zero objective. For transportation specifically, it also shows impressive versatility due to the possibility of using it in internal combustion engines (ICEs) or in fuel cells (FCs). Today, however, its production is costly due to the lack of infrastructure and the complications for its distribution, and governments and companies will have to invest in its development in order to make $H_2$ accessible and a viable solution for the reduction of GHG emissions.

## 1.2 LITERATURE REVIEW

### *1.2.1 Hydrogen*

Hydrogen is the first element of the periodic table, formed by one proton and one electron. It is colourless, odourless, and has the lowest density of all elements, as well as a high energy content per mass. It is also an extremely flammable substance and reacts with oxygen ($O_2$) with ease producing water ($H_2O$).

$$H_2 + \frac{1}{2}O_2 \rightarrow H_2O \qquad (1.1)$$

As can be seen, the combustion of $H_2$ does not produce any GHG. Because of that, it is viewed as a possible green fuel for the future and a replacement for the more established diesel and gasoline.

Currently, $H_2$ is produced by two main methods: steam methane reforming (SMR) and water electrolysis. SMR relies on the reaction of methane ($CH_4$) and water at high temperatures to produce $H_2$ as well as carbon monoxide (CO).

$$CH_4 + H_2O \rightarrow CO + 3H_2 \quad (1.2)$$

Today, about 70% of all $H_2$ in Europe is produced via this method, using natural gas or biogas as feedstock for the reaction [3]. Currently, it is the most cost-efficient process of $H_2$ production. However, the CO emissions make it the most polluting method, and will require a large amount of carbon capture and storage (CCS) and an increase in the use of biogas as feedstock to become the dominant approach in the future.

The other main production method is water electrolysis, which uses electricity to split $H_2O$ into $H_2$ and $O_2$.

$$H_2O \rightarrow H_2 + \frac{1}{2}O_2 \quad (1.3)$$

As opposed to SMR, this reaction is completely carbon-free. This pathway could establish itself with two different distribution strategies: either centrally or regionally. Central electrolysis consists of the use of electricity from the energy mix to produce $H_2$ at large scales and later transport it, while regional electrolysis has the potential of producing $H_2$ at smaller rates closer to refuelling stations and using 100% renewable energy. Water electrolysis is currently the best strategy for production in terms of emissions, but its high cost and energy requirement makes it difficult to compete with SMR today. Currently, just 10% of all European $H_2$ is produced via electrolysis, meaning that the remaining 20% is obtained as a byproduct of industrial processes [3].

Depending on the production pathway, $H_2$ can be sorted into colours: green, if $H_2$ is produced through electrolysis using renewable energy sources, blue, when using SMR with CCS or electrolysis with nuclear power, grey, when applying SMR but releasing the produced CO to the atmosphere, or black, when producing $H_2$ through electrolysis powered by fossil fuels.

Considering the expected rise in demand of $H_2$ in the next 30 years, the current production scenario will change considerably, depending especially on the European political and economic measures. If objectives are to be accomplished, infrastructure for $H_2$ production must increase massively, costs must dimmish considerably and carbon-neutral production pathways must be heavily encouraged.

### *1.2.1 Fuel cell vehicles*

Fuel cell vehicles (FCVs) are one of the most promising solutions for the decarbonization of transportation, with potential of being viable alternatives for diesel or gasoline vehicles. FCVs combine a fuel cell stack with an electric battery, both of which provide electricity to power an electric motor.

The fuel cell (FC) is an electrochemical cell that uses $H_2$ to produce electricity through reduction-oxidation chemical reactions, typically using a proton exchange membrane (PEM) to separate

the anode and the cathode and platinum (Pt) as a catalyser for the reaction, which takes place at temperatures between 60°C and 80°C.

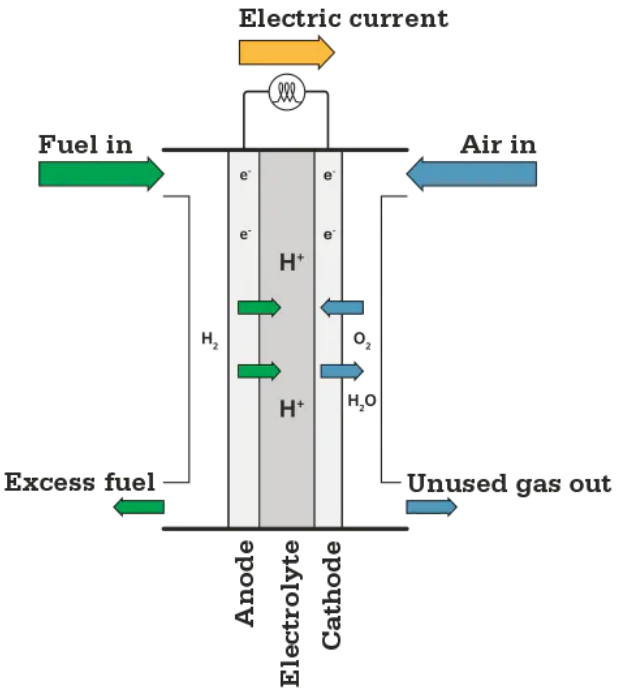


Figure 1.1: Fuel Cell Scheme [4]

As sketched in the previous figure, $H_2$ with a purity of 99.999% is introduced in the anode, where its proton ($H^+$) and electron ($e^-$) are separated. The $H^+$ is able to travel through the PEM into the cathode, allowing the $e^-$ to be used as electric continuous current to power the vehicle.

$$H_2 \rightarrow 2H^+ + 2e^- \quad (1.4)$$

Then, this current is redirected to the cathode, where it reacts with the protons that come from the PEM and the $O_2$ in the air to produce $H_2O$.

$$\frac{1}{2}O_2 + 2H^+ + 2e^- \rightarrow H_2O \quad (1.5)$$

Globally, the reaction results as follows:

$$H_2 + \frac{1}{2}O_2 \rightarrow H_2O \quad (1.6)$$

This technology, due to its high efficiency, simplicity, and non-carbon emissions, shows a large potential to compete with conventional vehicles powered by diesel or gasoline, while the large energy content per mass of $H_2$ makes this type of vehicle better than battery electric vehicles (BEVs) in terms of range and component manufacturing emissions due to a smaller dependency

of batteries. However, the use of FCs is not exclusively meant for transportation purposes, as the generation of power and heat are also possible applications.

It is important to point out that FCs are not the only way of using $H_2$ to power a vehicle, as this is also possible by a combustion reaction in an ICE. This is an attractive approach too, due to its simplicity and the possibility of mixing $H_2$ with diesel or natural gas in dual fuel engines. However, the high detonation power of $H_2$ and the formation of nitrogen oxides ($NO_x$) due to the high reaction temperatures are a series of inconveniencies that FCs do not have.

Although they present a large number of advantages, FCs are not perfect for a number of reasons. First, their use is considerably more expensive than conventional diesel or gasoline systems to power vehicles. The high cost of $H_2$, especially at a purity of 99.999%, the expensive components of the FC system, like the Pt needed to catalyse the electrochemical reaction, alongside the limited number of refuelling stations available pose a series of economic and logistical problems for the general public. Second, the use of $H_2$ as an energy vector, although similar to carbon-based fuels in terms of efficiency, is significantly worse electricity for BEVs in this area. For electric vehicles, the produced electricity is stored directly in the batteries and then used to power an electric motor at efficiencies of over 90%. However, $H_2$ needs to be produced through electrolysis or SMR using a considerable amount of energy, and then reacted in an FC system with efficiencies of around 60%, making it less competitive than BEVs in this area and similar to conventional ICEs, which usually have efficiencies of around 35%. Finally, the low durability of FC systems is another obstacle. For instance, the Department of Energy (DoE) estimates that, for realistic driving conditions, FC systems are expected to run for around 5000 hours [5]. Even though these issues pose problems as of today, it is expected that some of these trends will change in the near future, especially with the strict $CO_2$ emission limitations on the horizon and the focus of the scientific community on efficient $H_2$ production and use as well as improvement in FC degradation.

In order to reduce fuel costs and make the operation more flexible and affordable, FCVs in range-extender configuration (FCREx) have been studied. As opposed to traditional FCV configurations, which feature a small battery and a high-power FC stack with large $H_2$ tanks, FCREx vehicles propose architectures with larger batteries and smaller FC stacks and storage units. By doing so, the battery is able to provide a larger amount of energy, decreasing the dependence on $H_2$, increasing the operation flexibility, and an overall improvement of performance, as concluded by Desantes et al. (2022) [6]. For instance, if the FCREx vehicle is used in an urban context, its circulation can be mainly powered by electricity, which is efficient and cheap, with $H_2$ used for longer trips that require a larger energy demand. However, increasing the energy content of the battery is not an ideal solution, due to the limited space available in vehicles, the increase in weight and the larger amount of emissions caused to manufacture them.

Currently, the private sector is more focused on FCV applications of light duty vehicles (LDVs). As of today, there are three of these vehicles in the market: Honda Clarity, Hyundai Nexo, and Toyota Mirai. These LDVs have adopted a traditional FCV architecture: they count with powerful FC systems, in the range of 100 kW, alongside large $H_2$ tanks with masses in the neighbourhood of 6 kg. Their catalogues assure solid characteristics in terms of performance, highlighted by ranges of around 700 km, as well as zero carbon emissions. However, the prices are considerable, as most of them are worth around 70 000 €. This, along with the formerly

mentioned lack of refuelling stations and the high cost of $H_2$, make these vehicles very difficult to access for the general public today. Probably, if an FCREx structure is adopted, the operation could become more flexible and less dependent on $H_2$, which could help decrease the price of the energy needed to power the vehicle.

Although vehicle companies are yet to develop large FCV fleets, there have been numerous studies and publications that have investigated this subject with the objective of sizing the components of the vehicles. Mainly, these investigations have focused on heavy vehicles, such as buses or urban logistic vehicles, due to the rising interest in decarbonizing cities. One of the earlier studies conducted on this topic was published by Xu et al. (2013), focusing on a typical FCV design with a small lithium-ion battery [7]. This article, centred on the decrease of $H_2$ consumption, concludes that increasing the efficiency of the PEM system, decreasing the resistance of the battery, increasing braking energy ratio, and decreasing auxiliary power demands all result in considerable reductions in $H_2$ consumption.

Now, more recently published articles are focusing more on FCREx configurations. For instance, Hu et al. (2016) published a paper with the objective of targeting component sizing for urban buses [8]. On this occasion, a larger battery is considered, reaching the conclusion that using a 150 Ah battery alongside a 40 kW FC would be optimal in terms of cost and system durability. Other investigators, like Wu et al. (2019), have targeted the optimization of a plug-in FC urban logistics vehicle, again including a large battery to diminish the dependence on $H_2$. As a result, it was concluded that an optimal architecture consisted of a 54 kW FC and a 29 kWh battery, which is able to run the vehicle between 40 km and 60 km using the battery exclusively [9]. Furthermore, other researchers have focused on the effect of the use of the battery on the performance of the vehicle. Shojaeefard et al. (2023), when investigating the optimization of the battery sizing in FCREx vehicles to reduce consumption, considered that battery capacity must be maximized to minimize the number of charges and discharges of the battery, reducing degradation and improving performance [10].

Currently, a large number of investigators have targeted the optimization of lighter cars that are used commonly by the general public. Molina et al. (2021), researchers at Instituto CMT – Motores Térmicos, optimized the components of an FCREx vehicle applied for a passenger car [11]. This article, by varying the power of the FC, the energy content in the battery and the mass of $H_2$ in the tank, states that increases in battery capacity and FC power decreased $H_2$ consumption and reached ranges of around 700 km with 5 kg of $H_2$ in the tank. The optimal architecture in terms of cost and targeting maximum efficiency was set at 80 kW of FC stack power and a 30 kWh battery. Some of these researchers also collaborated with J.M. Desantes et al. (2022), performing a similar study but adapting the components to a C-class SUV. Here, evaluating FC powers between 40 kW and 100 kW, it is observed how large FC stack powers decreased $H_2$ consumption and increased FC durability [6]. Other studies from different research facilities have also produced articles related to this topic. Feroldi et at. (2016), for example, performed a sizing study on FC / supercapacitor hybrid vehicles, reaching the conclusion that supercapacitors with high energy content decreased overall $H_2$ consumption, while increases in FC size could result in increases in consumption due to increases in the weight of the vehicle [12].

As can be seen, the scientific community is interested in FCVs and their potential of decarbonizing the environment. However, the number of studies on light commercial vehicles (LCVs) is still limited. These, mainly vans and pick-up trucks, are used primarily for urban deliveries due to their small size and easier mobility in comparison to that of large trucks. Therefore, due to their current applications, the use of FC technology for this type of vehicle is ideal and will help reduce urban carbon emissions. Today, there are almost 30 million LCVs in Europe, 91% of which are powered by diesel and 6% by petrol, meaning that only about 3% of all the European LCV fleet is powered by alternative and more sustainable energy sources [13]. In order to reduce GHG emissions, radical changes must happen in this industry in the near future. The adoption of FCs as one of the new, green technologies could be part of the solution, which demonstrates the interest in the research made in this BSc thesis.

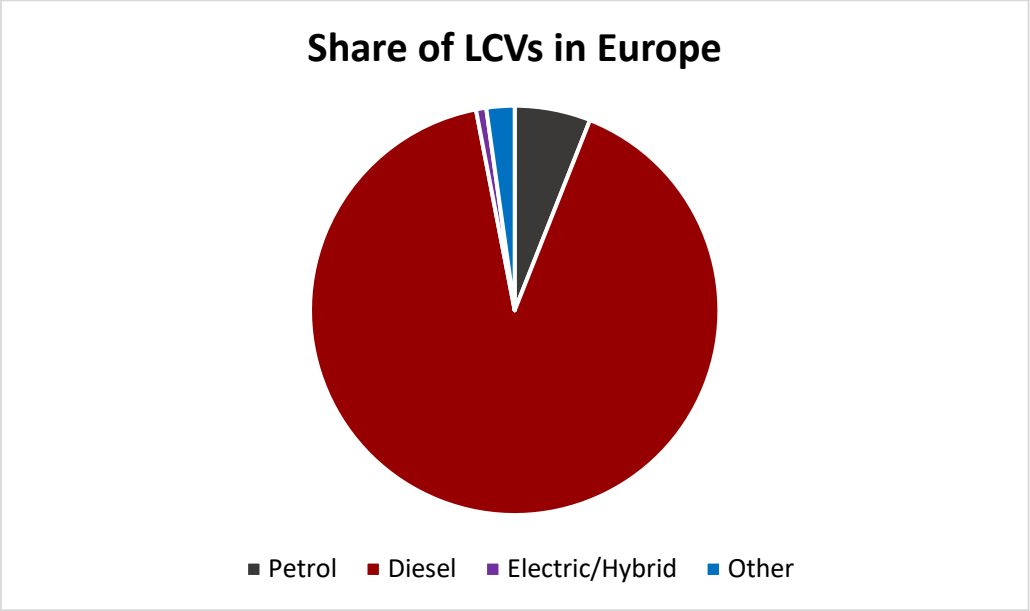


Figure 1.2: Share of LCVs in Europe in 2021 [13]

### *1.2.3 Life cycle assessment*

In order to determine if FCVs and $H_2$ are part of the climate change solution, their environmental impact must be analyzed. To do so, a life cycle assessment (LCA) can be made performed. This methodology is used worldwide to evaluate the impact of any product or process throughout the stages of its life. There are many different types of possible LCAs, such as well-to-tank, which evaluates the impact of the production of a certain source before its use, tank-to-wheel, which measures the consequences of the use of the source, or cradle-to-grave, which considers a complete life cycle from the creation to the end-of-life treatment of the studied product, among others.

Any LCA methodology is based on four main phases [14]. First, a goal and scope are determined, where the study, scenario, or functional unit around which the study centres are defined.

Second, a life cycle inventory (LCI) is produced. This process consists of the extraction and calculation of the necessary data regarding the inputs and outputs of the system, which includes energy, materials or emissions, that are present in the life cycle studied. Next, the life cycle impact assessment (LCIA) is produced using the data from the LCI section. At this stage, the emissions calculated are evaluated and attributed to a series of environmental occurrences such as global warming, eutrophication, ozone depletion or land use. Finally, the results are interpreted in the final phase of the assessment, and the environmental footprint of the life cycle is evaluated.

An LCA methodology is crucial to evaluate FCVs, as the primary objective of this vehicle is to reduce the environmental impact of conventional vehicles. Therefore, the production of the fuel, the manufacturing of the vehicle and its operation must be studied with the use of an LCA methodology to determine if FCVs can help Europe to accomplish its net-zero goal by 2050.

# CHAPTER 2: OBJECTIVES

The main goal of this study is to find the ideal architecture of a fuel cell light commercial vehicle, not only in terms of performance, but also focusing on its environmental impact. The study, by using a simulation model, will evaluate the behavior of each of the considered architectures, which will determine which of them is best for the operation of an LCV.

In order to accomplish this, it is necessary to achieve a number of secondary objectives. First, with the data obtained from the simulations, the effects of varying each of the components of the LCV must be identified. When understanding this information, it can be determined how factors like range and consumption are affected by changing the FC, battery or $H_2$ tank of the vehicle, which is crucial to analyze each architecture from both operational and environmental points of view. Second, an ideal energy management strategy must be identified. By varying how the FC and the battery provide energy to the vehicle, its performance can be optimized without changing any of the components of the vehicle. Furthermore, to evaluate its life cycle emissions, the impact of producing fuel, manufacturing the vehicle and its operation are evaluated considering present and future scenarios. By doing this with the studied LCV and with similar vehicles powered by diesel or exclusively by electric batteries, the current and future footprint of FCVs can be determined and compared with that of other LCVs. If H2 and FCVs prove to reduce the environmental impact of the transportation sector, the results of this study could help in reaching a number of the European Union Sustainable Development Goals, such as climate action, responsible consumption and production, or affordable and clean energy, among others.

Finally, from the perspective of a student, this project has the target of expanding knowledge on hydrogen and fuel cells. This fuel, alongside this technology, are promising solutions for some of the most critical problems in our current society. With this BSc thesis, the feasibility of the production of $H_2$ and the use of FCs for transportation applications are evaluated and could serve as the base for future academic research.

# CHAPTER 3: METHODOLOGY

In order to understand the operation of the LCV, determine the size of its components, and analyze its performance from an environmental point of view, this BSc thesis is divided into two main branches: a simulation line with a validated FC system developed with the GT-Suite v2020 and MATLAB R2020a software [17], and an LCA, using mainly GREET 2022 and complementary information from other databases.

First, the GT-Suite model for FCVs is adapted to replicate an LCV, changing the different variables that are being studied alongside other characteristics of the vehicle. Then, a series of simulations are launched following a charge-depleting and charge-sustaining strategy in order to understand the behavior of the LCV and to obtain data that will help compare the different architectures. Next, once the data is studied, a new set of simulations with combined energy management strategies (charge-blended) are tested with the goal of maximizing the range of the vehicle. Finally, a cradle-to-grave LCA is performed on target vehicle architectures in order to evaluate their environmental impact and determine whether or not the FCV is a promising alternative to those powered by conventional powertrains.

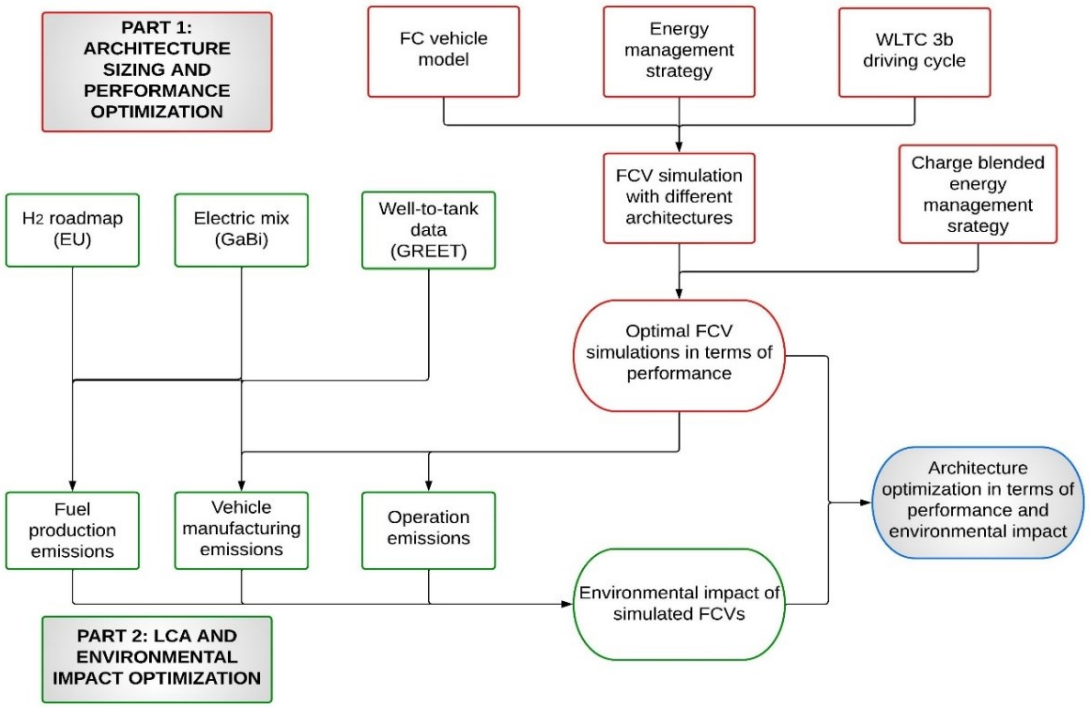


Figure 3.1: Methodology Flow Diagram

## 3.1 FUEL CELL VEHICLE MODEL

### *3.1.1 Vehicle model description*

In order to perform the simulations, GT-Suite v2020 is used. This software, developed by Gamma Technologies, is a 0D-1D modeling application used for engine performance simulations that provides accurate thermodynamic and energetic results and is widely used in the automotive industry. For this specific case, a validated fuel cell vehicle (FCV) model developed at CMT – Motores Térmicos is studied.

This model mainly features a FC, calibrated with experimental results extracted from [15], [16], which consisted of a series of experiments featuring a 20 kW FC stack with variations in the stack temperature and the cathode pressure and stoichiometry. Once the model was validated, it was integrated into a balance of plant (BoP) to form the following FC system.

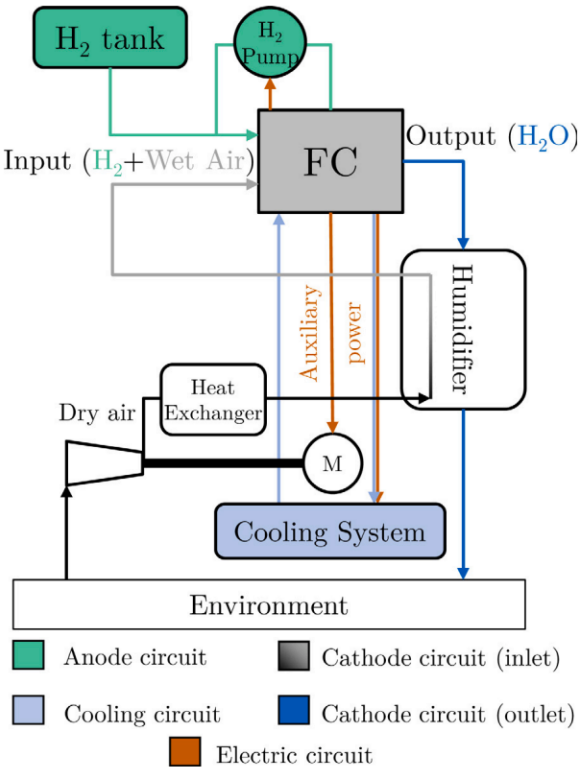


Figure 3.2: Fuel Cell System Outline [17]

The inputs of the FC are $H_2$ and $O_2$, as explained in the introduction section. $H_2$ is stored in a tank at a pressure of 700 bar to ensure an efficient and compact storage. An $H_2$ recirculating pump is also added to allow part of the unused $H_2$ back into the FC. As for $O_2$, it is obtained directly from the air of the environment, supplied into the system and compressed with an electric compressor. This component is followed by a heat exchanger that regulates the temperature of the incoming air. The output of the FC is the $H_2O$, produced from the reaction of $H_2$ and $O_2$, which is directed to a humidifier and, then, released to the environment. The purpose of this humidifier is to add moisture to the inlet air, which helps increase the efficiency of the FC by decreasing the ohmic losses. The model also includes a cooling system, used to keep the FC stack at

adequate temperatures by dissipating excess heat. Finally, the FC powers the electric motor (with a maximum power of 120 kW), which is responsible for the operation of the vehicle. The combination of all the components of the system creates an FC system with efficiencies of about 55-60%, including the power consumption of the balance of plant and the losses in electric current converters.

The vehicle to which this system is applied is an LCV, with its main characteristics based on a Renault Master van.

### *3.1.2 Energy management strategy*

The energy management strategy (EMS) is one of the main aspects of fuel cell vehicles (FCVs), as energy is provided from two different sources: the FCS and the battery. Imposing an EMS is crucial, as it allows the different vehicles to offer the optimal operation given a driving cycle and an architecture, and will therefore provide comparable information to perform a fair evaluation of their operation. To ensure this, optimal control (OC), a tool that provides the optimal power split for all the considered designs, is used [18].

For this BSc thesis, the objective is to minimize $H_2$ consumption, with the requirement of sustaining the battery state-of-charge (SoC) at the end of every driving cycle. Because of this, the objective of the simulations is to find an ideal control strategy *u(t)* that sustains the SoC of the battery after each cycle. The equations that describe the strategy are the following:

$$J = \int_{t_o}^{t_f} P_f\ (u(t), t)\ dt \qquad (3.2)$$

$$\int_{t_o}^{t_f} P_b\ (u(t), E_b(t), t)\ dt = 0 \qquad (3.2)$$

where *J* is the total $H_2$ consumption between the beginning ($t_o$) and the end ($t_f$) of the driving cycle and $P_f$ is the $H_2$ power consumed as a function of current density, which is the control variable *u(t)*. $P_b$ represents the power consumption of the battery, which also depends on the energy stored in the battery $E_b$.

In order to solve the OC problem, Pontryagin's Minimum Principle (PMP) is considered. This principle allows to solve an integral optimization problem by solving a set of differential optimization problems. The PMP implies that, if $u^*$ and $E_b^*$ are optimal trajectories of the control and battery energy throughout the driving cycle, then:

$$H\ (u^*, E_b^*, \lambda^*, t) \leq H\ (u, E_b^*, \lambda^*, t)\ \forall u\ \in U, t \in [t_o, t_f] \qquad (3.3)$$

where H is the Hamiltonian function, defined as

$$H\ =\ P_f - \lambda \dot{E}_b = P_f\ (u(t), t) + \lambda\ (t) P_b\ (u(t), E_b(t), t) \qquad (3.4)$$

The dimensionless variable $\lambda$ is constant throughout the driving cycle, and therefore, the optimization will consist of iterating the value of $\lambda$ until a result with minimum $H_2$ consumption and a sustained SoC is reached.

This EMS is used for a WLTC 3b cycle, which will be described in detail in section 3.2, and for the modeled FC-powered LCV described in the previous section.

### *3.1.3 Sizing*

This behavior of the vehicle is analyzed by varying the attributes of three of its main components: the $H_2$ FC, the battery and the mass of $H_2$ available in its tank. For the initial architectures that are contemplated, the assigned values are the following:

- FC stack power: 40, 60, 80, 100 kW
- Battery capacity: 20.5, 40, 60.3 kWh
- $H_2$ mass in the tank: 3, 5 kg

These values are determined after considering studies made on FCVs as well as the projections of the future FC LCVs expected to be in the market in the future. For instance, it is reported that the Renault Master van could have a maximum FC power of 30 kW, a battery capacity of 33 kWh and a $H_2$ capacity of 6.4 kg [19].

The FC power mainly affects the consumption of $H_2$. For greater powers, the current density in the cell decreases and, therefore, it can function more efficiently and decrease fuel use. Initially, an FC stack power of 20 kW was considered, but after observing an excessive $H_2$ consumption, this value was discarded. On the other hand, the improvements in range and consumption diminish each time the power increases due to the constant increase in weight, and therefore, architectures with a power of over 100 kW are not considered.

The battery, on the other hand, has a larger effect on the general performance of the vehicle, affecting its electric consumption and overall range. An increase in the battery capacity will result in a larger amount of energy available in the vehicle in exchange for an increase in weight. As the battery capacity is adjusted by varying the number of parallel cells in the battery, the values are not integers as the ones for the other parameters.

Finally, the $H_2$ tank capacity is contemplated for values of 3 and 5 kg. This parameter has a considerable effect on the operation of the LCV too, as it affects mainly consumption and range. The higher the amount of $H_2$ available, the more energy can be used in the vehicle without refueling, which translates into a greater range in exchange for an increase in the size and weight of the tank. A tank capacity of 3 kg of $H_2$ is adequate for last-mile transportation, while a capacity of 5 kg is more suited for situations that feature longer trips.

As stated before, the selected parameters will not only have an effect on the individual performance of the components that it affects, but also on the overall weight of the vehicle, which is a crucial factor when it comes the operation of the LCV. The following data was included in the GT-Suite model in order to estimate the total mass of the vehicle for each of the studied architectures:

| Parameter | Value |
|---|---|
| **Empty weight** | 1846.3 kg |
| **FC specific power** | 0.65 kW/kg |
| **Battery specific energy content** | 0.168 kWh/kg |
| **$H_2$ tank mass** | 0.052 kg $H_2$/kg |
| **Electric motor** | 73.4 kg |
| **Driver** | 75 kg |

Table 1: Data for Vehicle Mass Calculations [17], [20]

## 3.2 OPTIMIZATION PROCESS

### *3.2.1 Driving cycle*

In order to complete the simulations, the WLTC 3b driving cycle is implemented in GT-Suite. This specific test is meant for vehicles with a power-to-mass ratio of more than 34 W/kg, a characteristic that all of the vehicles fulfilled. This cycle is part of the Worldwide Harmonized Light Vehicles Test Procedure (WLTP), a world standard to determine consumption and emissions of light vehicles. The WLTC 3b cycle is especially interesting for the purpose of this BSc thesis, as it represents a diverse scenario that features low and high power demand zones (Figure 3.3). This helps provides a more accurate understanding of the characteristics of this LCV in different situations and gives a realistic view of the performance of the vehicle in real life situations.

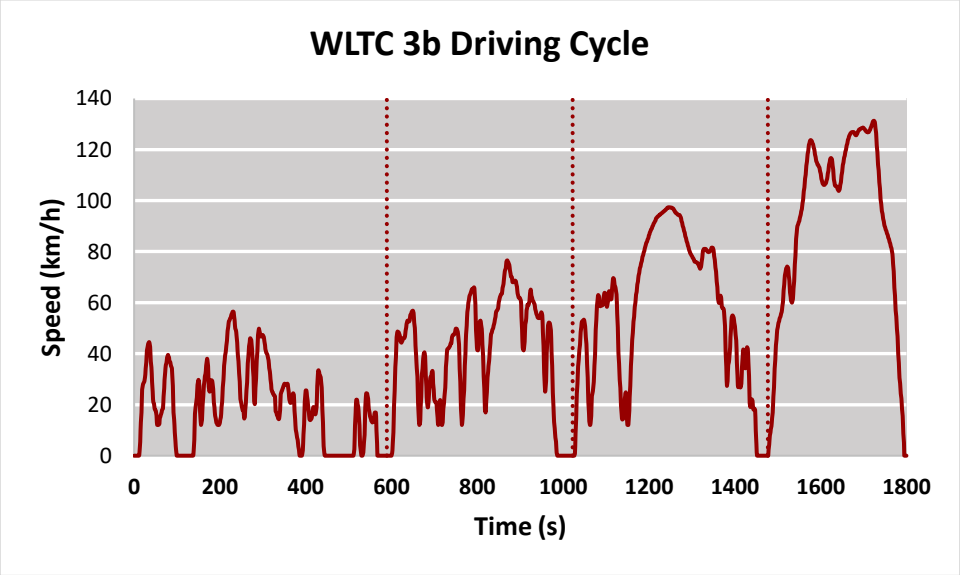


Figure 3.3: WLTC 3b Driving Cycle

The cycle features a 30-minute (1800 seconds) test throughout which the vehicle will run on low, medium, high and extra high speeds which aim to simulate urban, suburban, rural and highway scenarios [21].

### *3.2.2 Charge Depleting and Charge Sustaining modes*

Once the driving cycle is established, the energy consumption strategy is determined. For the initial cases, a charge-depleting mode (CD) is first used, followed by a charge-sustaining (CS) strategy until the energetic resources of the vehicles are exhausted. This strategy is considered as it is simple, conservative and helps analyze the behavior of the vehicle in each of the strategies separately. However, it is clearly not the ideal strategy if the objective is to maximize some of the performance parameters of the vehicle, which is the reason why charge-blended mode simulations will be launched and explained in the next sections of this BSc thesis.

First, the CD mode is applied. This strategy consists of operating the vehicle by just using the battery to provide electricity for the electric motor until the battery reaches a certain SoC. In this case, a final SoC of 0.25 is considered, which allows the vehicle to use a considerable amount of energy from the battery without causing an excessive discharge that would accelerate its degradation. Here, the variable that has the largest effect is the capacity of the battery, as the FC and $H_2$ in the tank are not used and only affect in the weight of the vehicle. To obtain the desired data, the simulation is launched from the GT-Suite software, selecting a number of cycles that assure that the battery discharges to 25% of its total capacity.

After the CD mode is completed and the SoC of the battery is 0.25, the CS mode is applied. This strategy is based on a combination of both the battery and the FC. FC will consume $H_2$ during the whole cycle, while the battery will be charged throughout some of the sections of the cycle and discharged to provide power to the LCV during others. To run these simulations, MATLAB and Simulink are also used to support the GT-Suite software. Using the mentioned tools, the balance between the FC and the battery is varied in order to find the strategy that assures a minimum $H_2$ consumption while maintaining an SoC of 0.25 after each WLTC 3b cycle is completed. The simulation ends when the vehicle runs out of energetic sources, at which point the desired values of range and consumption can be obtained.

A detail that must be taken into account is that all CS simulations start at the beginning of the WLTC 3b cycle, but all of them reach an SoC of 0.25 at different points depending on their battery capacity and weight. Therefore, all the CD simulations start at different points in the driving cycle, which could lead to an unfair comparison when analyzing different architectures. Therefore, additional CS simulations are launched for all the considered LCV architectures, starting at an SoC of 0.25 and at the beginning of the WLTC 3b cycle to ensure a fair comparison between each other.

These procedures are applied to all the possible combinations of FC power, battery capacity and $H_2$ tank mass parameters, obtaining tendencies in the behavior of the LCV.

### *3.2.3 Charge Blended mode*

In order to find an energy management strategy that could minimize the energy consumption and therefore maximize range, a series of new simulations are proposed. For these strategies, the CS and CD modes are substituted by a charge-blended (CB) mode, during which the FC and the battery will combine to provide energy from the beginning of the simulation, without a discharge cycle of the battery. In order to regulate these simulations, a target battery consumption per cycle is established, meaning that, at the end of each cycle, the SoC of the battery is reduced by 0.15, 0.10 or 0.05 from its start value. The CB mode will end when one of the two energy sources is exhausted. If the tank runs out of $H_2$ first, then the simulation will be completed in CD mode until the battery reaches an SoC of 0.25. If the battery reaches the mentioned value first, then the simulation continues in CS mode until the fuel available is finished.

For these simulations, FC stack powers of 100 kW were not considered, as it has been noticed that the increase in overall efficiency when changing the FC stack maximum power from 80 to 100 kW was not as significant as the other changes in this variable and are therefore not of great interest for this BSc thesis. Additionally, as the objective of these CB simulations is to maximize range, only $H_2$ tanks with a capacity of 5 kg are taken into account, as this value showed a large improvement over the 3 kg mass. Furthermore, after studying the results of the exploratory simulation, it is determined that the longer the FC and battery can work together without consuming all the $H_2$ available or reaching an SoC of 0.25 respectively, the lesser the overall energy consumption and the greater the range. Therefore, a final round of simulations is launched, with the objective of targeting a battery discharge that would maximize the number of cycles that the vehicle can complete in the CB mode. All the studied scenarios are summarized in the Table 2:

| Sizing | Battery discharge per cycle | | | |
|---|---|---|---|---|
| 40 kW – 20.5 kWh | 0.15 | 0.1 | 0.05 | 0.0438 |
| 40 kW – 40 kWh | 0.15 | 0.1 | 0.05 | 0.0377 |
| 40 kW – 60.3 kWh | 0.15 | 0.1 | 0.05 | 0.0334 |
| 60 kW – 20.5 kWh | 0.15 | 0.1 | 0.05 | 0.0425 |
| 60 kW – 40 kWh | 0.15 | 0.1 | 0.05 | 0.0418 |
| 60 kW – 60.3 kWh | 0.15 | 0.1 | 0.05 | 0.0369 |
| 80 kW – 20.5 kWh | 0.15 | 0.1 | 0.05 | 0.0418 |
| 80 kW – 40 kWh | 0.15 | 0.1 | 0.05 | 0.0368 |
| 80 kW – 60.3 kWh | 0.15 | 0.1 | 0.05 | 0.0331 |

Table 2: Charge-Blended Simulation Strategies

### 3.3 LIFE CYCLE ASSESSMENT PARAMETERS

Finally, this BSc thesis focuses on an LCA methodology to estimate the emissions produced during the complete life of the vehicle. This FCV produces minimal tank-to-wheel emissions, while other stages of its cradle-to-grave cycle, such as fuel production and vehicle manufacture, do produce considerable emissions that must be calculated, analyzed and compared with other types of LCVs.

#### *3.3.1 Scope and scenarios*

In order to analyze the future scenarios expected in Europe in the next years, a series of energy mixes from the years 2020 to 2050 are considered. As the exact mixes that will be present in Europe in the future are uncertain, three trends for the EU energy mix development are considered using GaBi, an LCA software from where the different mixes are obtained. These trends, named EU Energy Trend Reports (ETS), Normal Improvement in the sustainability policies (NI) and Significant Improvement in the sustainability policies (SI) estimate the change in the European energy mix following a series of different tendencies and show how the current energy mix is expected to change into others more reliant on renewable sources. The difference in the studied trends lies mainly in the rate at which this change is expected to happen. The data obtained is then adjusted for greenhouse gases using the CML-IA database from August 2016 [22]. By adjusting the energy sources of every energy mix and adding them to GREET, the GHG emissions for every scenario from the selected mixes and from the CML-IA database are matched in the global warming potential (GWP) 100 impact category, which reflects the effect of GHGs in the atmosphere for a period of 100 years.

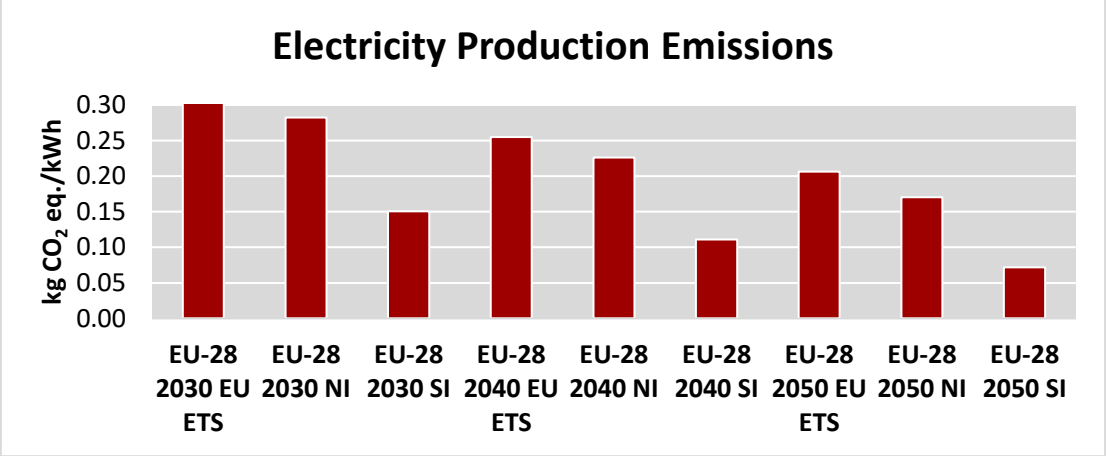


Figure 3.4: Electricity Production Emissions for every Estimated Scenario

The result of the combination of this information helps predict average scenarios for the years 2030, 2040 and 2050, which will show how the emissions for every step of the life cycle of the vehicle change as the energy mix becomes more reliant on renewable sources.

### *3.3.2 System boundaries*

The following diagram shows a simplified scheme of the processes studied for this LCA. The main inputs evaluated are raw materials and energy from each considered mix, which are directly involved for the fuel production, vehicle manufacturing and operation. There are a large group of outputs such as waterborne and solid wastes as well as atmospheric emissions. However, this BSc thesis will focus on GHG-100 as the main system output.

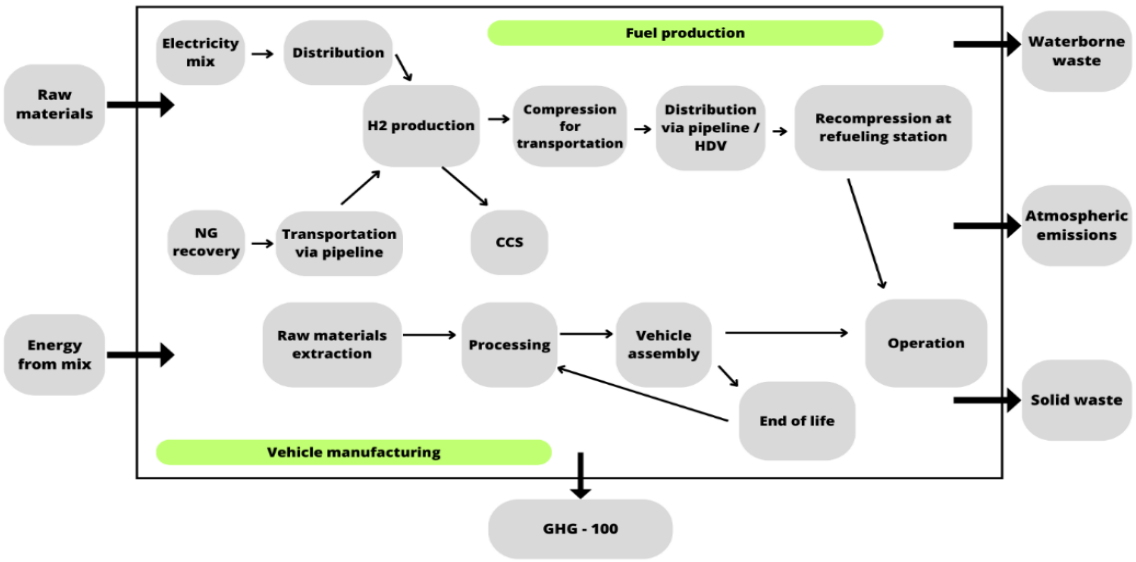


Figure 3.5: LCA Boundaries

The functional unit considered in this BSc thesis is the production of 1 vehicle, with an estimated lifetime distance of 240,000 km that should be covered in an average time of 10 to 15 years [23], [24]. Therefore, for the vehicle manufacturing calculations, the necessary materials to produce the components of an LCV are considered, while the emissions calculated per km will be multiplied by the distance that the vehicle is expected to cover during its life.

As the energy that powers the vehicle comes from two different sources ($H_2$ and electricity from the battery that is recharged from the energy mix), all the energy-related information is calculated in kWh in order to compare both.

### *3.3.3 Impact categories*

As explained previously, the impact category that is studied in this BSc thesis is GHG-100, which represents the GWP of gases over a period of 100 years. GHG emissions reduction is one of the main targets of the climatic policies of the EU, while it is also one of the main goals of the vehicles that aim to substitute those powered by ICEs, like BEVs or FCVs. GWP is measured in $CO_2$ equivalents, which represents the effect of greenhouse gases compared to carbon dioxide. The main gases considered are $CO_2$, $CH_4$ and $N_2O$, with a GWP of 1, 28 and 265 kg of $CO_2$ equivalent respectively [25]. Therefore, this is the formula that is used to calculate GHG-100:

$$GHG - 100 = m_{CO_2} \cdot GWP_{CO_2} + m_{CH_4} \cdot GWP_{CH_4} + m_{N_2O} \cdot GWP_{N_2O} \quad (5)$$

### *3.3.4 Life cycle inventory*

To obtain the emissions produced by all the considered processes, the GREET 2022 software (database version 14000) is used. This tool, which focuses on cradle-to-grave analysis, is globally used by researchers in both the public and private sectors to compare the environmental effect of different transportation options. As this BSc thesis is intended to include a cradle-to-grave study, data from fuel production, vehicle manufacturing and operation cycles is obtained.

*Fuel production cycle*

The fuel production cycle, known as well-to-tank, considers every step of the process of obtaining each fuel, including its extraction, treatment and distribution, and the emissions associated with them. For the $H_2$ production, six main methods were considered: central and regional electrolysis, SMR from natural gas (NG) with or without CCS, SMR from biogas and $H_2$ production as a byproduct. After the fuel is produced, it is compressed for transportation, distributed via pipelines and HDVs, and finally recompressed at the refuelling station.

To obtain precise results that adapt to the European scenario, a series of modifications are made in the GREET software before extracting data:

- First, a study is made on NG. This fuel, which is one of the main sources of $H_2$ today, is expected to see many changes both in its production and its composition in the next thirty years. Today, about 17 EJ of NG are demanded in Europe, but this number is expected to decrease gradually in the future years due to sustainability targets. As seen in Figure 3.6, the EU has estimated a series of scenarios for NG, stating that, by the year 2050, its consumption could be reduced to as little as 5 EJ [26]. This is important as, if the amount of NG decreases, the amount of $H_2$ that could be produced with it will decrease too. Furthermore, its composition is expected to change as well. Today, almost 100% of the NG available is produced conventionally. However, a steep rise in biogas demand is expected, as it is a source of energy with negative emissions due to the fact that its use avoids $CH_4$ to be released to the atmosphere. The European Biogas Association report for 2021 provides a series of trends for the increase in the demand of biogas (Figures 3.7 and 3.8): a Stated Policies Scenario (STEPS), which serves as an indication of where current policies stand, and a Sustainable Development Scenario (SDS), with the objective of reducing greatly the global carbon footprint [27]. These, together with the prediction of total NG consumption by the EU, allows us to calculate the composition of NG from today to 2050.

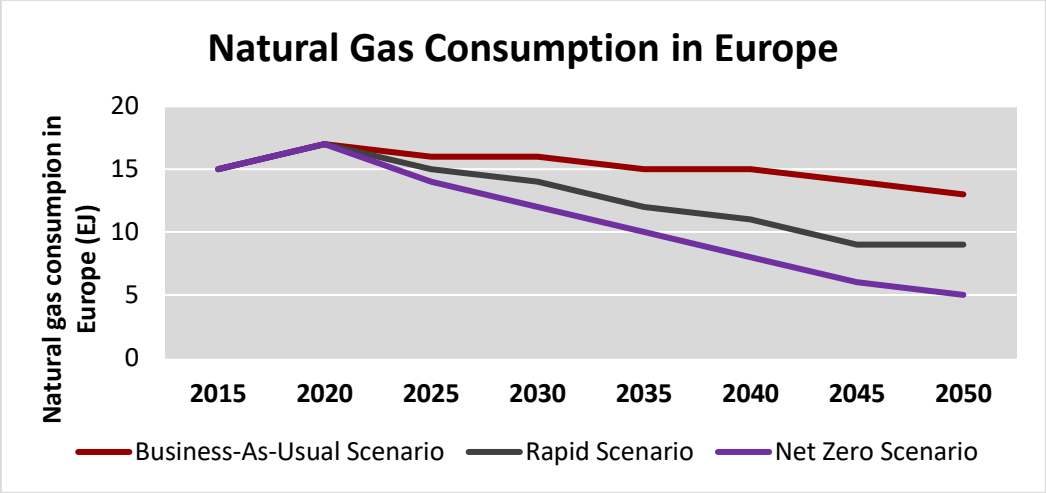


Figure 3.6: Natural Gas Consumption in Europe, Data retrieved from [26]

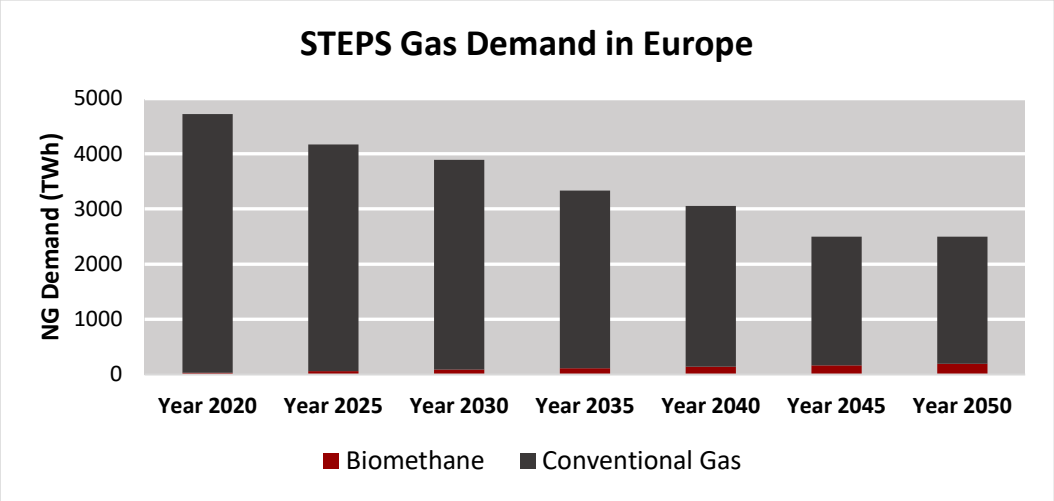


Figure 3.7: STEPS Gas Demand in Europe, Data retrieved from [27]

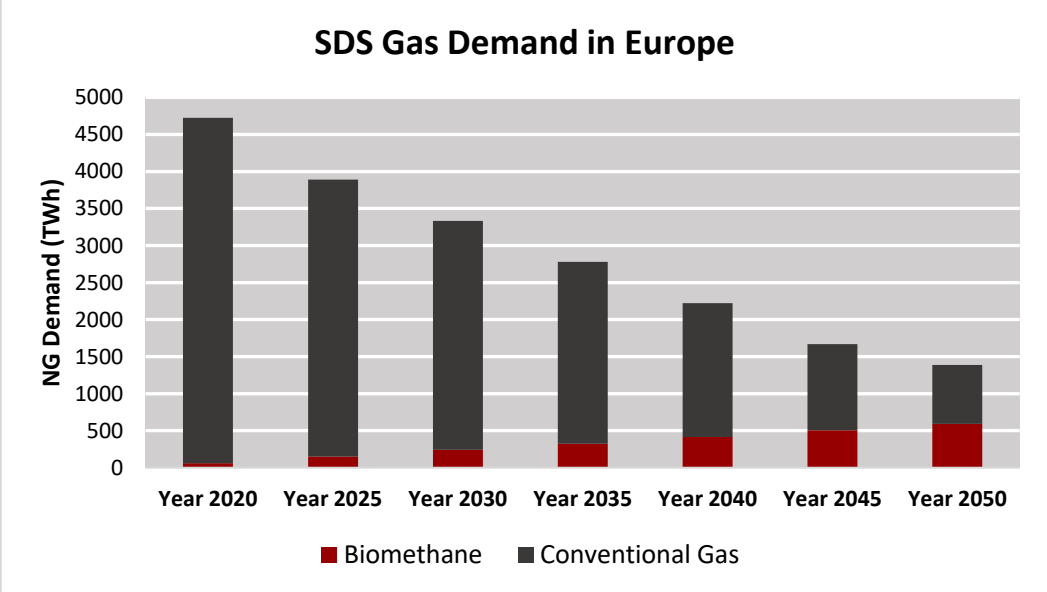


Figure 3.8: SDS Gas Demand in Europe, Data retrieved from [27]

- Next, the feedstock used for biogas production is adjusted. The International Energy Agency (IEA) states that almost 80% of biogas is produced in Europe through crop residues and animal manure, with the rest of it comes via municipal solid waste and wastewater sludge [28]. Due to the differences in the treatments of each of the former mentioned categories, the GHG-100 emissions could vary slightly for one another. Therefore, the data provided in the IEA is applied in the GREET model to obtain more accurate results.

- Finally, the energy source for the compression of $H_2$ produced via electrolysis must be considered, as this process could be completed using totally renewable energy instead of energy from the mix. However, it is impossible to determine the source of this energy as of today, and therefore, processes with both energy from the mix and from renewable sources are considered, with the deviation included in error bars.

With this information and with the different energy mixes considered, the GHG-100 emissions associated to every production method can be obtained using the GREET for all the studied scenarios. The data obtained is reflected in the following table, alongside with the emissions caused due to the production of electricity.

| $H_2$ production pathway | GHG-100 emissions (kg $CO_2$ eq./kWh) | | | |
|---|---|---|---|---|
| | 2020 | 2030 | 2040 | 2050 |
| Central electrolysis | 0.035 | 0.026 | 0.023 | 0.020 |
| Regional electrolysis | 0.025 | 0.016 | 0.013 | 0.010 |
| SMR w/o CCS | 0.319 | 0.275 | 0.216 | 0.104 |
| SMR w/ CCS | 0.136 | 0.084 | 0.020 | -0.102 |
| SMR from biogas | -0.478 | -0.517 | -0.614 | -0.716 |
| By-product | 0.330 | 0.305 | 0.296 | 0.287 |
| Electricity | 0.382 | 0.246 | 0.197 | 0.150 |

Table 3: $H_2$ and Electricity Production Emissions per Year and Pathway

The next step is to determine the amount of the total $H_2$ produced that comes from each of the mentioned processes. The EU predicts in its Hydrogen Roadmap two main tendencies when it comes to $H_2$ production: a “water electrolysis dominant scenario”, which expects that about three quarters of all the $H_2$ produced in Europe will come from central and regional electrolysis by 2050, and an “SMR dominant scenario”, which will rely on SMR to produce around 75% of the total European $H_2$ every year [3]. After studying these scenarios and considering the expected evolutions NG, it is determined that the SMR dominant scenario is very due to the

expected reduction in NG consumption and an increase in $H_2$ demand. The Hydrogen Roadmap poses two tendencies for $H_2$ demand: a business-as-usual scenario, that expects a demand of 780 TWh of $H_2$ in Europe by 2050, and an ambitious scenario, that predicts that this value could go up to 2251 TWh. Therefore, if the ambitious $H_2$ production scenario happens alongside the Net-Zero NG trend, more than 90% of the total NG available in Europe would have to be used exclusively for the production of $H_2$. This is highly unlikely, especially considering the fact that only about 4% of NG today is used for this means. BP, in its latest energy outlook, estimates that the maximum percentage of the global NG that could be used to produce $H_2$ could be as much as 24% in 2050 [29]. Therefore, the "SMR dominant scenario" proposed by the EU is corrected for this BSc thesis. Two scenarios, considering each of the $H_2$ production trends, are created from the original: an "SMR dominant with ambitious $H_2$ production scenario" and an "SMR dominant with business-as-usual $H_2$ production scenario". For scenarios where the $H_2$ demand remains low, a large percentage of it can come from SMR, while scenarios with a higher $H_2$ demand will need to rely more on electrolysis as the primary production method. Then, the results are be merged again in a "SMR dominant corrected scenario", considering the deviations in error bars.

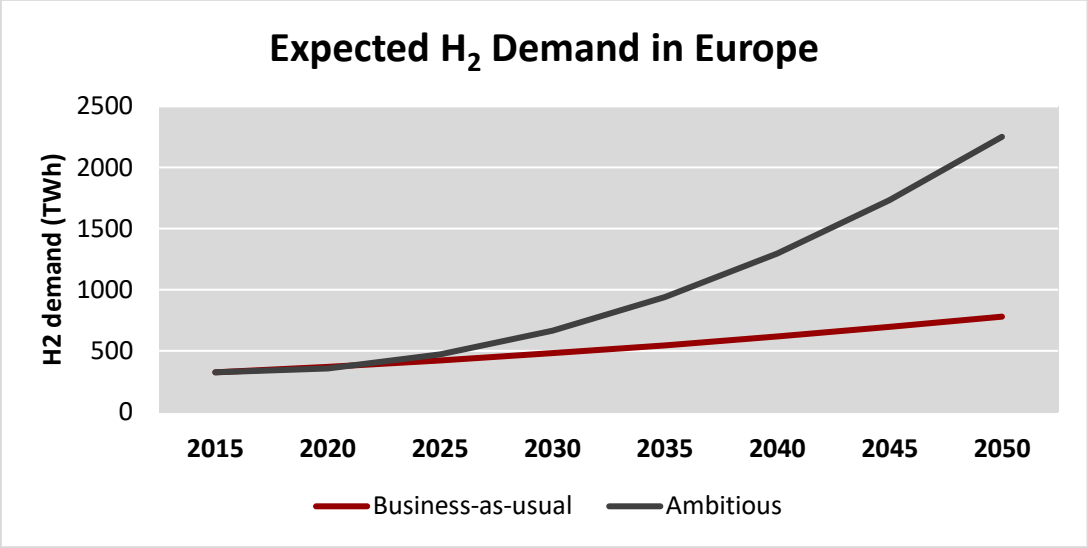


Figure 3.9: $H_2$ Demand in Europe, Data retrieved from [3]

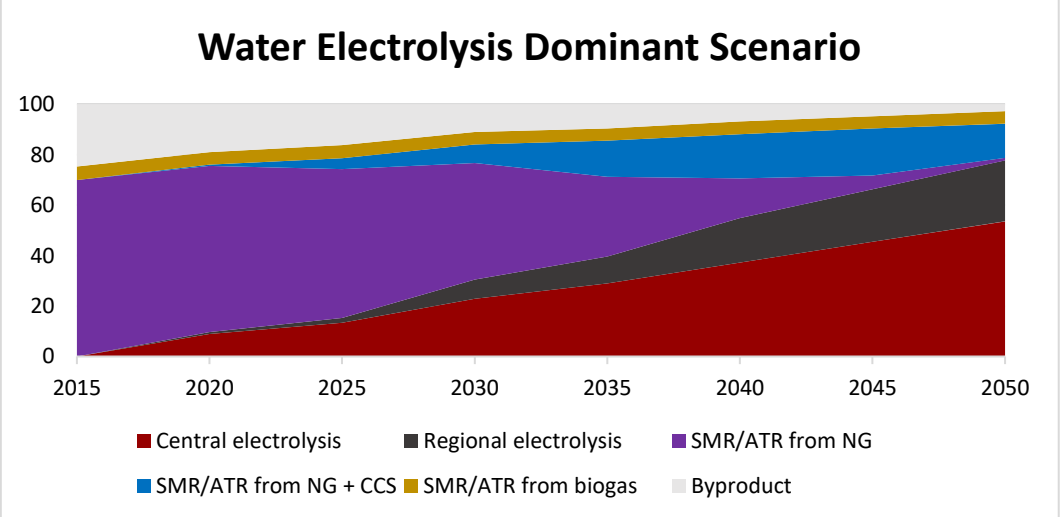


Figure 3.10: Water Electrolysis Dominant $H_2$ Production Scenario, Data retrieved from [3]

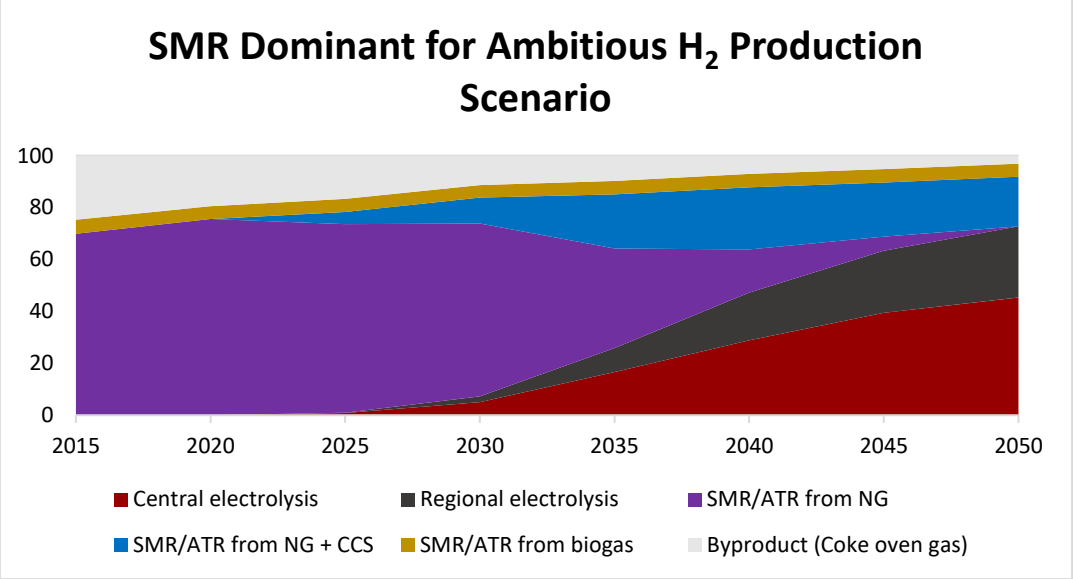


Figure 3.11: SMR Dominant for Ambitious $H_2$ Production Scenario, Data retrieved from [3]

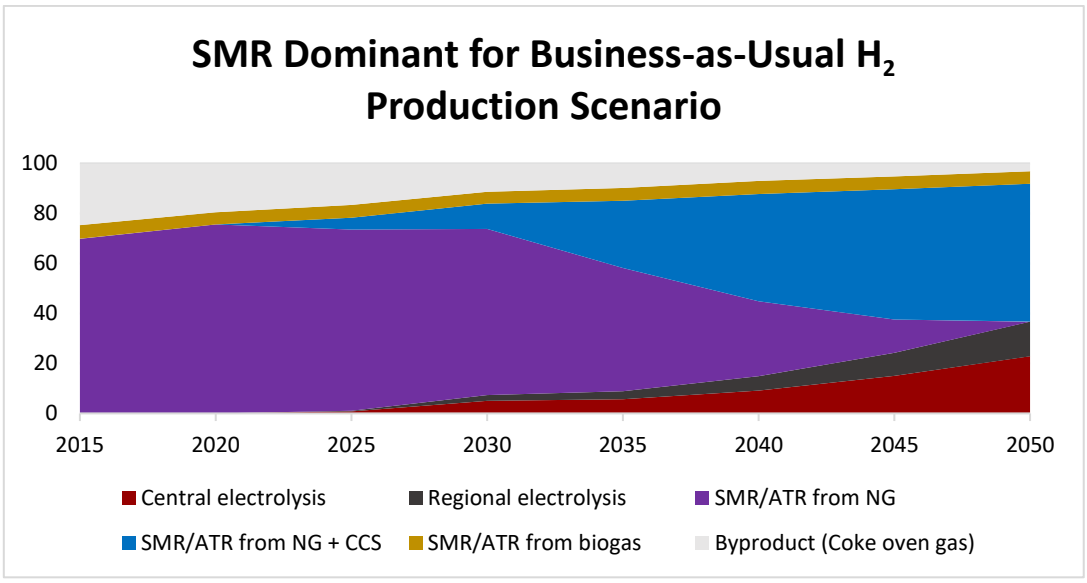


Figure 3.12: SMR Dominant for Business-as-Usual $H_2$ Production Scenario, Data retrieved from [3]

Finally, with the emissions calculated with GREET for each production method and year and knowing the percentage of the total $H_2$ that comes from each of the production pathways, the emissions to produce each unit of $H_2$ are obtained.

As the FCV is powered not only with $H_2$, but also with a battery, the emissions produced to obtain the necessary electricity, including the transmission losses, must also be evaluated. These emissions are known, as they were used in section 3.3.1, Figure 3.4, to adjust the different energy mixes.

*Vehicle manufacturing cycle*

The manufacturing of the components of the vehicle, as well as the production of other auxiliary elements needed for the proper operation of the LCV, produce a series of emissions that must be evaluated to perform an accurate LCA. To obtain the needed information, the weight of the vehicle is broken down into its different elements, and then the emissions associated with each unit of mass of the components of the vehicle are obtained using the GREET software for each of the future EU mixes. It is important to notice that the variation of the FC maximum power, the battery capacity, and the mass of the $H_2$ tank cause changes in the masses of the affected components, and therefore the emissions produced vary between architectures.

The vehicle is divided into its mechanical components, which include its body, fuel cell system (FCS), $H_2$ tank, chassis, electric motor, electronic controller and vehicle tire replacement, its battery pack, the assembly, disposal, and recycling (ADR) processes, and the fluids used in the vehicle, which include brake fluid, transmission fluid, coolant, windshield fluid and adhesives.

The raw materials needed for the manufacturing of the different parts of the vehicle are steel, aluminium, copper wire, magnesium, glass, plastic product, styrene-butadiene rubber, carbon fibre-reinforced plastic, zinc, glass, fiber-reinforced plastic, lithium, and other vehicle materials, which are inputs used in GREET for the calculation of the vehicle manufacturing emissions.

Once these details are taken into account, the emissions associated with the production of each of the simulated vehicles can be obtained.

*Operation cycle*

The operation cycle, also known as tank-to-wheel, evaluates the emissions produced when the fuel is used to power the vehicle. In the case of FC vehicles, $H_2O$ is the only product emitted from the reaction of $H_2$ with the $O_2$ in the air. This is one of the main incentives of FC vehicles, as others, such as those powered with conventional fuels in ICEs, produce a large number of greenhouse gases that are emitted directly to the atmosphere. $H_2O$, on the other hand, has a GWP of $5 \cdot 10^{-4}$ kg $CO_2$ eq. [30], which is far smaller than those of $CO_2$, $CH_4$ and $N_2O$. Knowing the $H_2O$ emissions per distance travelled during the operation, the total GHG-100 produced during the tank-to-wheel cycle of the vehicle can be calculated.

### *3.3.5 Vehicle market analysis*

Once the emissions for all the cycles in the life of the LCV are calculated and the full LCA assessment is performed, a comparison of this vehicle can be made with those already available in the market in terms of performance and environmental impact. In order to do so, a study of the Renault Master vehicles available in the market is made. Currently, Renault Master LCVs are powered by two different technologies: either fully by electricity or by a diesel ICE.

First, for the electrical vehicle, information can be found in the catalogue available at Renault [31]. This document provides information about the mass of the vehicle, the electric motor power and the energy capacity of the battery, among others. In order to have a vehicle with a

mass similar to that of the FC LCVs, the L3H2 propulsion electric vehicle is selected. The following table summarizes its main traits:

| Parameter | Value |
|---|---|
| **Mass** | 2349 kg |
| **Maximum mass** | 3500 kg |
| **Electric motor power** | 57 kW |
| **Battery capacity** | 52 kWh |
| **Range (WLTC class 2)** | 204 km |

Table 4: Electrical Renault Master Characteristics

To perform a complete LCA, fuel production, vehicle manufacturing and operation must be considered with the same method that was used for the calculation of emissions from the FC LCV. This is simple for this specific vehicle: the emissions associated with the production of electricity have already been estimated, the production of each of the components of the vehicle can be easily recalculated using the information from the previously described LCA and eliminating the FC and the $H_2$ tank, and the cycle emissions will be zero as the use of electricity in the LCV does not produce emissions.

On the other hand, the diesel vehicle does present considerable differences. General characteristics of the vehicle are obtained using an online automobile catalogue [32]. These parameters are represented in the next table, which will the help produce a performance evaluation of the LCV:

| Parameter | Value |
|---|---|
| **Mass** | 1971 kg |
| **Maximum mass** | 3500 kg |
| **Diesel engine power** | 134.23 kW |
| **Diesel consumption** | 9.5 L / 100 km |
| **Emissions** | 0.25 kg $CO_2$ / km |

Table 5: Diesel Renault Master Characteristics

As for the environmental analysis, a denser study is performed due to the differences in all of the sections of the LCA.

First, the emissions caused by the production of diesel are estimated. Using the GREET database and considering low-sulfur diesel as the main fuel as well as a 10% share of biodiesel in it, the GHG emissions for diesel production are obtained. This, alongside the expected distance that the LCV is expected to travel, provides the total emissions associated with fuel production throughout all its life. As data consumption is obtained in L / 100 km, emissions are obtained in kg $CO_2$ eq. / L.

| **Diesel production GHG-100 emissions (kg $CO_2$ eq./L)** | | | |
|---|---|---|---|
| 2020 | 2030 | 2040 | 2050 |
| 0.598 | 0.578 | 0.571 | 0.564 |

Table 6: Diesel Production Emissions

Next, the vehicle production cycle will also see a large number of changes when compared to the production of the FCV. Main changes are the substitution of the FC and the $H_2$ tank for a conventional ICE powertrain system, the use of a small lead-acid battery as opposed to the larger batteries needed to power the FCV, and other minor fluids added such as engine oil.

Finally, knowing the $CO_2$ emissions provided by the catalogue, the emissions throughout the whole life of the vehicle are estimated.

With all this information, a complete comparison of the performance of the environmental impact of the vehicles is performed in order to determine whether or not FCVs are a possible alternative for the current technologies available in the market.

# CHAPTER 4: RESULTS

After performing all the studies explained in the methodology section, a series of results are produced, providing information for the performance of the LCV as well as its environmental impact.

## 4.1 COMPONENTS SIZING RESULTS FOR STANDARD CD + CS STRATEGIES

By varying the maximum power of the FC between values of 40 and 100 kW, its battery capacity between 20.5 and 60.3 kWh, and the $H_2$ mass that can be stored in its tank between 3 and 5 kg, a total of 24 complete CD + CS simulations are produced.

### *4.1.1 Vehicle mass and payload*

The first noticeable effect of the change of the components is in mass of the vehicle. As the components grow in power or capacity, they do in overall mass as well, which leads to an increase in energy consumption. The mass of all the different architectures varies from 2226.63 kg (FC power of 40 kW, battery capacity of 20.5 kWh and $H_2$ mass of 3 kg) to 2577.85 kg (FC power of 100 kW, battery capacity of 60.3 kWh and $H_2$ mass of 5 kg). This affects directly to the payload of the vehicle, which is be a key parameter when analyzing performance.

### *4.1.2 Charge Depleting mode*

The CD mode consists of the discharge of the battery to 25% of its original value. The only energy source at this stage is the battery, reserving the $H_2$ mass to be used in the CS mode. Therefore, the battery capacity is the key factor in the performance of the LCV for this cycle. Increasing either the FC power or the $H_2$ mass in the tank only affects the overall weight of the vehicle, and therefore its consumption, but not the powertrain efficiency itself.

An example of the evolution of the battery SoC throughout the cycle is shown in the next graph. The information presented is obtained from the simulation with a maximum FC power of 60 kW, a battery capacity of 40 kWh and 5 kg of $H_2$ in the tank. It can be seen that, as time advances and the vehicle travels the corresponding distance, the SoC of the battery decreases until it reaches a level of 0.25, at which point the CD mode ends. The flatter lines represent to the least demanding sections of the WLTC 3b cycle, while the steeper parts represent the high-speed zones, which are responsible for the majority of the energy used from the battery.

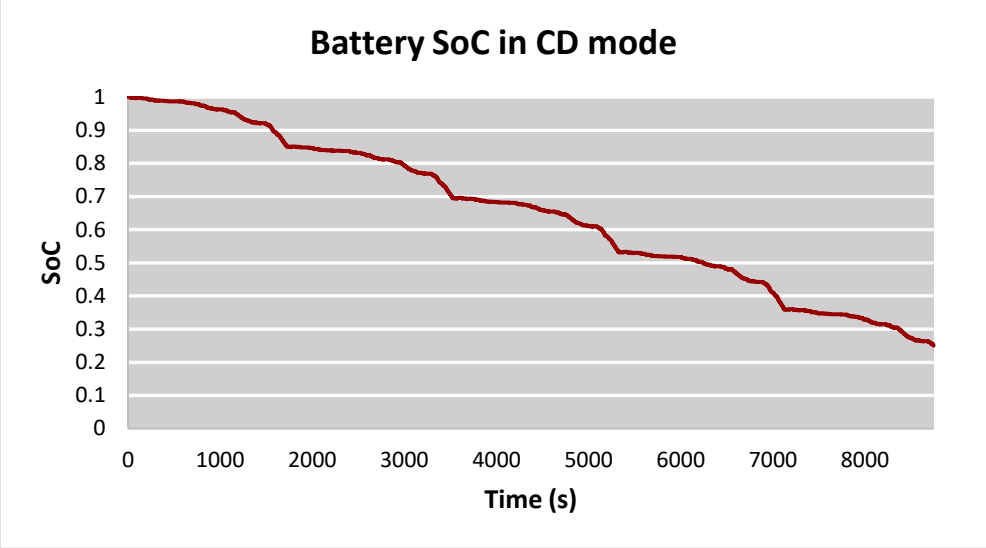


Figure 4.1: Evolution of Battery SoC during CD Mode

Once the simulations are completed, a series of parameters that will help determine ideal vehicle architectures are analyzed. First, the changes in range in CD mode are analyzed. For this specific parameter, the energy content of the battery is the variable with the greatest effect. As the capacity increases, the energy available in the battery to be used in the CD mode increases too. This translates directly into an increase in range for this strategy, as shown in the graph below. FC power and $H_2$ mass, on the other hand, increase the overall mass, and therefore decrease the CD range of the vehicle. However, for the studied parameter, the influence is minimal. For instance, increases from 40 to 100 kW of FC power with fixed battery capacities and $H_2$ masses only decrease CD range by an average of 1%, while increases from 3 to 5 kg of $H_2$ masses for fixed FC powers and battery capacities cause a decrease in CD range of under 0.5%. Therefore, due to their neglectable influence for this specific parameter, they are not represented.

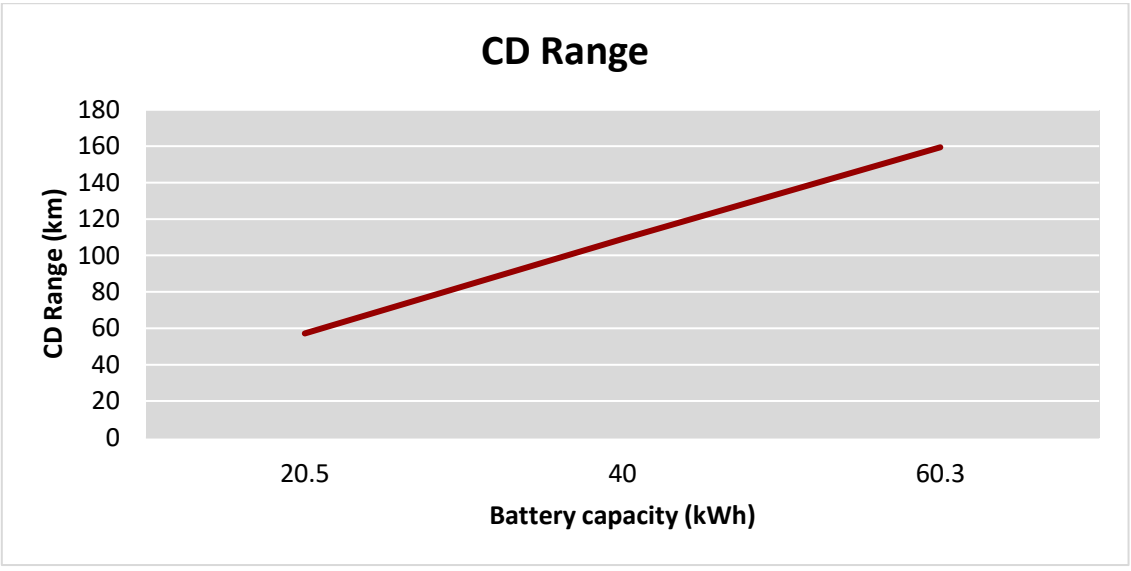


Figure 4.2: Variation of CD Range when changing the Battery Capacity

Next, changes in battery consumption, which is inversely proportional to the CD range, are explored. As explained throughout this section, FC power and $H_2$ mass only affect the vehicle in its weight during the CD mode. Therefore, increases in these values will result directly in increases in the consumption of the battery. Again, these changes are not of great significance, and this increase in consumption will be vastly compensated in the CS mode. As for changes in the battery, the same trends occur when increasing its capacity: when comparing the 20.5, 40 and 60.3 kWh architectures, it is seen that the increase in mass causes a rise in consumption, despite the increase in efficiency due to the lower discharge rate of the battery. However, as the amount of energy increases greatly from one value of capacity to the other, this increment in consumption does not noticeably affect the range and performance of the vehicle. For instance, when comparing simulations with batteries with capacities of 20.5 kWh and 60.3 kWh, it is seen that range increases by an average of 179.15% while only seeing a rise in consumption of 5.37%.

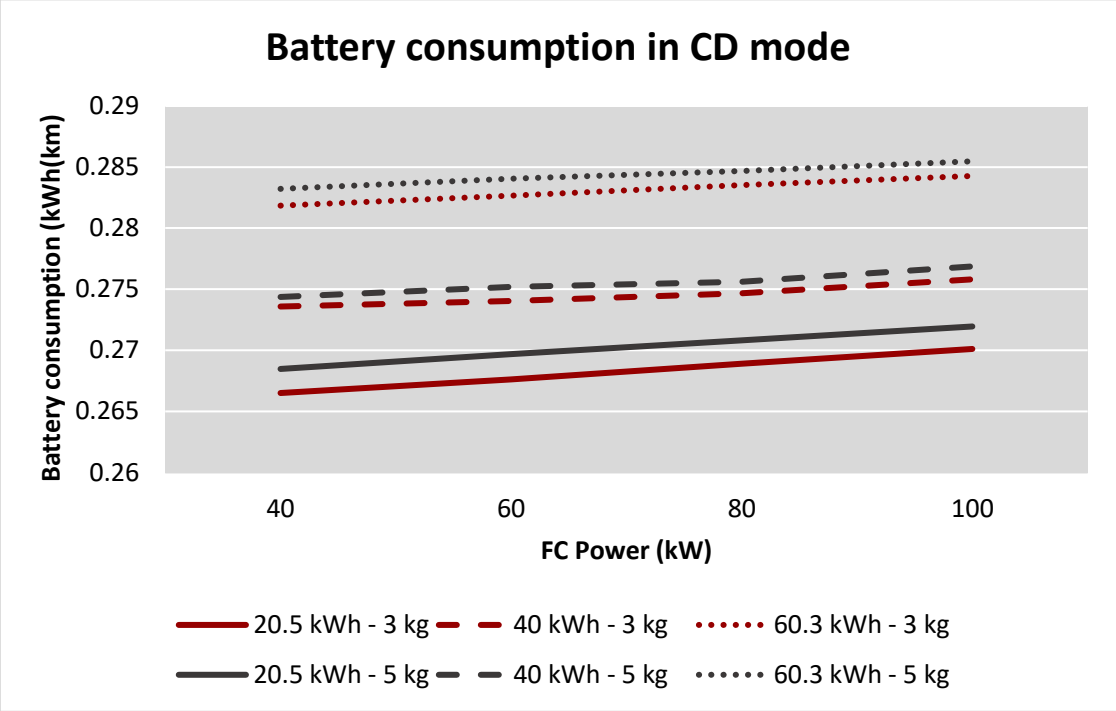


Figure 4.3: CD Battery Consumption for each Architecture

### *4.1.3 Charge Sustaining mode*

Once the battery reaches an SoC of 0.25, the CD mode ends and is replaced with the CS mode. Now, the FC uses the $H_2$ available in the tank (following the previously explained EMS strategy) to power the vehicle and maintain the battery at a stable SoC, ending the simulation when all the $H_2$ in the tank is consumed. In this cycle, FC power and $H_2$ mass will be the determining factors for the performance of the LCV, while the capacity of the battery will have a far smaller influence compared what it had during the CD mode. Figure 4.4 represents the SoC of the battery for a cycle in CS mode and belongs to the vehicle with the same architecture of the CD graph presented previously (60 kW – 40 kWh – 5 kg $H_2$), while the $H_2$ consumed per second during the simulation is presented in Figure 4.5.

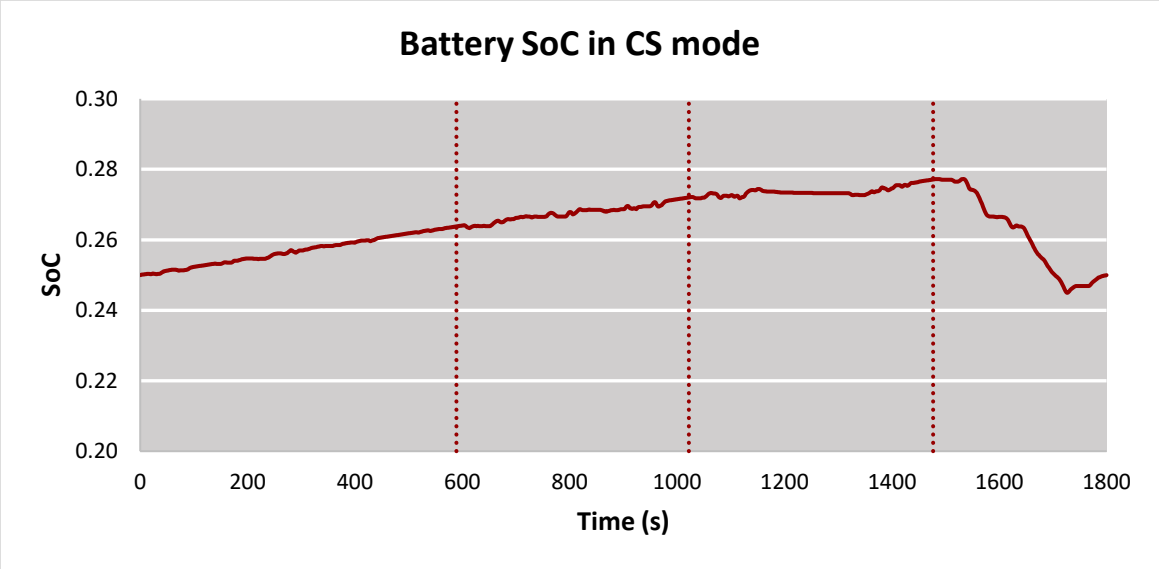


Figure 4.4: Evolution of the Battery SoC throughout a WLTC 3b Cycle

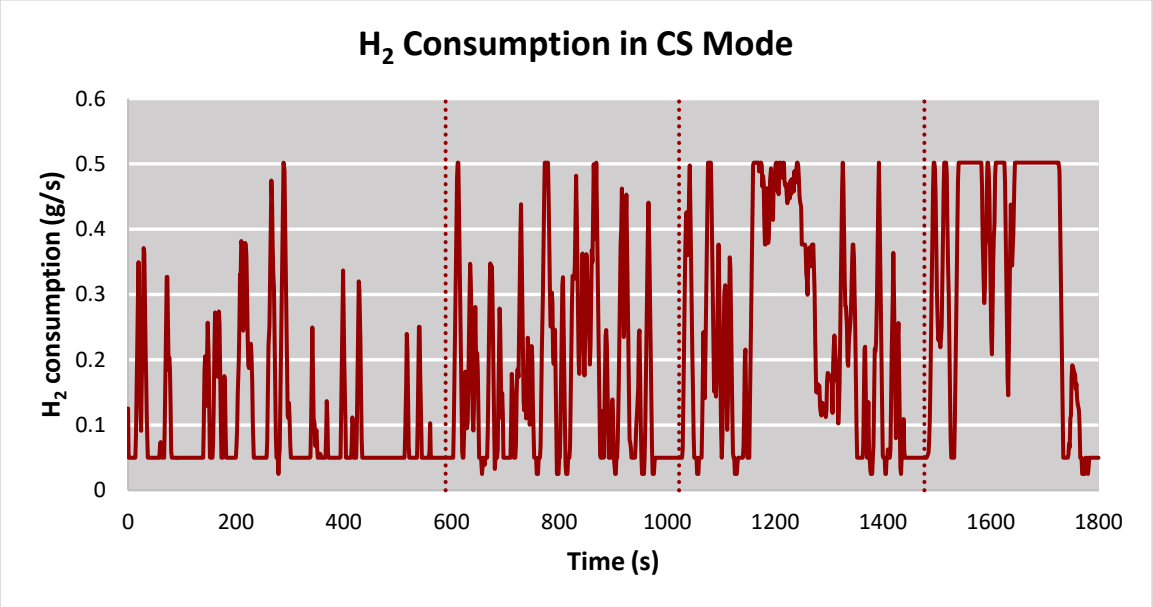


Figure 4.5: $H_2$ Consumption throughout a WLTC 3b Cycle

These graphs show clear differences in the behavior of the vehicle in the low, medium, high, and extra-high demand sectors of the cycle, separated by the discontinuous vertical lines. From them, it can be concluded that, in order to minimize $H_2$ consumption during the driving cycle and maximize range, the FC uses the $H_2$ in the tank to power the vehicle and to charge the battery to values of about 0.28 during the less demanding parts of the cycle. Then, for the extra-high power demand section, the battery and the FC both provide energy to meet the imposed requirements, which is shown by the steep decrease of SoC and the high values of $H_2$ consumption. The result obtained is a simulation at the end of which the SoC of the battery is maintained equal to that at the beginning and that consumes the smallest amount of $H_2$ possible to achieve it.

After completing the simulations and understanding the operation of the FC and the battery, a series of parameters of interest are analyzed. First, the range of all the different vehicles is calculated from the simulation data, obtaining Figure 4.6.

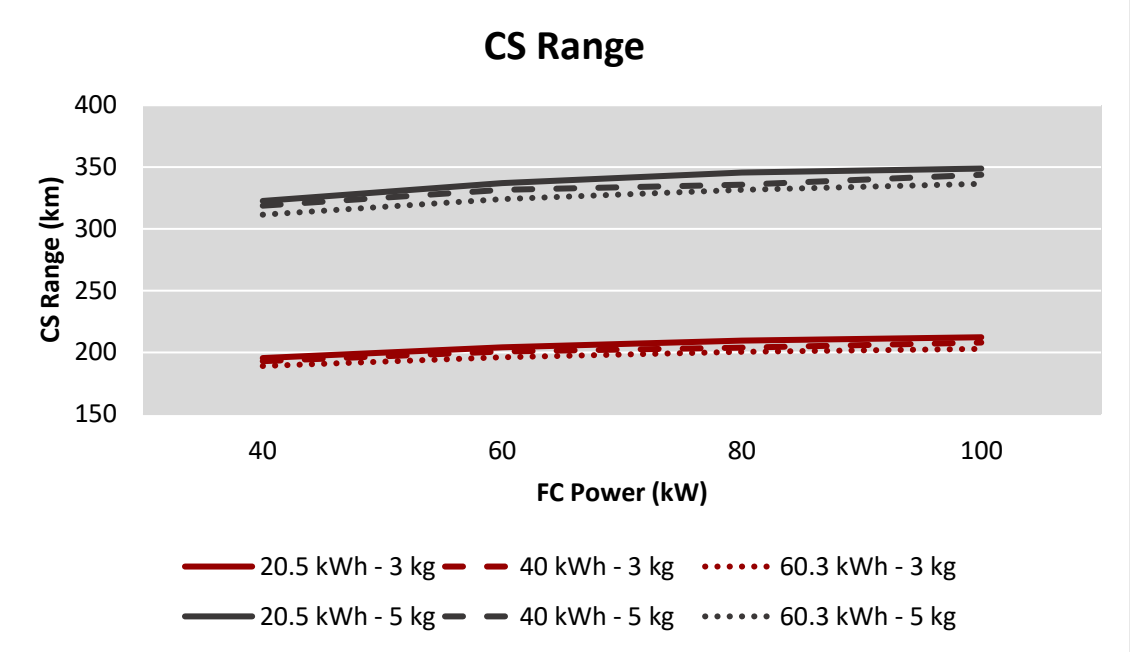


Figure 4.6: CS Range for each Architecture

For this performance parameter, the mass in the tank is the most influential parameter. Increasing the mass from 3 to 5 kg of $H_2$ means that a larger amount of energy is available in the tank without needing to refuel, which translates in increase of CS range of about 65% for simulations with the same FC and battery but different $H_2$ masses. Another important parameter that must be considered is the power of the FC. This variable affects mainly the FC current density, which measures the amount the electric current per unit of area. When increasing the FC stack maximum power, the FC can work at lower current densities, which translates into a more efficient behavior and, therefore, a lower $H_2$ consumption. If simulations with the least and most powerful FCs are compared, an average increase of 8% in CS range can be seen between them, as shown in Figure 4.7. However, after each increase in FC power, the gain in range decreases. For instance, when comparing all the simulations that feature an FC of 40 and 60 kW, an increase in range of about 4.1% is seen for all simulation, while this increase is only of 1.5% when comparing vehicles with FCs of 80 and 100 kW. This happens because an FC with a maximum stack power of 80 kW already operates naturally at a current density that provides an efficiency close to its maximum possible value. Therefore, increasing this parameter from 80 kW to 100 kW does not show a large influence in the performance of the vehicle. Finally, it is noticed that increases in the battery capacity reduce slightly the range of the vehicle due to the increase in weight. This is the least significant change, as the range only decreases by an average of 3.8% when comparing the smallest and the largest batteries.

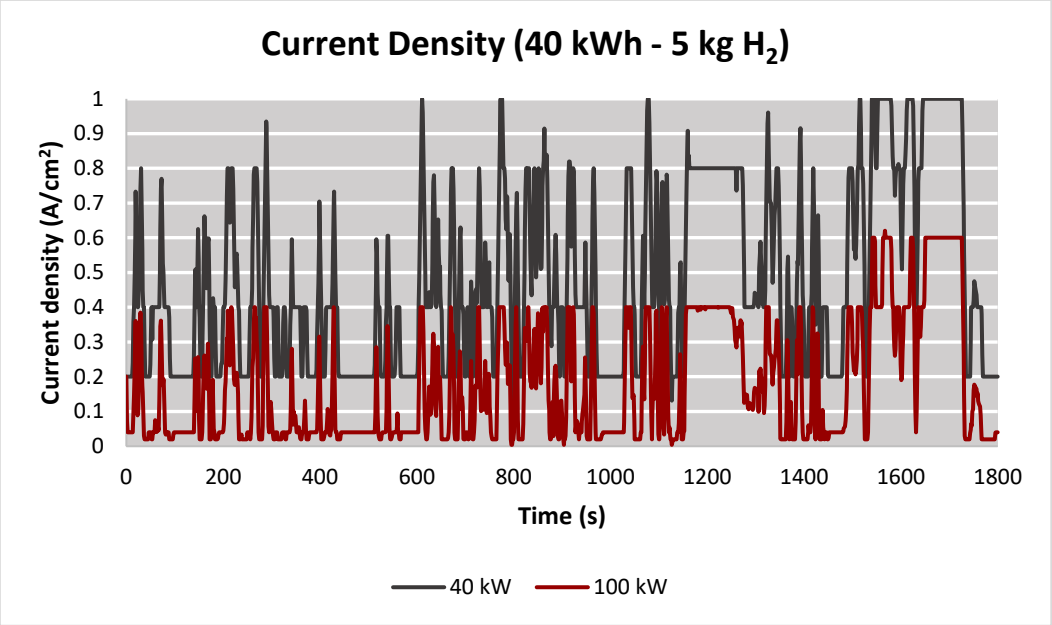


Figure 4.7: Comparison of Current Density for Vehicles with different FC Stack Power

Similar changes are seen in Figure 4.8, which compares $H_2$ consumption in CS mode for all the different architectures. When increasing FC power, consumption is reduced, as expected by the decrease in current density perceived in Figure 4.7. On average, a decrease of 7.4% in $H_2$ consumption is seen when comparing the 20 and 100 kW FC designs. Again, it is observed how the tendencies become less steep when moving towards higher FC power, which is the same shift that is observed when analyzing the vehicle range. Increases in the $H_2$ mass cause slightly higher consumption due to the increase of the weight of the vehicle, but this is greatly compensated by the increase in range. On average, increasing the mass in the tank from 3 to 5 kg causes an increase in consumption of 0.9% in exchange for an increase in range of 65%. As far as the battery is concerned, increases in its capacity cause a rise in the weight of the LCV, increasing consumption in CS mode by 4% when comparing the biggest and smallest batteries.

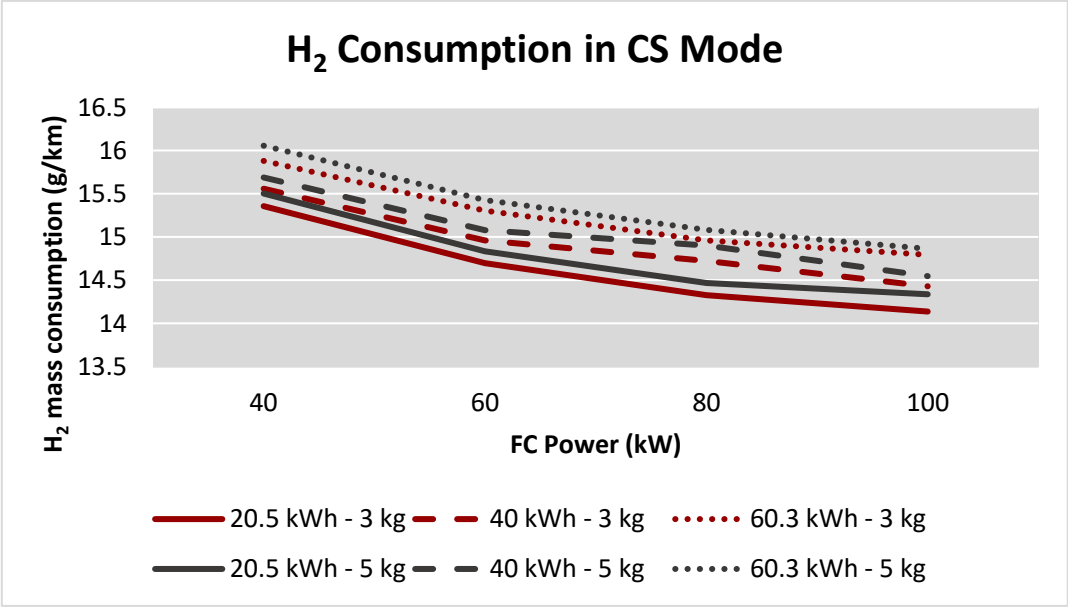


Figure 4.8: $H_2$ Consumption in CS Mode for each Architecture

### *4.1.4 Charge Depleting + Charge Sustaining mode*

Once the CD and CS simulations are launched and the data analyzed, a complete picture of the characteristics of each architecture is obtained.

When calculating the total range as the total distance travelled in both the CD and CS modes, the following results are produced. The tendencies observed are due to combinations of all those that are seen when analyzing CD and CS modes separately. Clearly, the most determining factor is the mass of $H_2$ in the tank. The range for vehicles with the same battery and FC but different $H_2$ masses is improved by an average of 42.8% when substituting the 3 kg tank with the 5 kg one. This change is even more significant for vehicles with smaller batteries, as these have a smaller CD range and rely on $H_2$ to power the LCV for the majority of its operation. The capacity of the battery is another influential variable, as increasing this value by about 20 kWh creates an increase in range of about 13.7%. However, this value decreases when the size of the vehicle rises due to an increment in weight and energy consumption. Finally, increasing the FC maximum power also rises the range, as the vehicle can operate with smaller current densities at higher efficiencies. A rise in 20 kW of FC power will, on average, increase the range of the vehicle by 1.75%. Nevertheless, as explained when analyzing CS range, increases in range become gradually smaller FC powers grow bigger. For instance, the 40 kW architectures show an improvement of 2.83% compared to those with a 20 kW FC, while simulations that feature a 100 kW cell only increase the distance travelled by the 80 kW vehicle by just under 1%.

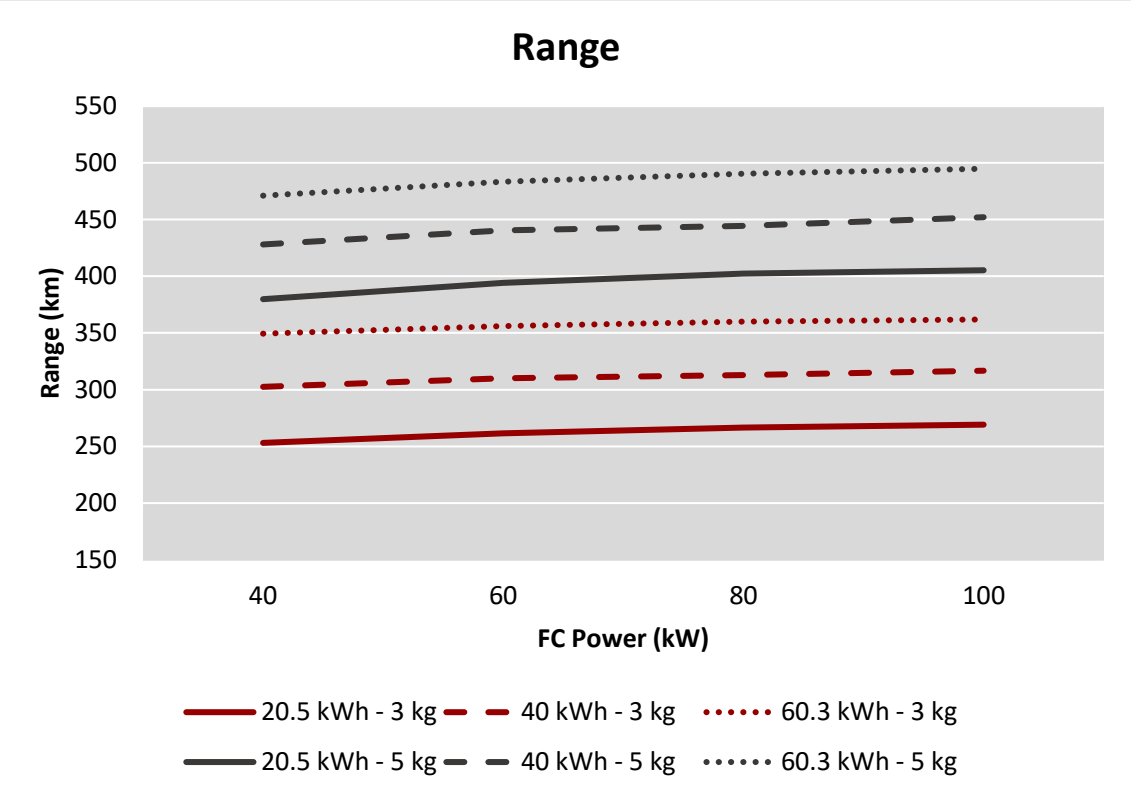


Figure 4.9: Evolution of Overall Range for every Architecture

Next, the difference in energy consumption in each vehicle can also be evaluated. Knowing that 75% of the energy stored in the battery is used and the mass of $H_2$ available in the tank

(considering a lower heating value of 33.33 kWh/kg of $H_2$), the total energy consumption per km travelled can be calculated (Figure 4.10). It can be seen that increasing the $H_2$ mass causes increases of 6.2% in consumption, but its increment in range heavily outweighs this. It is also noticeable that consumption decreases when the power of the FC does too, by values of around 1.85% when rising power by 20 kW. Finally, smaller consumptions are observed for bigger batteries. This is explained by the fact that, the larger the energy content in the battery, the longer the distance the LCV can travel in CD mode. As the battery system has an efficiency of over 90%, compared to a value of 55-60% for the FC system, being able to use the CD mode for a larger number of cycles translates into a lower overall energy consumption. Increasing the capacity of a battery by 20 kWh would result in decreasing the total energy consumption by 2.95%.

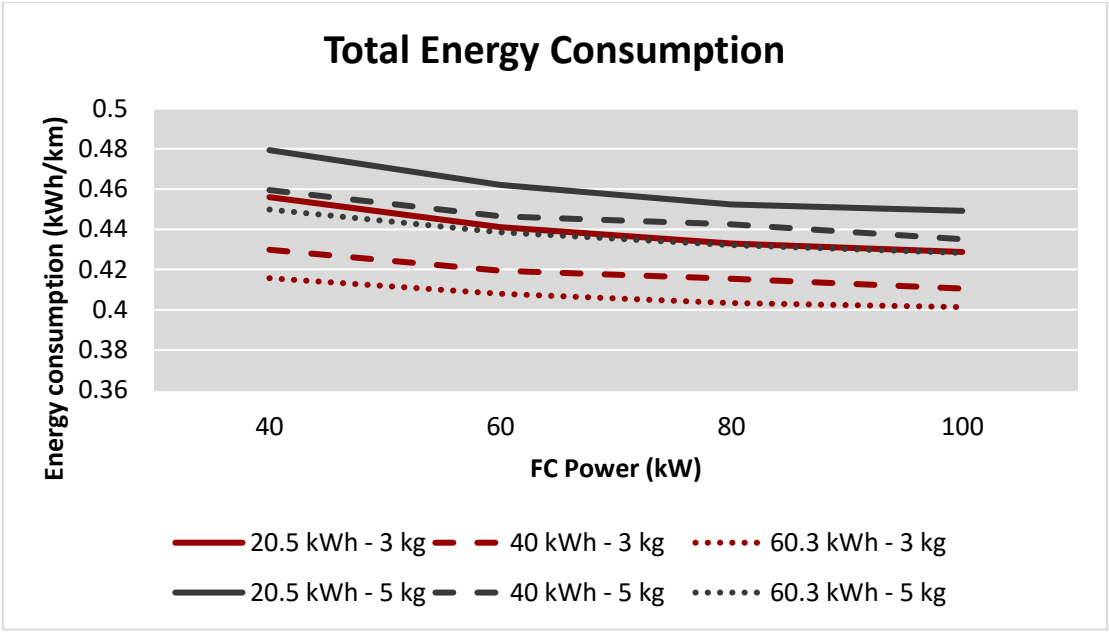


Figure 4.10: Total Energy Consumption for each Architecture, including Electricity and $H_2$

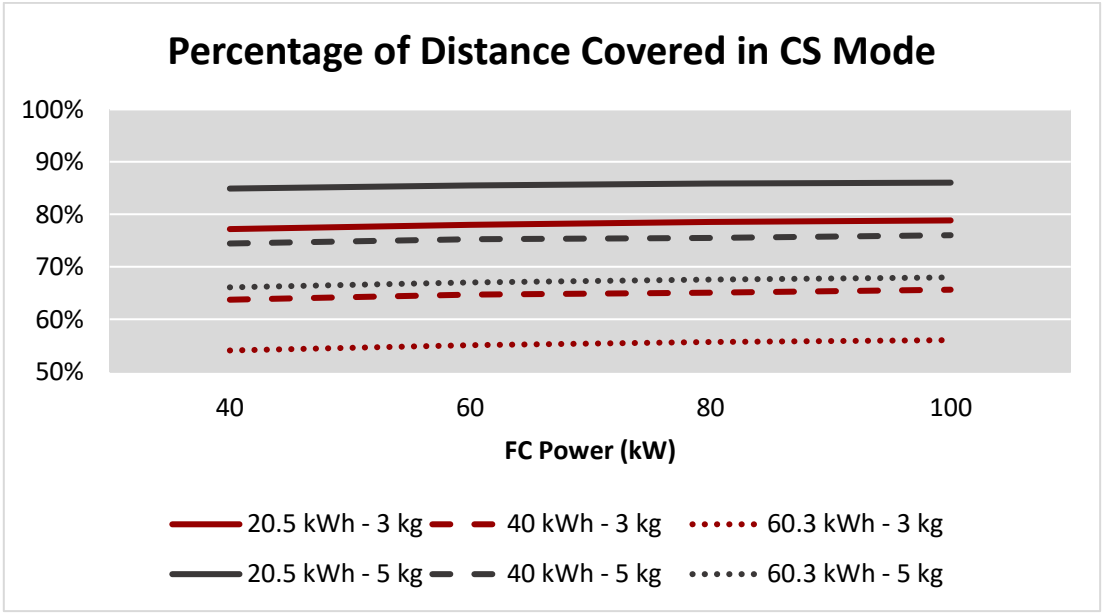


Figure 4.11: Percentage of Distance covered in CS Mode for all the Architectures

A final display of information is seen in Figure 4.12, comparing the range of all the simulations launched. To do so, the payload of each architecture is calculated as the difference between the maximum authorized mass of the vehicle (3500 kg) and the total mass of each LCV. This data does not only help compare the different performances with sizes, but will also help locate the simulated LCV with others with similar characteristics and powered by different technologies. The general trend is that, for smaller payloads, the range become larger. This happens because those vehicles with smaller payloads feature the most powerful FCs and the largest batteries, making them able to travel a longer distance. The two groups that are separated vertically correspond to those with a 5 kg of $H_2$ tank (above) and 3 kg (below), with the change in range symbolized by a purple arrow. Furthermore, the points that seem to be united in groups of 4 are those with the same battery capacities but different FCs, showing the evolution of range when changing FC stack power with a red arrow. Finally, changes in battery capacity are represented with a grey arrow, being those with higher battery capacities the ones with lesser payloads and higher ranges.

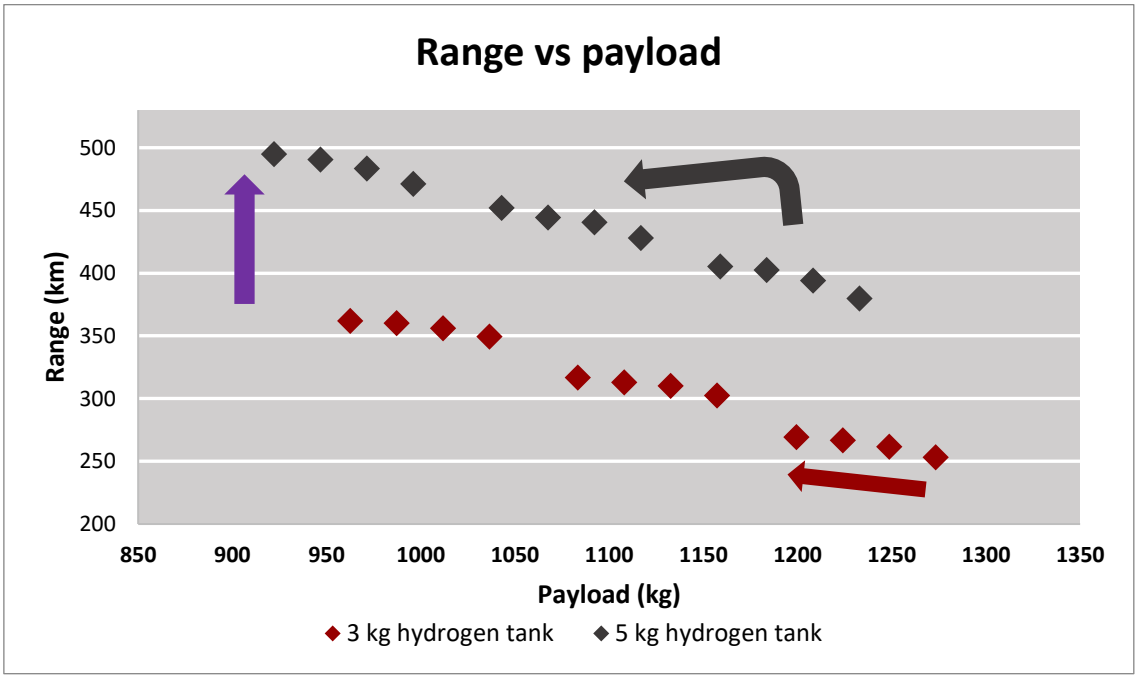


Figure 4.12: Range and Payload Comparison for all Architectures

From all the data obtained, the ideal architecture of the LCV is determined in terms of performance. To maximize range, the vehicle should feature a large $H_2$ tank, a large battery, and a medium-to-large FC stack, providing a considerable amount of energy onboard with an efficient FC operation. By selecting the maximum considered values for these three categories (100 kW FC stack, 60.3 kWh battery, 5 kg $H_2$), a range of 494.8 km is obtained, resulting in an increase of 95.54% in this parameter when compared to an architecture with the smallest possible components. As for consumption, it is minimized with a small $H_2$ tank, reducing the weight of the vehicle, and with a large FC and battery, providing an efficient energy use. The overall energy consumption for this specific architecture is of 0.40 kWh/km, reducing this value from the worst possible architecture in this category (40 kW of FC power, 20.5 kWh of battery capacity, 5 kg of $H_2$ in the tank) by 16.28%. Therefore, considering the fact that range can be increased considerably with small increases in consumption alongside the small changes when

comparing 80 kW and 100 kW FC systems, it is concluded that performance for a light commercial vehicle is optimized by using a large $H_2$ tank (5 kg), a large battery (60.3 kWh) and a medium-to-large FC (80 kW), resulting in a range of 490.4 km and an energy consumption of 0.43 kWh/km. It is important to point out that this architecture is ideal in terms of vehicle operation. However, if other factors such as environmental impact are evaluated, the optimum size of the components of the LCV could differ.

### 4.2 SYSTEM OPTIMIZATION RESULTS

The data obtained with these simulations gives a general idea of the behavior of the LCV, as well as its characteristics related to range and consumption. However, as explained before, the energy management strategy is only optimal for the CS+CD modes, but it does not mean that these modes are ideal. Therefore, a new CB strategy, consisting of the use of both the FC and the battery at a controlled level, will substitute the CD and CS modes. By operating the FC and the battery together, it is possible that the vehicle can work at higher overall efficiencies, reducing energy consumption. As the objective is maximizing range, the mass of $H_2$ in the tank will remain fixed at 5 kg, while the FC power of 100 kW is discarded due to its limited influence in terms of performance. For all the 9 combinations of FC power and battery capacity possible, three exploratory simulations that discharge the battery by 15%, 10% and 5% are carried out for each one, as well as a final simulation that targets the maximum possible range for each architecture.

In order to compare the behavior of the vehicles when changing the energy management strategy, the evolution of the SoC of the battery and the $H_2$ consumption for the 60 kW – 40 kWh – maximum range case is presented in Figures 4.13 and 4.14.

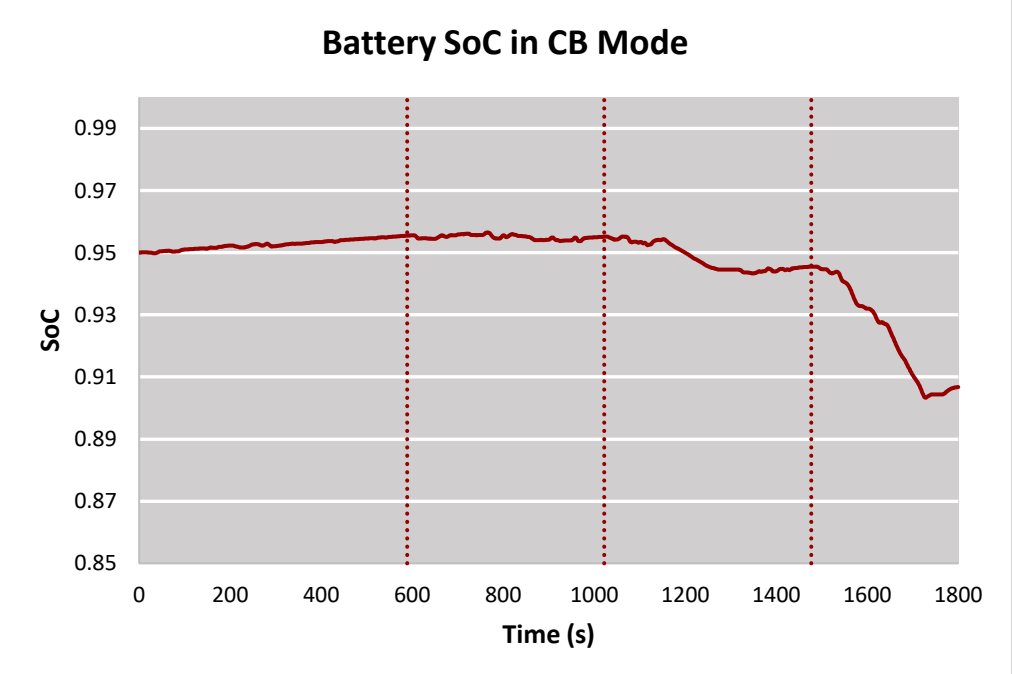


Figure 4.13: Evolution of the Battery SoC throughout a WLTC 3b Cycle in CB Mode

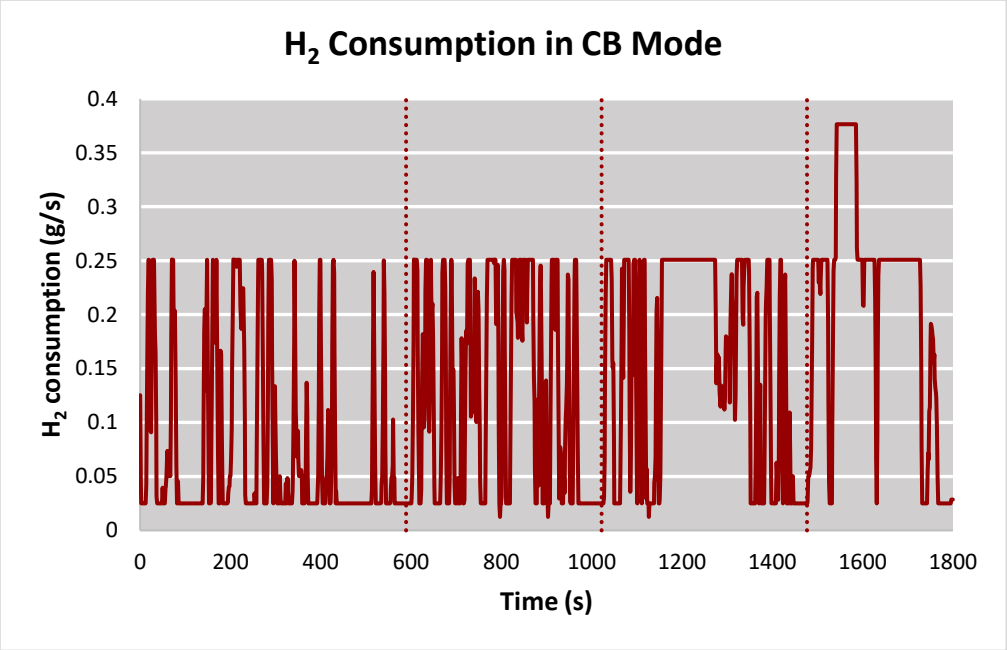


Figure 4.14: Evolution of $H_2$ Consumption throughout a WLTC 3b Cycle in CB Mode

Clear changes are observed in both of these parameters when compared to those of the standard CD + CS simulations. First, the least demanding sections of the cycle are analyzed. Here, the SoC, starting with a 0.95 value to assure that the GT-Suite simulation does not force the SoC to be greater than 1, presents numerous variations when matching it to the CS SoC evolution. For the early stages, the SoC remains close its initial value, as the FC is able to power the vehicle without needing to recharge the battery excessively due to the energy management strategy, as it does not require the FC to sustain the battery SoC completely. For instance, for a simulation featuring a 60 kW FC, a 40 kWh battery and 5 kg of $H_2$ with the CS strategy, the difference between the maximum SoC reached during the cycle and the initial 0.25 value is of 10.9%. However, for a vehicle with the same components but with a CB cycle implemented, the difference between the maximum and the initial SoC is only of 0.7%. As the FC does not need to recharge the battery excessively and focuses mainly on the vehicle operation, $H_2$ consumption decreases. As for the high demanding stages, the energy in the battery is used until the target value is reached at the end of the cycle. As the battery can provide a greater amount of energy, $H_2$ is consumed at a lower rate than in the CD + CS simulations, decreasing overall consumption and therefore range. If $H_2$ consumption is to be compared between vehicles with the previously mentioned architecture and different energy management strategies, it can be seen that the average consumption value for the CS strategy is of 0.195 g/s, with a peak value of 0.502 g/s, while the CB strategy shows an average of just 0.132 g/s and a maximum value of 0.376. This information is presented in Figure 4.15.

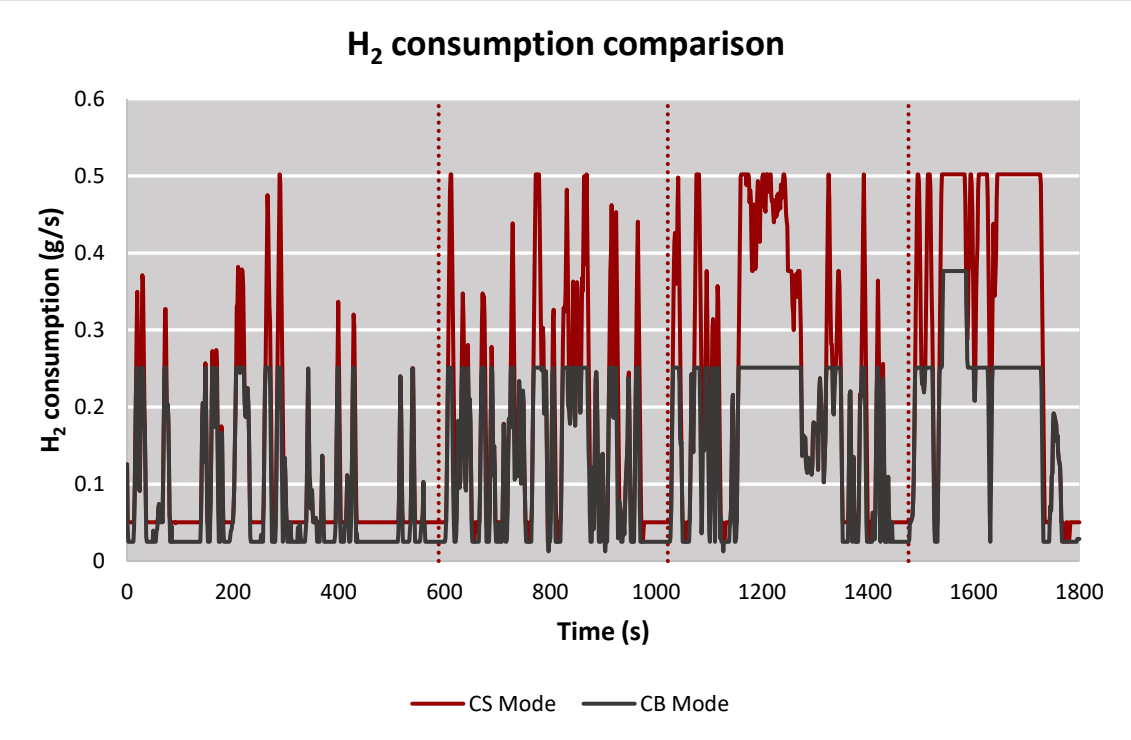


Figure 4.15: $H_2$ Consumption Comparison of different Energy Management Strategies for a Vehicle with 60 kW FC Stack Power, 40 kWh Battery Capacity and 5 kg of $H_2$ in its tank

Additionally, it is important to notice that, if not properly designed, one of the energy sources is consumed before the other when operating in CB mode, at which point the vehicle starts working in either CS or CD mode. In general, for simulations that target 15%, 10%, and 5% discharges of the battery per cycle, the energy content of the battery is used completely before the $H_2$ in the tank, meaning that the simulations switch to CS mode when the battery reaches a SoC of 0.25 until all the $H_2$ is used.

Before discussing the data obtained, it is important to highlight that simulations that feature a 60.3 kWh battery are unable to complete the CB simulation with a 15% battery discharge per cycle. This happens because 15% of the energy content of these batteries provides more energy that what is needed to complete a standard CS cycle. Therefore, these three specific simulations are not represented in the results.

Once the behavior of the LCV in CB mode is understood and analyzed, data is extracted from the simulations to compare it with the standard CD + CS modes. As the objective of the CB strategy is to maximize range, this is the first parameter to be compared. General trends are the same as they were for the CD + CS simulations. First, it is seen how more powerful FC stacks increase range due to the decrease in current density, showing an average increase of 1.94% each time the FC maximum power is increase by 20 kW. As in the first simulations, this improvement becomes less noticeable as the FC stack grows more powerful. Second, larger battery capacities increase range due to the larger amount of energy available in them, replicating the trend of the standard energy management simulations. Increasing the energy content in the battery by 20 kWh supposes an average increase in range of 11.4%. However, the real interest of these

simulations relies on evaluating how the change in battery discharge per cycle affects range. The following graphs shows the total range that each of the studied architectures can travel, with all the CB and CD + CS simulations represented and showing both the change in battery SoC per distance travelled. On the right, the CD + CS simulations are show, which represent the largest possible discharge of the battery due to its operation in CD mode. On the left, the CB simulations with ideal discharge are represented, showing the increase in range in this configuration. The rest of the graph represents the evolution in range as the discharge per cycle is minimized to target an optimal value.

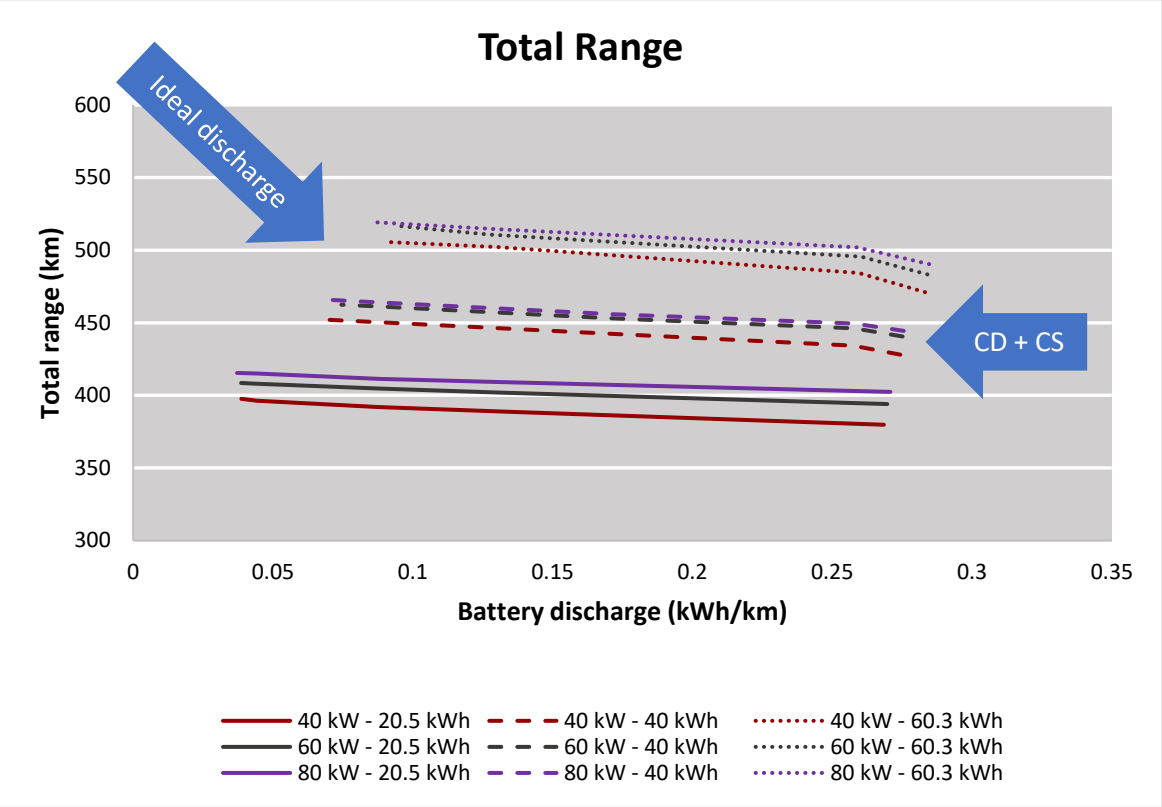


Figures 4.16: SoC Discharge and Range Comparison for all studied Architectures

Clearly, it is seen how a smaller discharge of the battery increases the range of the vehicle. This happens because decreasing the change in SoC towards the optimal value (lower than 5% for all architectures) increases the number of cycles that the vehicle can travel in CB mode. This strategy, that reduces $H_2$ consumption, allows the vehicle to travel for a longer distance by only changing its energy management strategy. Therefore, managing energy in order to make the vehicle operate in CB mode as much as possible is key in order to achieve minimum energy consumption. Simulations with high battery discharges allow the LCV to function with the CB strategy for a limited amount of time, while decreasing this parameter makes the vehicle able to travel a larger number of cycles in this mode. To achieve the maximum possible range, the final set of simulations target an optimal change in battery SoC, permitting the LCV to stay in CB mode for an average of 96.76% of the time. An example of this trend is portrayed in Figure 4.18, which represents the changes in range distribution for a vehicle with an FC power of 60 kW and a battery capacity of 20 kWh:

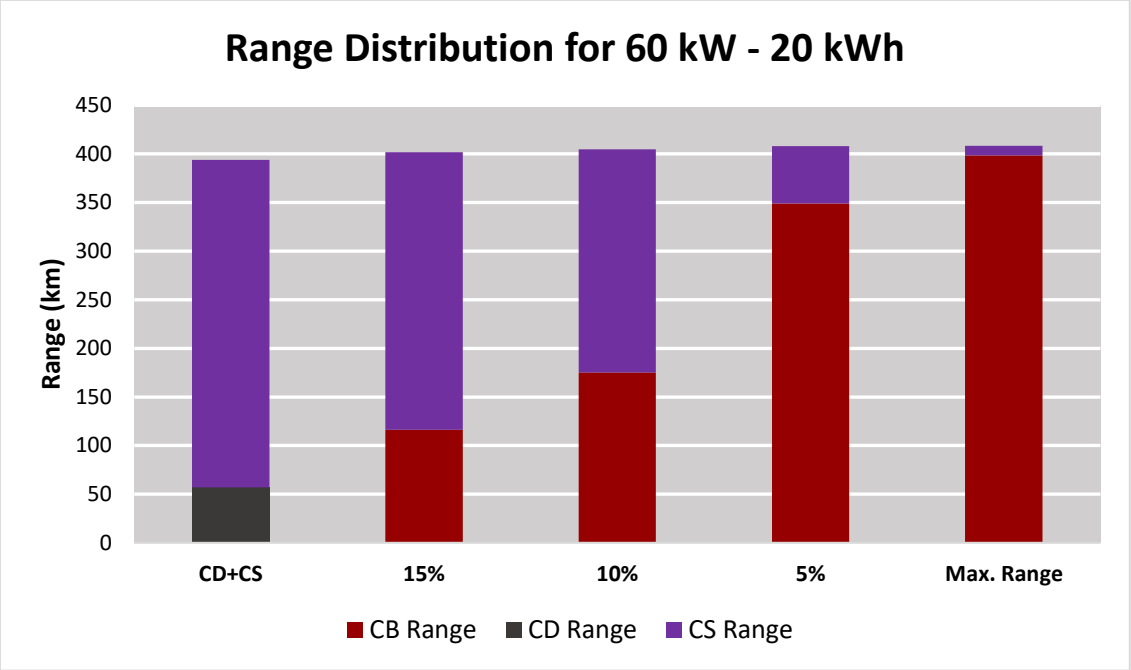


Figure 4.17: Range Distribution for all Energy Management Strategies

The implementation of the CB control strategy proves effective in terms of range for all the contemplated simulations. Table 7 summarizes the results obtained:

| Architecture | Optimum discharge per cycle | Range in CD + CS mode (km) | Maximum range in CB mode (km) | Change |
|---|---|---|---|---|
| 40 kW – 20 kWh | 0.0438 | 379.78 | 397.63 | 4.70% |
| 40 kW – 40 kWh | 0.0377 | 428.03 | 452.32 | 5.67% |
| 40 kW – 60 kWh | 0.0334 | 471.07 | 505.59 | 7.33% |
| 60 kW – 20 kWh | 0.0425 | 394.04 | 408.53 | 3.68% |
| 60 kW – 40 kWh | 0.0418 | 440.57 | 462.44 | 4.97% |
| 60 kW – 60 kWh | 0.0369 | 483.28 | 516.72 | 6.92% |
| 80 kW – 20 kWh | 0.0418 | 402.40 | 415.46 | 3.24% |
| 80 kW – 40 kWh | 0.0368 | 444.42 | 466.14 | 4.89% |
| 80 kW – 60 kWh | 0.0331 | 490.37 | 519.14 | 5.87% |

Table 7: Range Evolution in CB Mode for all studied Architectures

Increases in range are linked to a decrease in energy consumption, as explained when analyzing the CD + CS simulations. The graph shown below represents the total energy consumption per distance travelled of the vehicle, with includes electricity from the battery and energy produced with $H_2$:

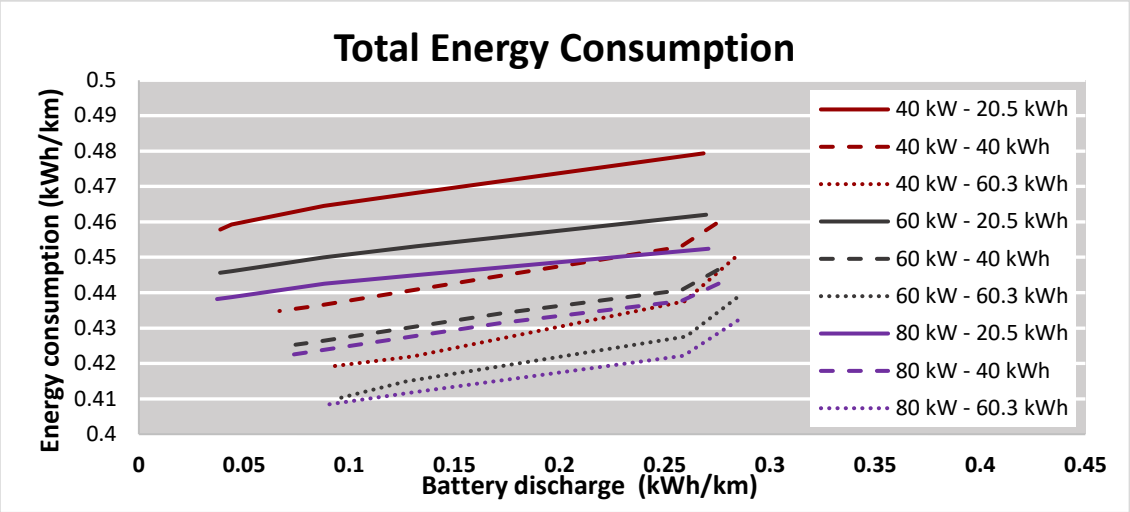


Figure 4.18: Battery Discharge and Consumption Comparison for all Architectures in CB mode

Here, a series of trends for the three contemplated variables are observed. First, increases in the FC stack power decrease total energetic consumption in all cases. This is the same evolution that was seen for CD + CS simulations, as more powerful FC stacks can operate at lower current densities, which then leads to an increase in efficiency and a decrease in $H_2$ consumption. Increasing the FC power by 20 kW results in an average decrease in consumption of 1.89%, with this decrease being larger for smaller FC stacks. Next, it is seen how increases in battery capacity decrease overall energy consumption. Batteries with a large energy content, at the cost of increasing the overall mass of the vehicle, are able to provide more energy, making the system less dependent on $H_2$ and therefore reducing overall consumption. An example of this behavior in shown in the following figure, where the effect of changing the energy content of the battery on the consumption of $H_2$ is shown.

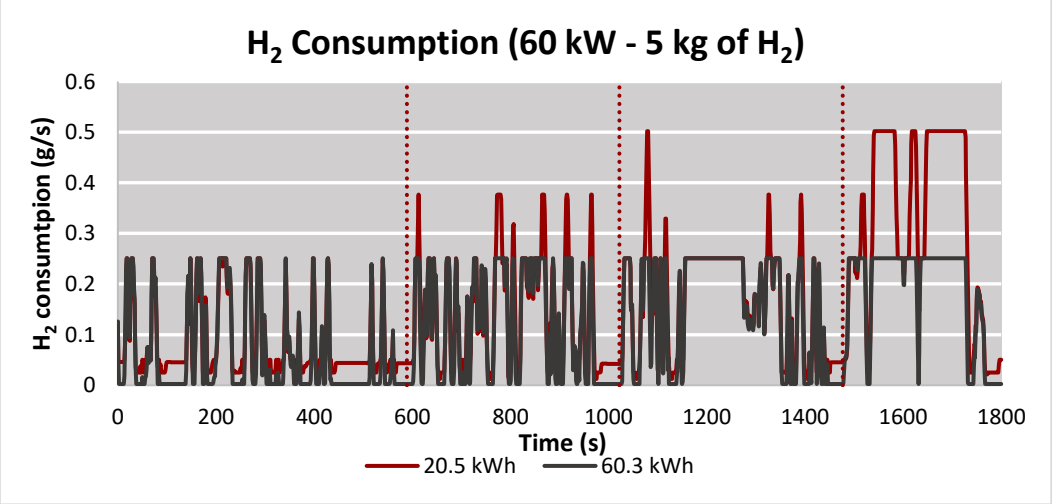


Figure 4.19: Variation in $H_2$ Consumption when changing Battery Capacity

Clearly, it is seen how larger batteries allow the vehicle to consume $H_2$ at a steadier rate with smaller peaks in all sections of the driving cycle. On average, total energy consumption is decreased by 3.13% when the battery capacity is increased by 20 kWh. Finally, decreases in battery discharge allow the vehicle to operate in CB mode for a larger amount of time, during which energy consumption is smaller than in CS mode. To synthesise the results, Table 8 is presented to help compare the consumption data for the CD + CS and the CB simulations:

| Architecture | Consumption in CD + CS mode (kWh/km) | Minimum consumption in CB mode (kWh/km) | Change |
|---|---|---|---|
| 40 kW – 20 kWh | 0.479 | 0.458 | -4.49% |
| 40 kW – 40 kWh | 0.459 | 0.435 | -5.37% |
| 40 kW – 60 kWh | 0.450 | 0.419 | -6.83% |
| 60 kW – 20 kWh | 0.462 | 0.446 | -3.55% |
| 60 kW – 40 kWh | 0.446 | 0.425 | -4.73% |
| 60 kW – 60 kWh | 0.438 | 0.410 | -6.47% |
| 80 kW – 20 kWh | 0.452 | 0.438 | -3.14% |
| 80 kW – 40 kWh | 0.443 | 0.422 | -4.66% |
| 80 kW – 60 kWh | 0.432 | 0.408 | -5.54% |

Table 8: Consumption Evolution in CB Mode for all Architectures

In order to make data more visual and help compare all vehicles with each other, the following graphs that match each vehicle payload with their range and consumption are presented:

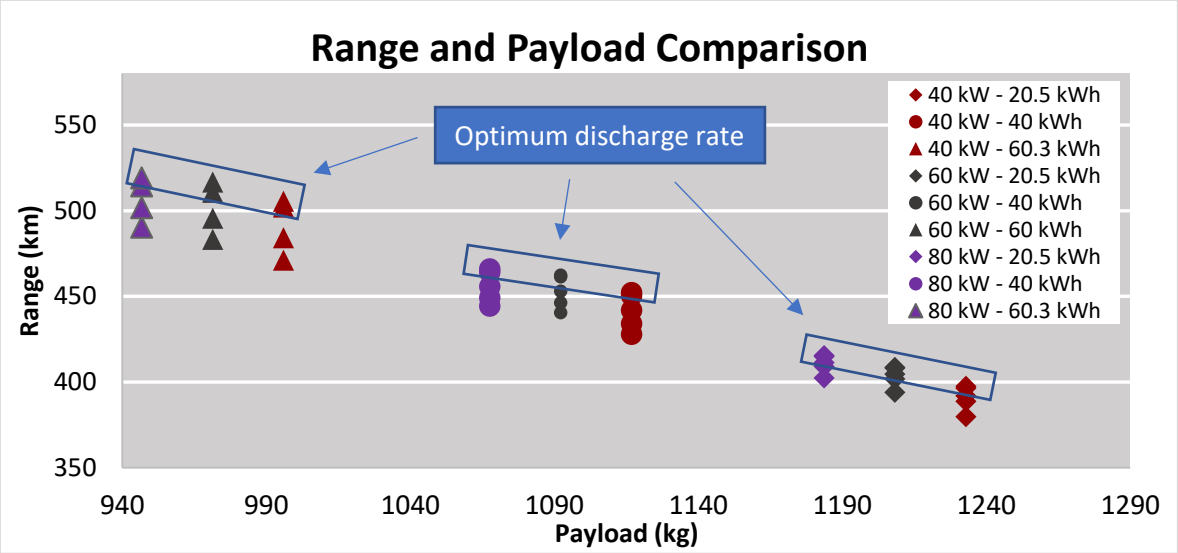


Figure 4.20: Range for all Architectures in CB mode

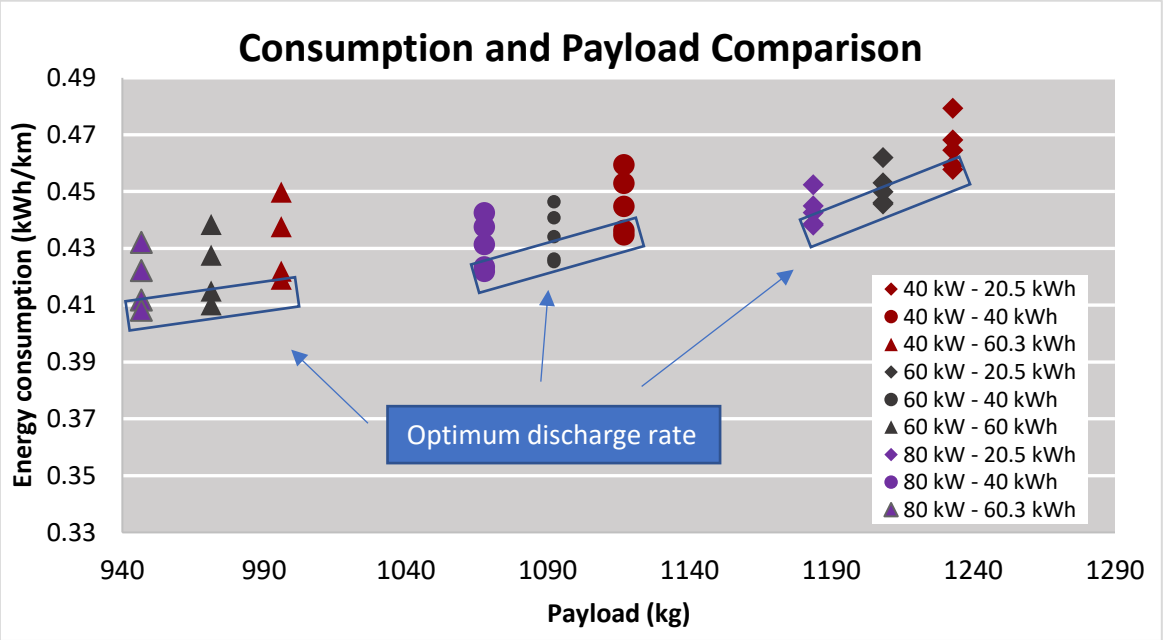


Figure 4.21: Consumption for all Architectures in CB mode

These graphs are useful as they allow to show information in a simple manner without having an overwhelming amount of data displayed. Vehicles are sorted in payload groups. Clearly, vehicles with less powerful FC stacks and smaller batteries have a smaller mass, and therefore a larger payload. These vehicles, due to their limited energetic resources, present the smallest ranges, while more inefficient FC systems and small batteries also cause larger consumptions. Heavier vehicles, which possess smaller payloads, have larger ranges and smaller consumptions due to their powerful and efficient FCs and the high energy content of their batteries. The vertical groups in these graphs include vehicles with the same architectures, but with different energy management strategies, being the designs with maximum range those with the close to

optimal CB mode. General trends are seen in the figures below, which represent the changes in range and consumption for a fixed FC stack and battery:

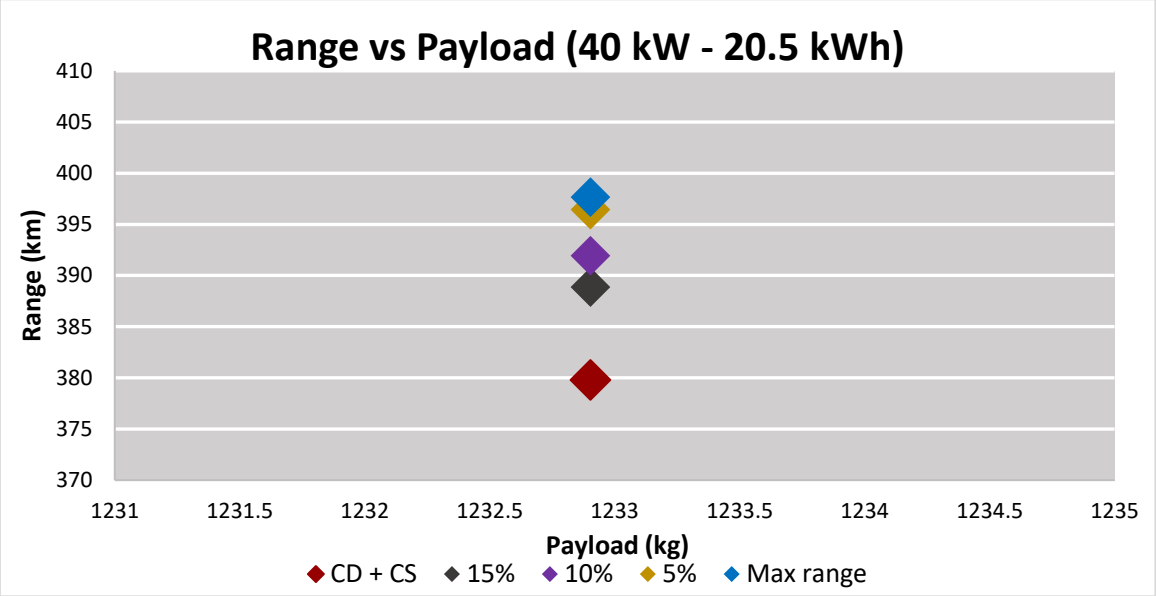


Figure 4.22: Range for different Energy Management Strategies

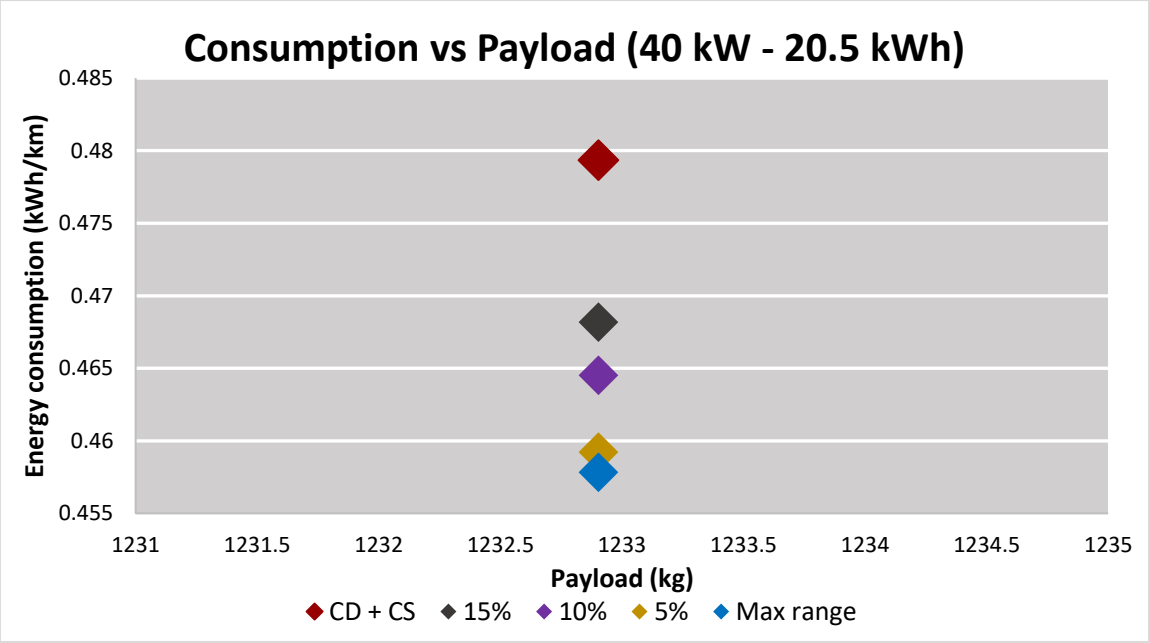


Figure 4.23: Consumption for different Energy Management Strategies

Here, it is seen how, without needing to modify any of the components of the vehicle, the range increases while the consumption falls when the CB energy management strategy is implemented and optimized to provide maximum range. Considerable improvements are seen when comparing the CD + CS results with the less strict CB control strategies, while changes in these categories become smaller as the ideal battery discharge rate per cycle is approached.

In conclusion, this section shows that implementing a CB strategy improves the range and consumption values for all architectures contemplated for this LCV without needing to change any of the vehicle components. If performance is to be optimized, the energy management

system should implement a CB strategy adjusted to allow the vehicle to operate using both the FC and the battery for the longest amount of time possible. Again, as in the last section of this BSc thesis, the use of a CB mode optimizes range and consumption specifically. However, if other parameters such as cost or environmental impact are evaluated, it is possible that the conclusion could be different, as the CD + CS modes could provide more flexibility than the CB strategy in different aspects. For instance, if cost is evaluated, due to $H_2$ having a higher price currently than electricity, it is possible that a standard CD + CS operation would be less expensive for users of the LCV.

## 4.3 LIFE CYCLE ASSESSMENT

Once the performance of the vehicle is studied, an assessment with the objective of evaluating the environmental impact of the proposed architectures is carried out. As explained previously, GHG-100 are the emissions that the study focuses on, while an expected life of 240 000 km for the FCV is also a determining factor of the results. As explained in the methodology section, the LCA is composed of three stages: the fuel production cycle, the vehicle production cycle, and the operation cycle. Each of these is responsible for a set of emissions and, when analyzed together, show the total GHGs emitted throughout the life of the vehicle. Due to the large number of architectures, it is inefficient to apply the LCA results for every simulation. Therefore, the study focuses on four simulations that feature the CB energy management strategy: a conservative architecture, featuring a 40 kW FC and a 20.5 kWh battery, an ambitious one, with an 80 kW FC and 60.3 kWh battery, and intermediate solutions that approach a traditional FCV configuration, although with a bigger battery (80 kW FC and 20.5 kWh) and an FCREx configuration (40 kW FC and 60.3 kWh battery). To simplify, the 20.5 kWh and 60.3 kWh batteries will be referred to as 20 kWh and 60 kWh respectively.

### *4.3.1 Fuel production cycle*

The LCV is powered by two energy sources: electricity, provided by the battery, and $H_2$, used in the FC to power the electric motor. The method used to obtain these emissions is detailed in Section 3.3.

For electricity, data is obtained using the CML-IA database, which specifies the GHG emissions per kWh of electricity. This information is given for all the three energy trends scenarios (ETS, NI, SI), meaning that each of the studied years counted with three different possible values. Therefore, to represent the information accurately, the average value between the three is calculated and the deviation is represented through error bars in Figure 4.25.

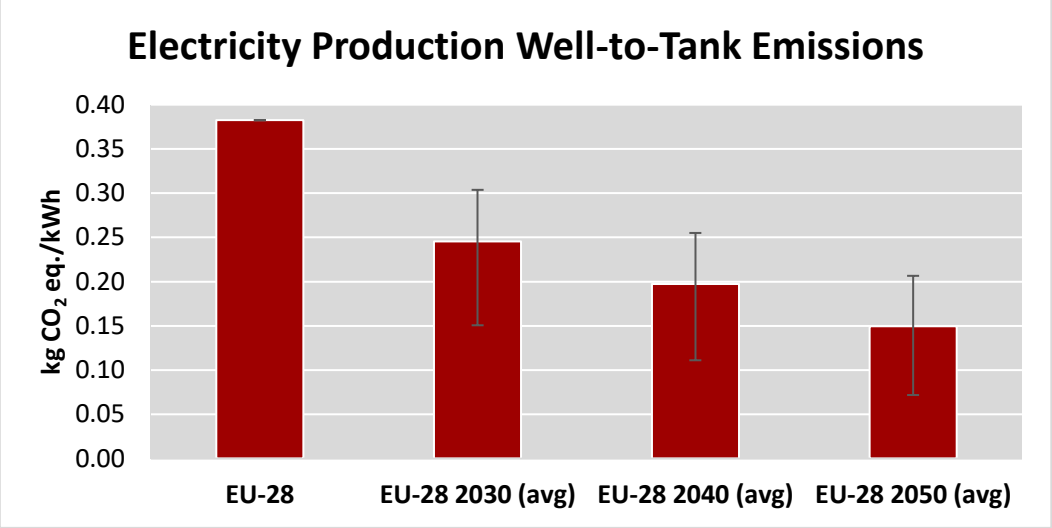


Figure 4.24: Electricity Production Well-to-Tank Emissions for all the Scenarios

On average, it is expected that emissions caused by electricity production will be reduced by over 60% in 2050 due more renewable energy mixes expected in Europe. In the figure, large deviations are seen in error bars, due to the ETS scenario being very conservative while the SI trend shows a more aggressive change.

This information can then be applied to the mentioned vehicles. To do so, the average electric energy used per km throughout the driving cycle is calculated, considering an electric energy loss of 15% in the battery recharge processes [33].

| Architecture | Electric energy to the vehicle (kWh/km) | Electric energy consumed from the grid (kWh/km) |
|---|---|---|
| 40 kW – 20 kWh | 0.039 | 0.045 |
| 40 kW – 60 kWh | 0.089 | 0.105 |
| 80 kW – 60 kWh | 0.037 | 0.044 |
| 80 kW – 60 kWh | 0.087 | 0.102 |

Table 9: Electricity consumed to power different FCV Architectures

This information, alongside the expected distance that the vehicle will cover, provides the emissions caused by the production of electricity throughout the life of the FCV.

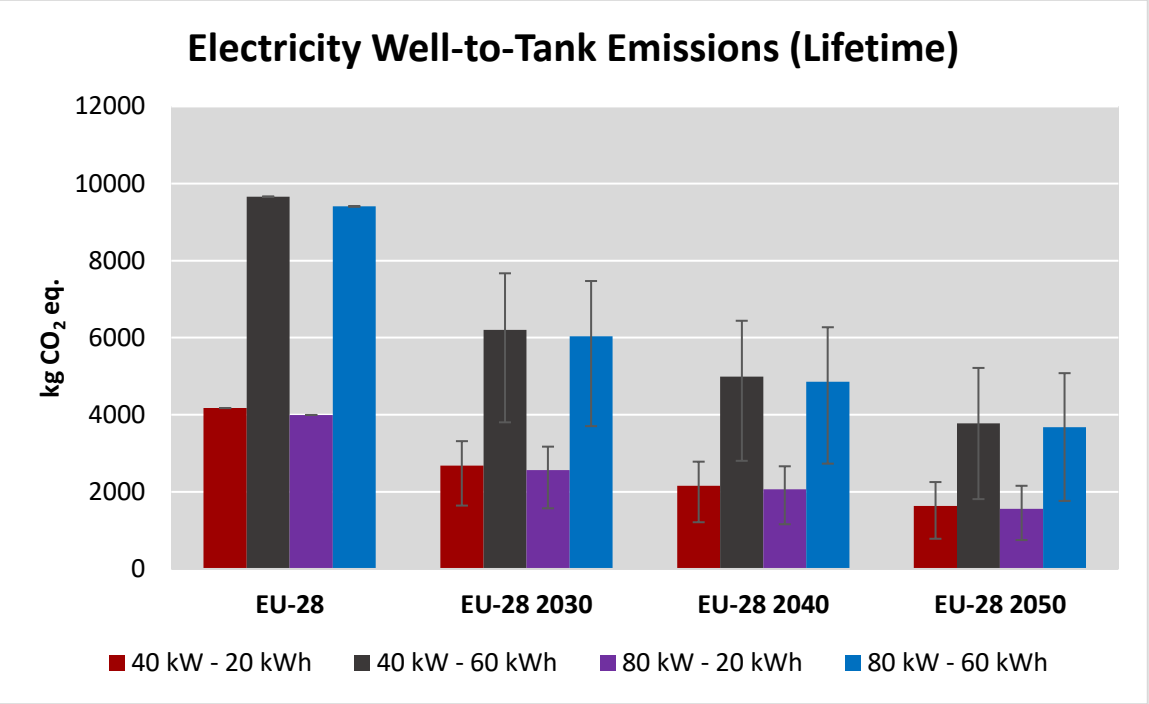


Figure 4.25: Electricity Production Emissions per Lifetime for all the Scenarios

Due to the difference in the energy content in the batteries, those with smaller capacities require less electricity to operate, and therefore present smaller GHG emissions. Changing a 20 kWh battery for one with a capacity of 60 kWh while maintaining the rest of the components constant implies an average increase of 133.4% in GHG emissions.

The second and main fuel in FCVs is $H_2$. As explained in this BSc thesis, the future of this energy source is quite uncertain, as it is affected by many different factors such as its demand, its method of production, the NG future production and the origins of biogas feedstock. Therefore, a set of different scenarios must be considered, with uncertainties represented as error bars. Using the GREET software, emissions caused to produce $H_2$ with every method are calculated for all of the energy mixes considered. With these, different scenarios are constructed, considering the proposed $H_2$ production scenarios, the different compression possibilities, and the future developments of natural gas. The effect of all of these variables is analyzed separately in order to understand the different results and explained trends.

- *$H_2$ production scenarios*

  As mentioned when describing the methodology of this project, two $H_2$ production trends are contemplated: one dominated by water electrolysis, and another with a majority of the fuel coming from SMR. The difference between these two scenarios is the main focus of this section, as it is key to compare the difference in emissions from embracing one strategy or the other.

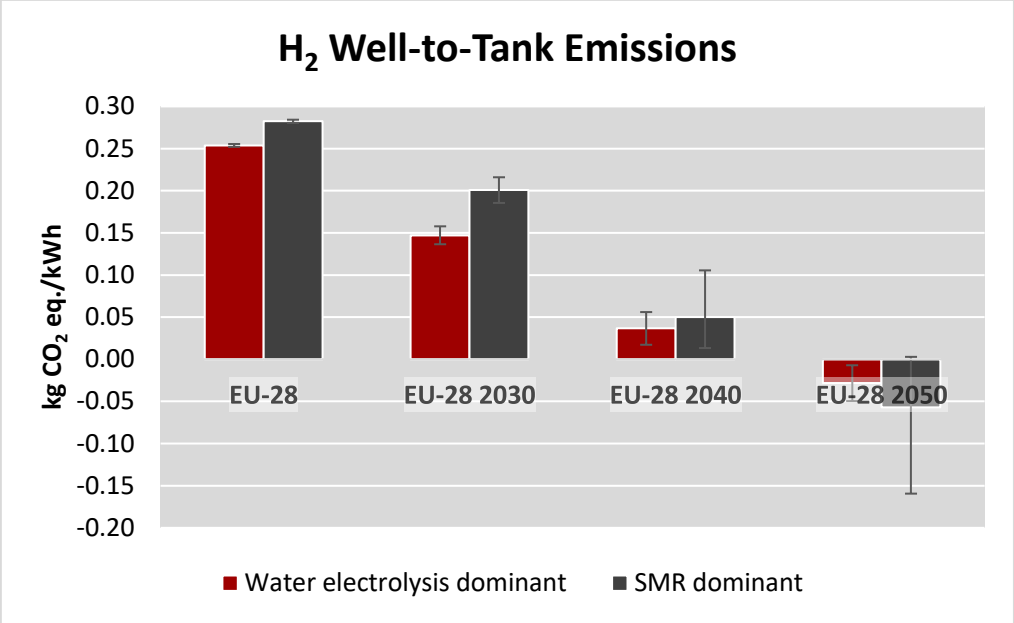


Figure 4.26: $H_2$ Well-to-Tank Emissions Comparison for different $H_2$ Production Trends

These results will function as the base to obtain all the results for this part of the study. In general, a clear trend of reduction is seen for both proposed scenarios. This is due to the energy mixes becoming more reliant on renewable energy, and therefore emissions in all the steps of $H_2$ production are reduced. For the earlier years, it is seen how the water electrolysis dominant scenario presents lower emissions. This would have been easy to infer, as this trend relies mainly on electricity to produce $H_2$, which ire more environmentally friendly than reforming $CH_4$ and releasing $CO_2$ to the atmosphere. However, when looking more into the future, it is seen how the SMR dominant scenario presents lower emissions. This is due to the increase in biogas in the NG share. Biogas is the only source from which $H_2$ can be produced with a balance of negative emissions. As the SMR dominant focuses mainly on this process, a large amount of biogas is expected to be used in this scenario, and therefore the average well-to-tank emissions for this scope could produce more negative emissions than the other scenario. For the remaining sections of this study, an average scenario between these two is calculated, with the deviation included in the represented error bars.

- *NG scenarios*

Two main natural gas trends are considered: the STEPS scenario, which proposes a conservative reduction of NG consumption alongside a small rise in biogas, and the SDS scenario, which targets a large decrease in NG use and an increase in biogas share that reaches over 40% of the total gas produced in the year 2050. As seen when analyzing the different $H_2$ production trends, larger quantities of biogas help the overall well-to-tank emissions. This statement is proven by the information shown in Figure 4.28.

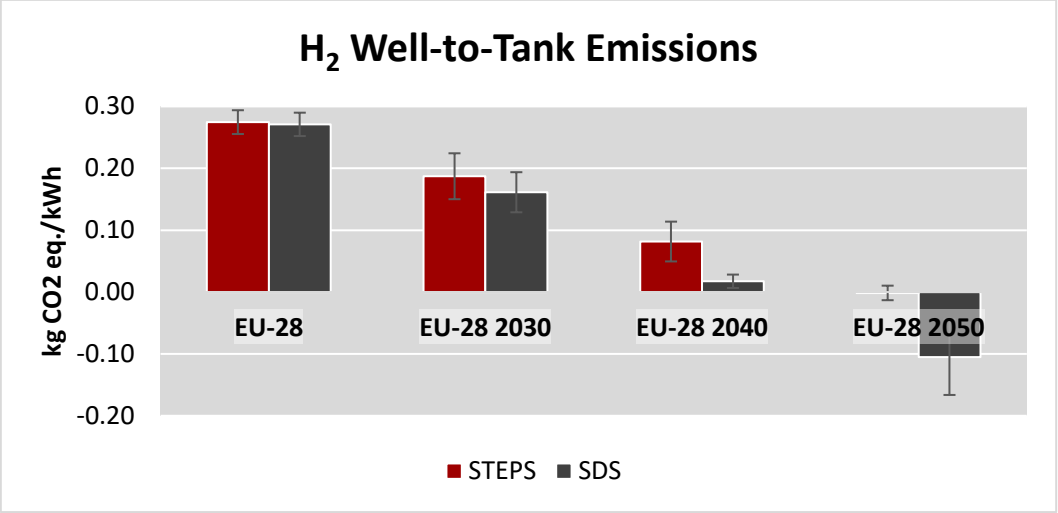


Figure 4.27: $H_2$ Well-to-Tank Emissions Comparison for different NG Trends

Again, the influence of the composition of NG is proven. Even for the earlier years, when there is not an extreme difference between both scenarios, it is shown how increasing the amount of $H_2$ produced through biogas can help reduce GHG impact. This difference becomes more noticeable as time advances. For instance, in the year 2050, the average expected emissions for $H_2$ production can vary from -0.001 kg $CO_2$ eq./kWh down to an impressive -0.105 kg $CO_2$ eq./kWh when comparing both scenarios.

- *$H_2$ compression scenarios*

Due to its extremely low density, it is critical to compress $H_2$ before its distribution and at refueling stations. For the former process, GREET contemplates two possibilities when $H_2$ is produced via electrolysis: either compressing using the energy from the mix or utilizing renewable energy. As it is impossible to know how this aspect of production is going to develop in the upcoming years, both possibilities are considered and represented in Figure 4.29 in an average $H_2$ production scenario.

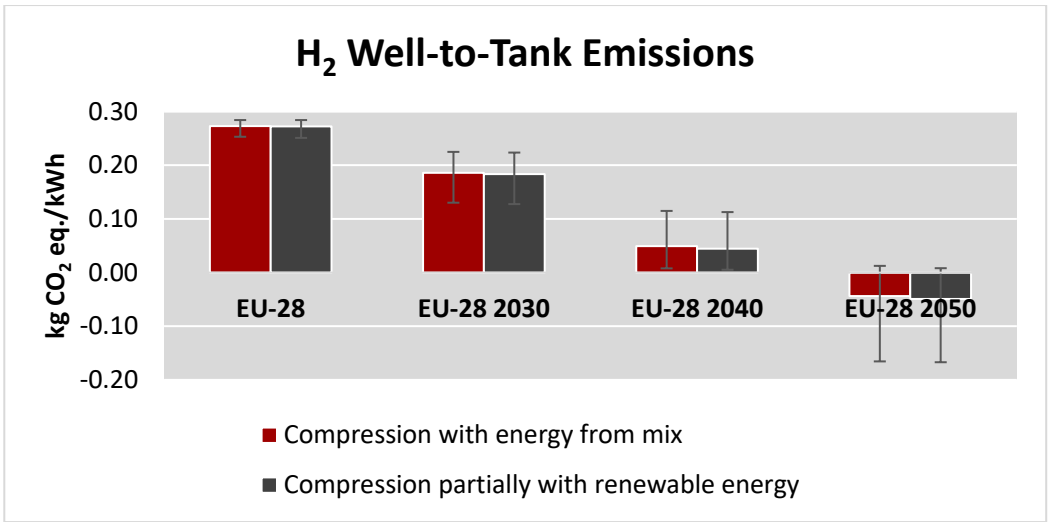


Figure 4.28: $H_2$ Well-to-Tank Emissions Comparison for different $H_2$ Compression Strategies

It is seen how this variable is the less determining of them all, as the difference between bars for the same year in minimal. This is due the first compression of $H_2$ only representing a small fraction of the process, and therefore the variation of this trait is not important when looking at the bigger picture.

Once all the different trends are comprehended, the well-to-tank data extracted is used to estimate the $H_2$ well-to-tank emissions of each of the considered LCVs. Again, the average value between all the different combinations of the previously mentioned scenarios is extracted, with the variations represented as error bars.

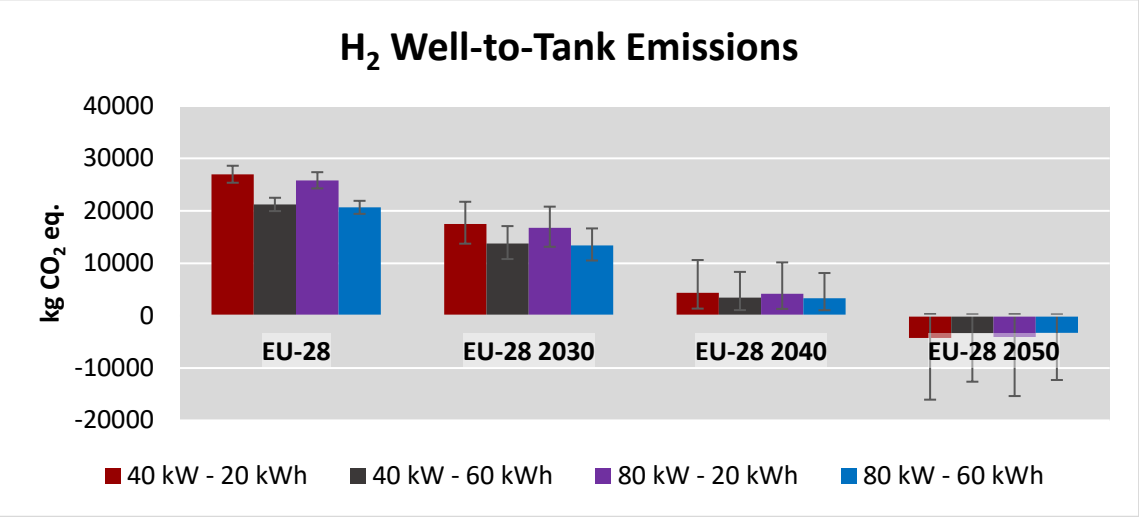


Figure 4.29: $H_2$ Production Emissions per Life

Two different trends can be analyzed from this figure. First, as expected, the evolution in time reduces GHG emissions due to two main factors: the increase of renewable energy present in the European mix and the increment of biogas available as the years pass. The former helps diminish the emission values, mainly in processes like SMR treatment or $H_2$ compression, while increasing the share of biogas rises the amount of negative emissions, to the point where it is expected that negative emissions for $H_2$ production can be reached in 2050. Second, if the different vehicles are to be compared, it is seen how those with bigger components produce less emissions associated with $H_2$. This trend is directly linked to the $H_2$ consumption of each vehicle. As studied when exploring the simulation results, more powerful FC stacks can operate with smaller current densities, making the vehicle more efficient and therefore reducing consumption. A vehicle with a lesser consumption requires less $H_2$ throughout its life, and therefore reduces its carbon footprint. It is important to point out that, for the year 2050, due to the expected negative emissions, smaller vehicles will present less overall $H_2$ production emissions as they will need more fuel to function.

Therefore, knowing the well-to-tank emissions associated with electricity and $H_2$, the total energy production values can be produced, which reveal the emissions needed to produce all the energetic resources that each of the architectures need during their expected life.

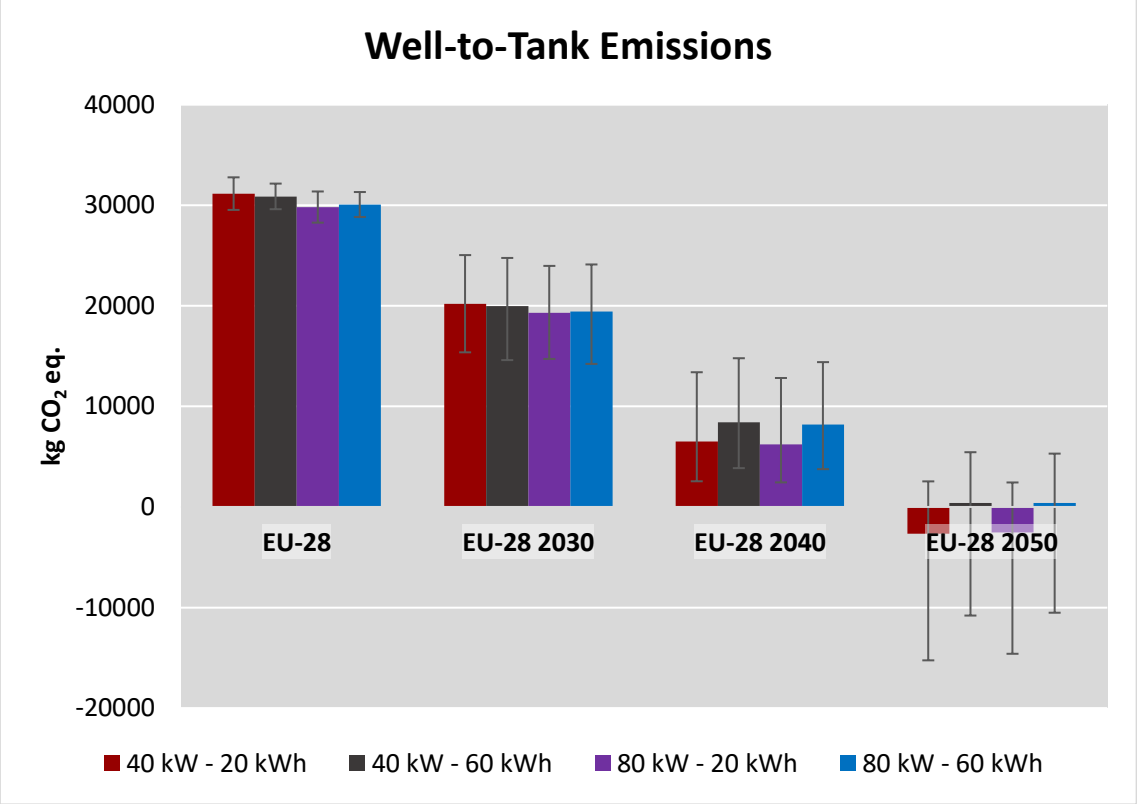


Figure 4.30: Energy Well-to-Tank Emissions per Life

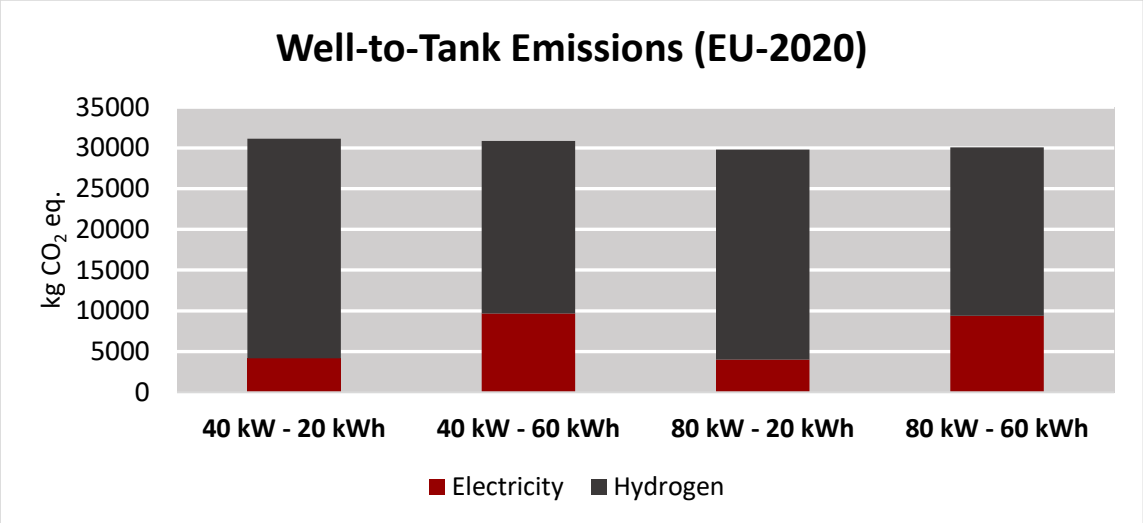


Figure 4.31: Energy Well-to-Tank Emissions per Life in EU-2020 Scenario

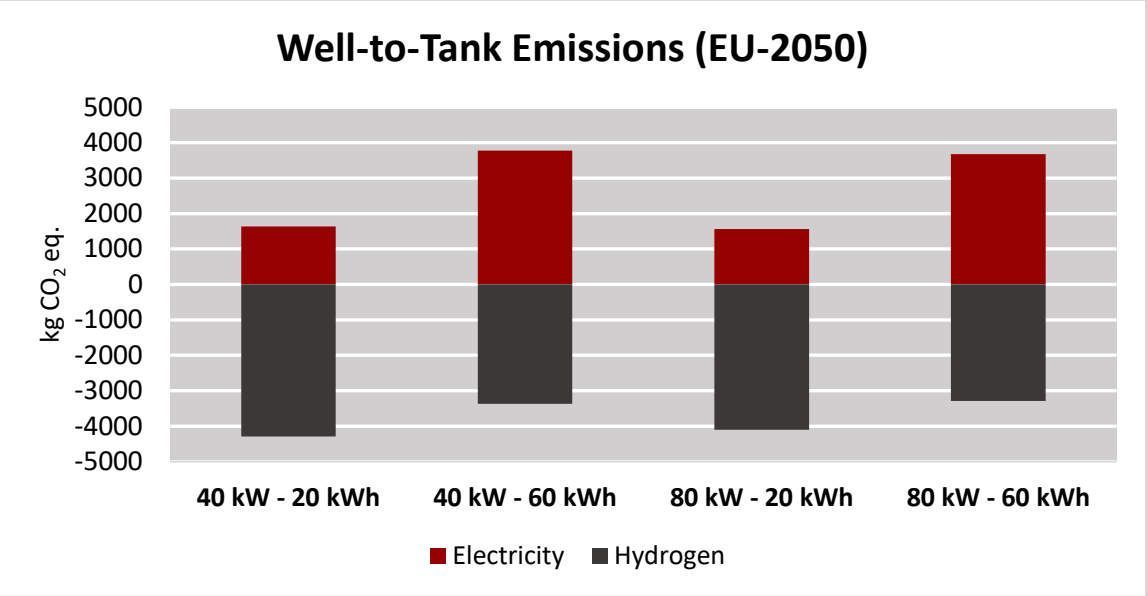


Figures 4.32: Energy Well-to-Tank Emissions per Life in EU-2050 Scenario

Referring to the different energy mixes, the well-to-tank emissions follow a clear trend, as a larger quantity of renewables present in these mixes reduce emissions in the production of both energy sources. However, trends do seem to change when studying the emissions of the different architectures. For the first years, it is seen how vehicles with smaller FC power stacks imply more well-to-tank emissions due to increases in $H_2$ consumption and, therefore, a larger amount of $H_2$ needed to power the vehicle. This is proven by Figure 4.32, which shows that, in the year 2020, the production of $H_2$ would be responsible for just under 27 000 kg $CO_2$ eq. for the 40 kW – 20 kWh vehicle, which is 6 000 kg $CO_2$ eq. more than what the 80 kW – 60 kWh architecture emits. Even if the former does require less electricity in its battery, it still does not compensate the well-to-tank $H_2$ emissions. On the other hand, when focusing on the more distant years, a change in this trend is observed due to the drastic change in $H_2$ production emissions. At this point in time, with an important presence of renewable energies and a large amount of biogas available, $H_2$ emissions become negative, which is even more noticeable in vehicles with more inefficient consumption. Because of this, architectures with small batteries and high reliance on $H_2$ produce less GHGs throughout their lives, making the 40 kW – 20 kWh architecture the one with the least expected well-to-tank emissions. It is important to notice the large errors bars present in the preceding figure. As explained before, future scenarios are uncertain, especially those involving fuels that are in early stages of development like $H_2$. Its demand and production methods as well as the other possible changes explained in this section make the future be somewhat unpredictable, causing the possible uncertainties represented in the graphs.

### *4.3.2 Vehicle manufacturing cycle*

The next part of the LCA that is explored is the vehicle manufacturing cycle, which studies the GHG emissions cause by the production of the different components of the vehicle. For the case of this FCV, components are grouped into six main groups: the FC system, the $H_2$ tank, other mechanical components, the battery pack, the ADR process and a series of fluids needed for the

correct operation of the FCV. For fluids as well as for tires, a number of replacements must be considered taking into account the expected life of the LCV.

With the use of the GREET software as well as information from the GT-Suite simulations, the mass of each of the components is extracted, as well as the GHG emissions expected per kg of each component in each of the proposed energy mixes. With this data, the GHG emissions related to the manufacturing of each vehicle are obtained and presented in Figure 4.34.

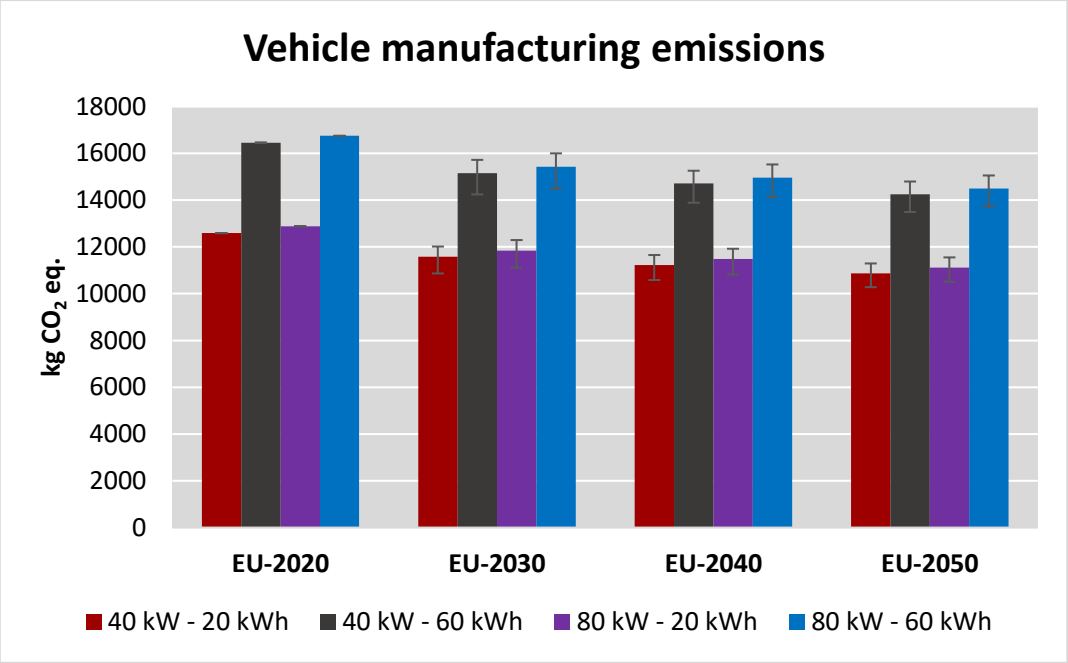


Figure 4.33: Vehicle Manufacturing Emissions for all Architectures

As in the well-to-tank results, two different trends can be observed: the change in GHG emissions between each of the studied years as well as the variation of this value between the different architectures.

First, a decrease in emissions is observed for future scenarios in every case. This, as in the well-to-tank cycle, is due to the changes in energy mix, which become more reliant on renewables. However, this change is not as drastic as the one seen in the previous cycle as, on average, emissions are reduced by 13.6% from the present to the year 2050 for all architectures.

As for the different vehicles, visible differences are observed and remain somewhat constant throughout all scenarios. Cleary, the difference in the energy content in the battery is the determining aspect in this matter. Both for architectures with 40 kW and 80 kW FC powers, a significant change in the manufacturing cycle emissions is seen when changing from a 20.5 to a 60.3 kWh battery due to the increase in the mass of the battery needed to increase its capacity. On average, the difference in emissions between LCVs with the same FC power but different battery capacities is 30.6%. In order to identify the source of these emissions, some of the previously displayed data can be segmented into the different groups of components of the vehicles with the following results:

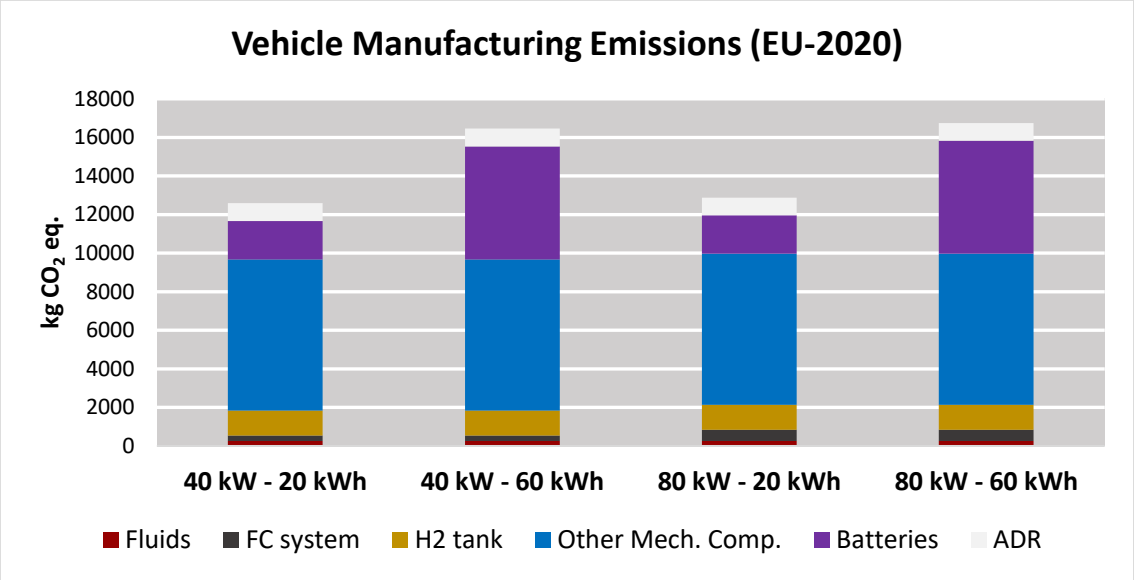


Figure 4.34: Segmented Vehicle Components Manufacturing Emissions in EU-2020 Scenario

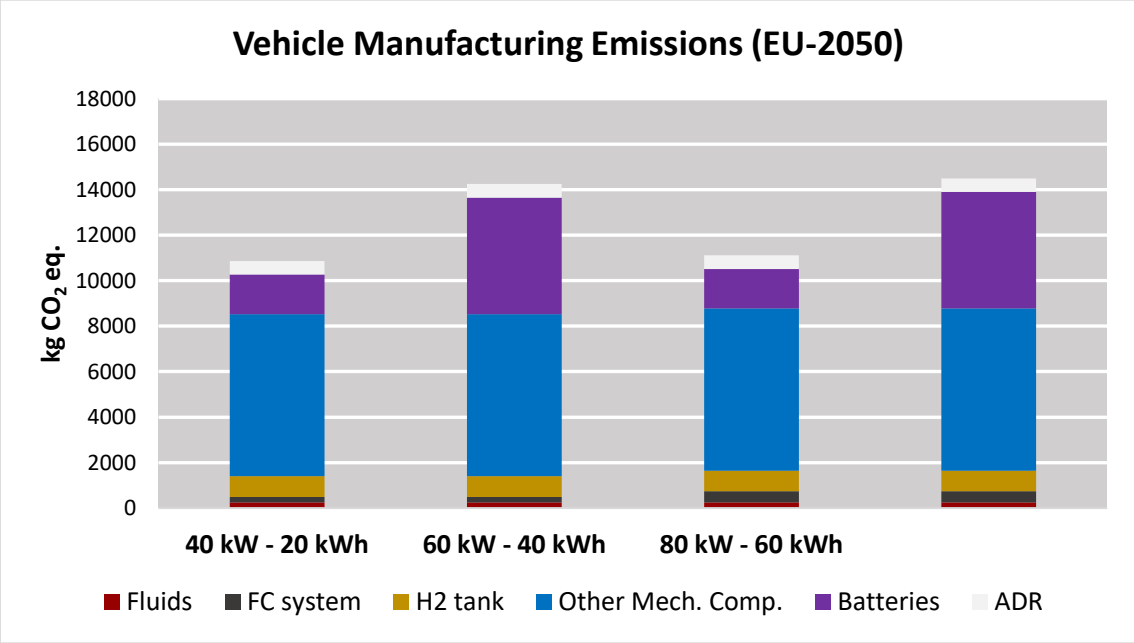


Figure 4.35: Segmented Vehicle Components Manufacturing Emissions in EU-2050 Scenario

It is clear, both for the earliest and the latest possible scenarios, that the majority of the vehicle manufacturing emissions are associated with the production of mechanical components, followed by batteries, ADR and fluids. Mechanical components for all vehicles are similar, and therefore, the difference in battery capacities are the factor that provokes the difference in emissions which explains the previously discussed trends. Furthermore, it is seen that the FC systems and the $H_2$ tank, which provide energy to the vehicle through $H_2$, cause significantly lesser emissions than the electric battery. Table 10 presents the percentage that each group represents of the total manufacturing emissions of each architecture on average for all the considered scenarios, which helps show the difference in the battery production emissions compared to the production of the FC system in this part of the life cycle:

| | Emissions associated with each group of components | | | |
|---|---|---|---|---|
| | 40 kW – 20 kWh | 40 kW – 60 kWh | 80 kW – 20 kWh | 80 kW – 60 kWh |
| Fluids | 2.16 % | 1.65 % | 2.11 % | 1.62 % |
| FC System | 2.30 % | 1.75 % | 4.49 % | 3.45 % |
| $H_2$ tank | 9.15 % | 6.99 % | 8.94 % | 6.87 % |
| Other Mechanical Components | 64.18 % | 49.01 % | 62.74 % | 48.17 % |
| Batteries | 15.94 % | 35.81 % | 15.59 % | 35.19 % |
| ADR | 6.26 % | 4.78 % | 6.12 % | 4.70 % |

Table 10: Vehicle Components Emissions Share in each Architecture

Therefore, if the objective is to minimize the environmental impact, the ideal solution for vehicle manufacturing emissions includes the smallest possible components, especially targeting the use of a small battery. Nevertheless, this would have an impact on the performance of the vehicle. Hence, to extract meaningful conclusions, both the well-to-tank, tank-to-wheel and vehicle manufacturing emissions must be put together and compared for each architecture.

### *4.3.3 Operation cycle*

In an FCV, $H_2O$ is the only product that is emitted from the vehicle during its operation. Therefore, this cycle, also known as tank-to-wheel, presents a very small number of emissions compared to conventionally powered LCVs, as $H_2O$ has a much smaller effective GWP than gases produced in diesel or gasoline ICEVs. Knowing the $H_2$ consumption of each vehicle from the CB simulations, the production of $H_2O$ can be calculated per distance and per life of the vehicle. For the three considered architectures, the results are as follows:

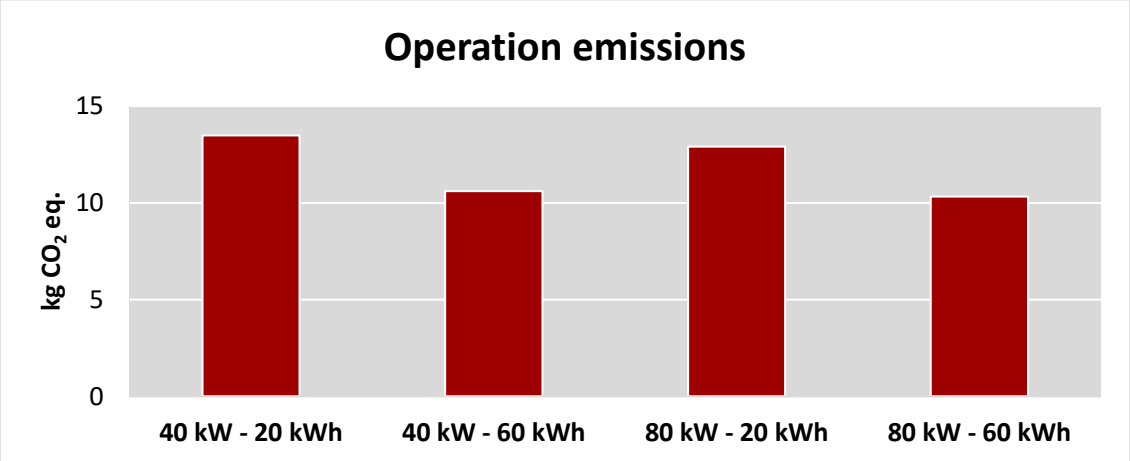


Figure 4.36: Tank-to-Wheel Emissions for all Architectures

Here, two main trends are observed when changing the components of the vehicle can be observed. First, increasing the capacity of the battery translates in a larger part of the operation being completed in CB mode, which, as stated previously, decreases $H_2$ consumption and, therefore, decreases $H_2O$ production. Second, increasing the maximum power of the FC stack allows the vehicle to operate with lower current densities, which causes a smaller use of $H_2$ and a lesser emission of $H_2O$. However, the importance of these results relies not on the comparison between architectures, but with the emissions caused by other parts of the life cycle. For instance, the 40 kW – 20 kWh produces around 13 kg $CO_2$ eq. during its operation, which is neglectable compared to the more than 30 000 kg $CO_2$ eq. associated with the well-to-tank cycle for this vehicle in the EU-2020 scenario or the 12 500 kg $CO_2$ eq. caused by the manufacture of this vehicle. This proves that FCVs are able to operate with almost zero emissions, which highlights one of its main advantages compared to other vehicles powered by carbon-based fuels.

### *4.3.4 Complete life cycle*

Finally, by obtaining the emissions for all the steps of the life cycle of each vehicle, a complete assessment can be made to determine how the environmental footprint varies between each architecture. The results of the combination of each of the different cycles is shown in the next figure:

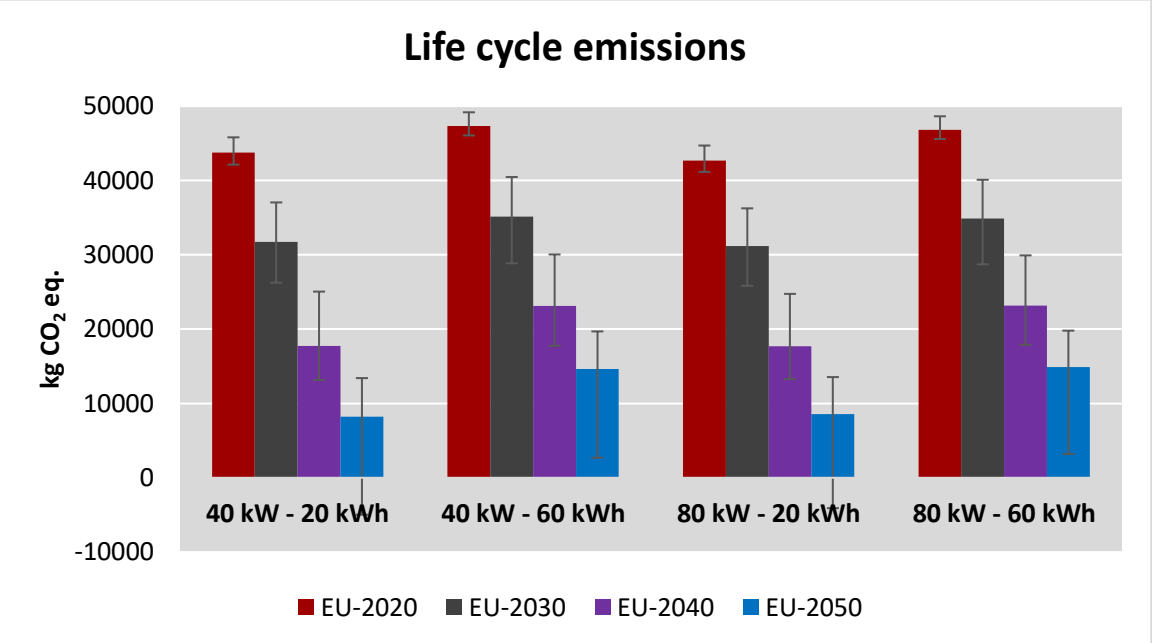


Figure 4.37: Life Cycle Emissions for all Architectures

Again, two clear tendencies can be detected: one related to the timeframe, and another focused on the simulated vehicles.

The evolution of GHG emissions throughout the years is as expected. A series of factors, like the development into less carbon-based energy mixes and the increase in biogas use, help decrease overall emissions in the life cycle of the LCVs. The change in environmental footprint is noteworthy in all vehicles, as supported by the in Table 11:

| | Change in GHG emissions from 2020 to 2050 | | | |
|---|---|---|---|---|
| | 40 kW – 20 kWh | 40 kW – 60 kWh | 80 kW – 20 kWh | 80 kW – 60 kWh |
| Absolute value (kg $CO_2$ eq.) | -35 521 | -32 671 | -34 116 | -31 920 |
| Percentage | -81.2 % | -69.0 % | -79.9 % | -68.2 % |

Table 11: Change in GHG Emissions for all Architectures between 2020 and 2050

The other tendency observed involves the different vehicle architectures. The data represented in Figure 4.38 shows that, when increasing the components of the vehicles, the overall life cycle emissions increase in every scenario, especially when battery capacity increases. In order to analyze this in detail, the bars are segmented into different sections to reveal the relationship between fuel production, vehicle manufacturing and operation in terms of emissions and represented in the following graphs.

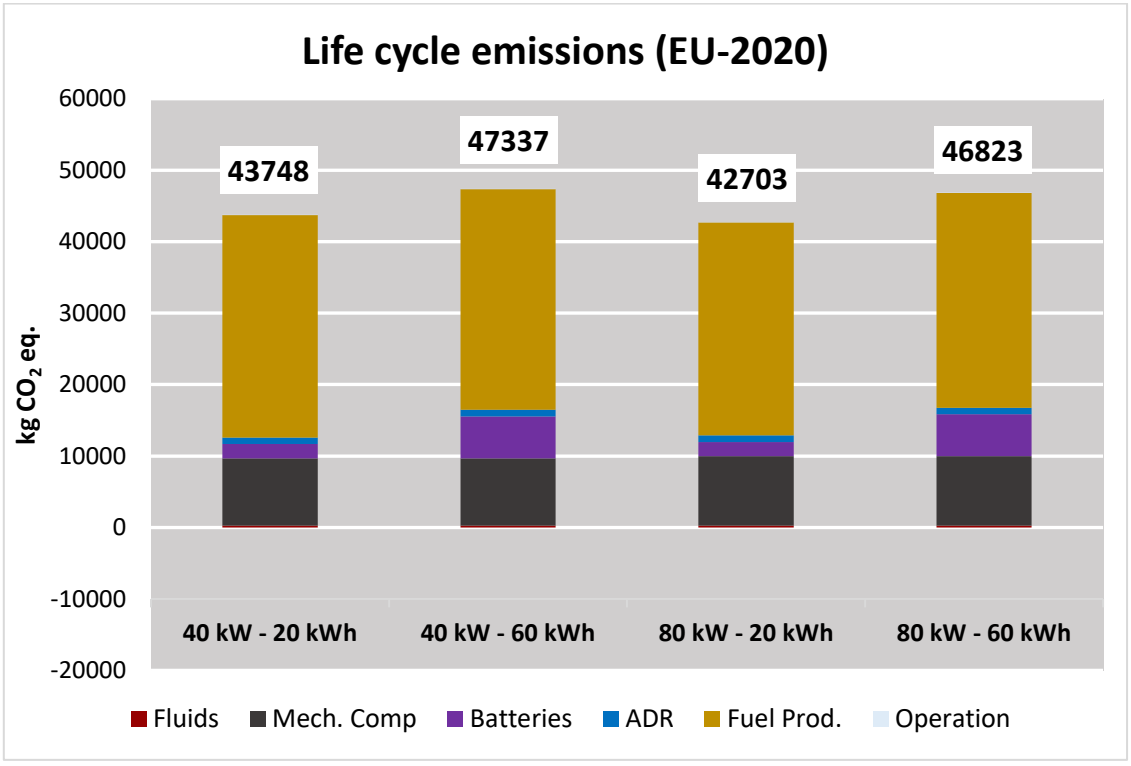


Figure 4.38: Life Cycle Emissions Segmentation for EU-2020 Scenario

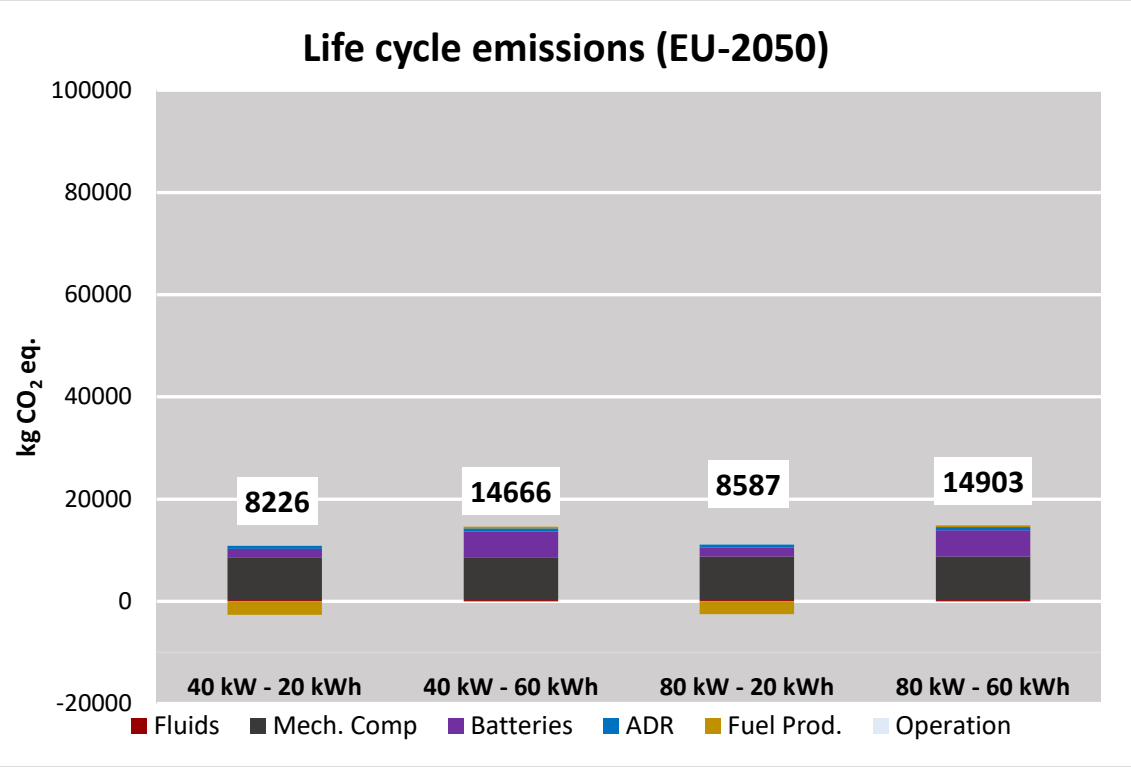


Figures 4.39: Life Cycle Emissions Segmentation for EU-2050 Scenario

These graphs clarify what occurs in the portrayed scenarios and explain the changes in emissions. Clearly, the main cause of differences in emissions between each architecture are the batteries. When comparing emissions in the same year, fuel production, mechanical components and all the other categories do not show a large difference between vehicles, but batteries do change drastically, causing the differences that are observed in the figure that represents all life cycle emissions. Therefore, changes in emissions from the most polluting architecture (80 kW – 60.3 kWh) to those with a 20.5 kWh battery are explored in Table 12, showing that the vehicle with an 80 kW FC does not show a large difference compared to one with a 40 kW FC in terms of emissions while showing a larger range and smaller consumption.

| Emission changes from an 80 kW – 60 kWh architecture | | | | |
|---|---|---|---|---|
| Scenario | 40 kW – 20 kWh | | 80 kW – 20 kWh | |
| | Absolute value (kg $CO_2$ eq.) | Percentage (%) | Absolute value (kg $CO_2$ eq.) | Percentage (%) |
| EU-2020 | 3 079 | 7.0 % | 4 122 | 8.8 % |
| EU-2030 | 3 111 | 8.9 % | 3 711 | 10.6 % |
| EU-2040 | 5 423 | 23.4 % | 5 445 | 23.5 % |
| EU-2050 | 6 680 | 44.9 % | 6 318 | 42.4 % |

Table 12: Emissions Changes from an 80 kW – 60 kWh Architecture

In conclusion, it is determined that vehicles with large batteries, which show the best performances in the GT-Suite simulations, produce more GHG emissions throughout their life cycle than those with a smaller energy content in their battery. Therefore, if the objective is to minimize environmental impact while maintaining a decent performance, an interesting solution is considering a medium-to-large FC stack and a small battery. By using this information, a comparison can be made with other LCVs currently in the market, determining this way the viability of FCVs.

### *4.3.5 Vehicles comparison*

In the methodology section, it is explained that there are currently Renault Master LCVs in the market powered either by diesel ICEVs or with batteries and electric motors. By using the results of the simulated FCVs, a comparison in terms of performance and environmental impact can be made between the different technologies to determine where the FCV ranks among currently commercial vehicles.

The BEV operates similarly to the FCV, with the difference of the former not having an FC system or an $H_2$ tank. The catalogue presented by Renault states that, following a WLTP procedure, the electric vehicle has a range of up to 204 km by using a 52 kWh battery. However, this range corresponds to a different driving cycle than the one used for the simulated FCV. As the BEV has a power-to-mass ratio of 23.5 W/kg, the cycle assigned to it is the WLTC class 2. This cycle, meant for vehicles between 22 and 34 W/kg, is similar to the WLTC 3b, but omits the extra-high demanding section, which is responsible for the highest energy consumption in the FCV simulations. Therefore, in order to obtain a fair comparison between all vehicles, a WLTC class 2 (Figure 4.41) simulation is carried out, adjusting it to the characteristics of the BEV, to compare the given range with one provided by a simulation.

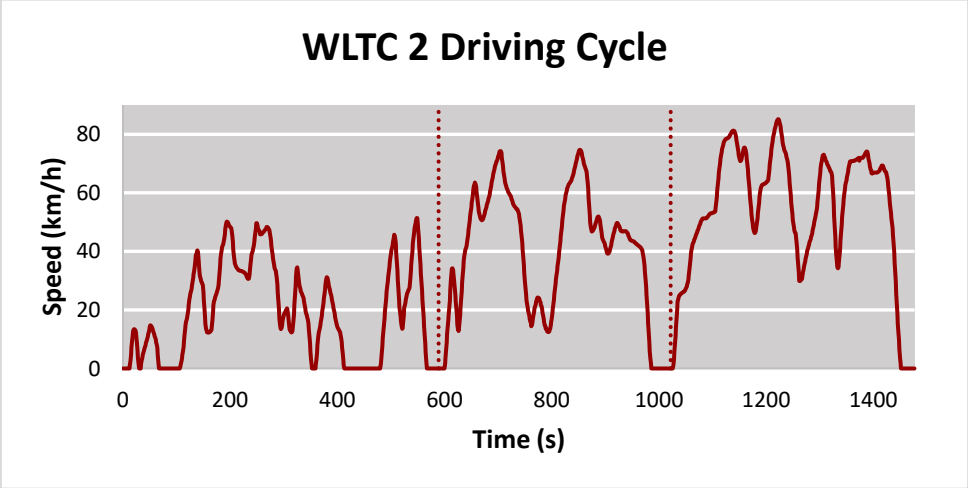


Figure 4.40: WLTC class 2 Driving Cycle

When the simulation is analyzed, an electric range of 199 km is obtained. This value is considered valid, as it only differs by around 2.5% from the range stated in the catalogue. Therefore, a WLTC 3b simulation for the BEV is done to evaluate its performance and compare it fairly with the

FCVs. This simulation, as with the FCVs, will start with a battery SoC of 1, and will run with the battery powering the electric motor until a value of SoC = 0.25. By doing so, and due to the appearance of the extra-high demanding section of the cycle, it is determined that the range of the EV with this driving cycle is 139.6 km, much less than the initial 204 km.

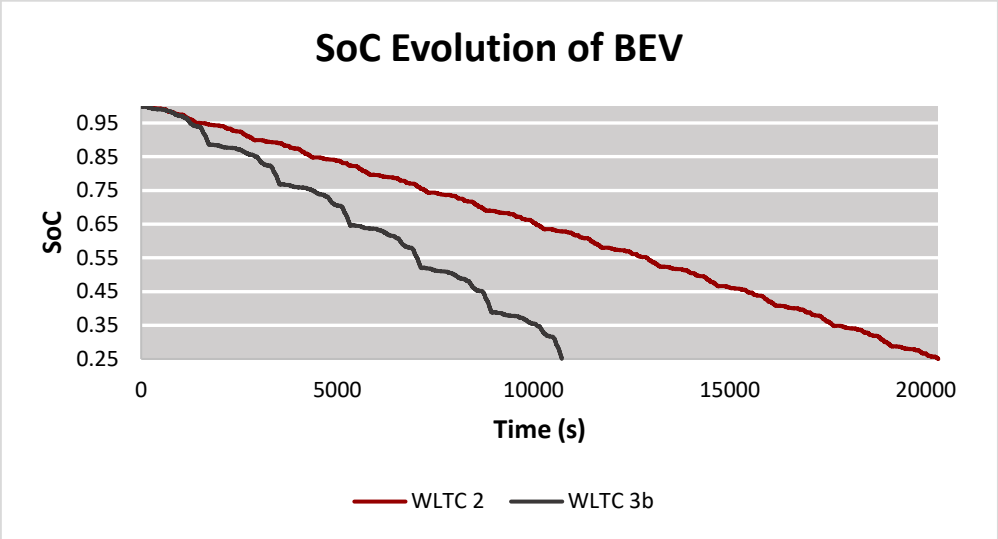


Figure 4.41: Battery SoC Evolution in the BEV for both WLTC Cycles

The diesel vehicle, on the other hand, has a power-to-mass ratio that corresponds to the WLTC 3b driving cycle. Knowing its consumption, emissions, and using the same expected life for all vehicles, a table that compares all their characteristics can be produced:

| | FCV (40 kW – 20 kWh) | FCV (40 kW – 60 kWh) | FCV (80 kW – 20 kWh) | FCV (80 kW – 60 kWh) | BEV | Diesel |
|---|---|---|---|---|---|---|
| Mass (kg) | 2 267 | 2 504 | 2 316 | 2 553 | 2 424 | 1 971 |
| Maximum mass (kg) | 3 500 | 3 500 | 3 500 | 3 500 | 3 500 | 3 500 |
| Electric motor power (kW) | 120 | 120 | 120 | 120 | 57 | 0 |
| ICE power (kW) | 0 | 0 | 0 | 0 | 0 | 134 |
| Battery capacity (kWh) | 20.5 | 60.3 | 20.5 | 60.3 | 52 | 0 |
| Payload (kg) | 1 232 | 996 | 1 184 | 947 | 1076 | 1529 |
| Range (km) | 398 | 506 | 415 | 519 | 140 | 1 105 |

Table 13: Characteristics of all Vehicles

Knowing these characteristics, a relationship of the payload and range of the vehicles can be represented. Here, it is seen how the diesel vehicle stands out over the rest. The fact that it doesn't have a large battery makes it have a small mass compared to the others, while diesel can power the vehicle for the longest distance without refuelling. As for the BEV, it shows a payload close to that of the simulated FCVs, but with a much smaller range which will require the user to recharge frequently. Finally, the FCVs, represented by the four points close to the centre of the graph, show larger ranges than that of the BEV, due to the use of $H_2$, but still much less than that of diesel, with payloads similar to the one presented by the electric LCV. In general, the diesel vehicle counts with a range that is 113% larger than that of the best FCV in this aspect and 692% more than that of the electric LCV, while the FCV has the potential of increasing the range of the BEV by up to 272%.

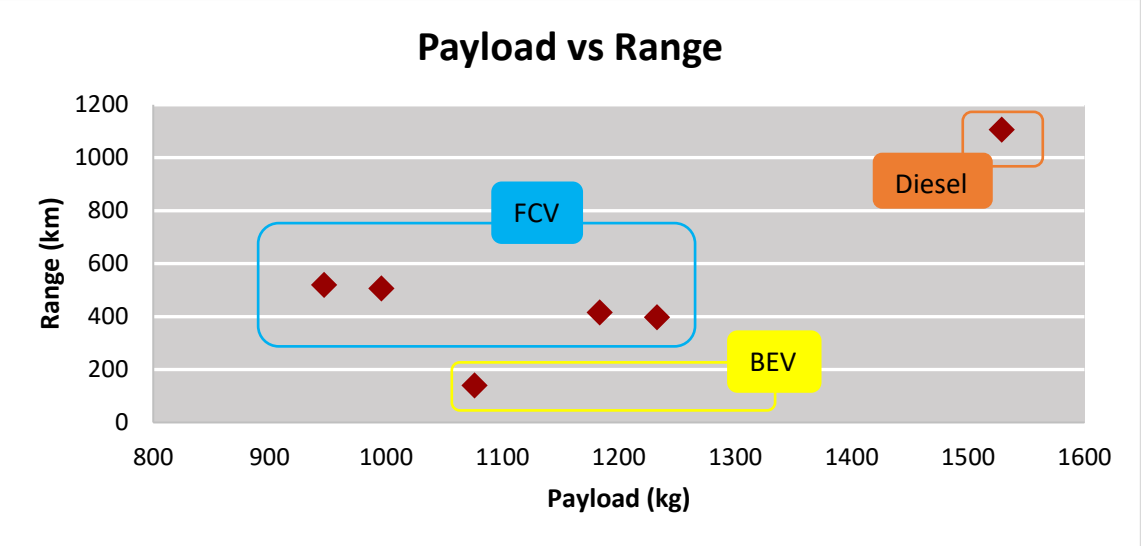


Figure 4.42: Payload and Range Comparison for all Vehicles

Furthermore, by considering the traits of each vehicle, an LCA can be made for the electric and diesel vehicles using some of the data used to perform the LCA from the previous section. To make a comparison between them and the studied FCVs, the EU-2020 and EU-2050 scenarios are considered:

- *Fuel production*

  First, the electricity needed to power the BEV is calculated knowing the capacity of its battery, its range, and the expected distance that the vehicle covers throughout its life. Then, considering power losses in the electricity recharging processes and knowing the GHG emissions caused by its production for every scenario, the total emissions associated with the production of this energy source are obtained.

  As for diesel, using the emissions per litre of diesel data detailed in the methodology section, the fuel consumption of the vehicle, and its expected life, well-to-tank emissions are obtained for the diesel vehicle.

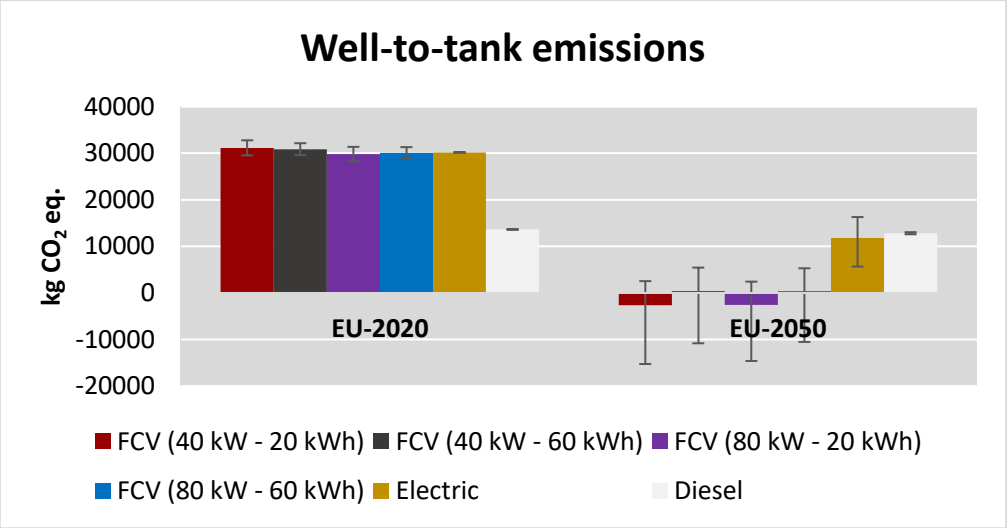


Figure 4.43: Well-to-Tank Emissions for all Vehicles

It is seen how, for the current scenario, FCVs and electric vehicles imply more emissions in the production of their fuel, due to an energy mix with a low share of renewable energy, dominance of $H_2$ production methods where $CO_2$ is released into the atmosphere (in the case of the FCVs) and large amounts of electricity needed due to a high energy consumption (for the BEV). At this time, the production of diesel results in the least well-to-tank emissions. However, this trend changes with time: the use of electrolysis and biogas to produce $H_2$ as well as the increase of renewables in the energy mix reduce the fuel production emissions for vehicles not powered by ICEs, especially for FCVs, while the diesel production does not see dramatic changes to its current state.

- *Vehicle manufacturing*

The vehicle manufacturing processes, with the changes detailed in the methodology section, produce the following results:

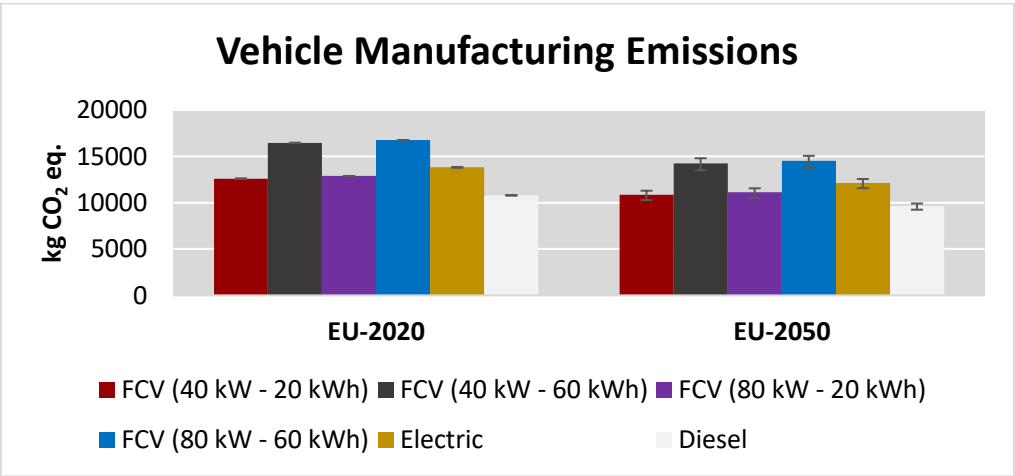


Figure 4.44: Vehicle Manufacturing Emissions for all Vehicles

It is seen how the production of the diesel vehicle emits the least amount of GHGs for both scenarios. This happens mainly due to the batteries used in FCVs and BEVs, which represent a considerable amount of emissions that the manufacturing of an ICE vehicle does not produce. As the diesel LCV does not have a large battery, then its vehicle production emissions are notably reduced. With the years and the more environmentally friendly mixes, emissions will diminish, especially for vehicles featuring large batteries, but not in the same extent that well-to-tank emissions will.

- *Operation*

Knowing that BEVs do not cause emissions throughout their operation and using the $CO_2$ emissions for the diesel LCV, a series of results are produced and displayed in Figure 4.46.

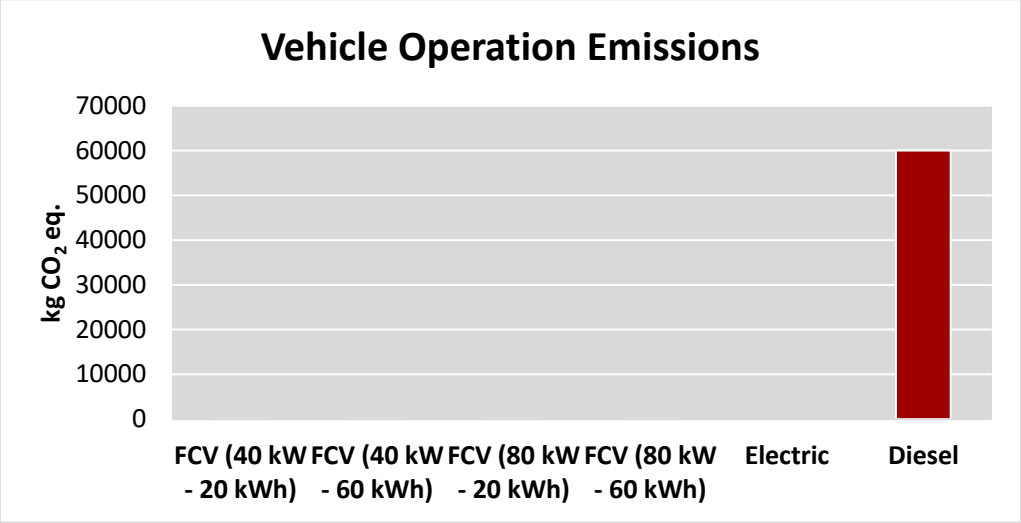


Figure 4.45: Vehicle Operation Emissions for all Vehicles

Here, the main difference between vehicles powered by carbon-based fuels and all others. Burning diesel to power the LCV causes a total of 60 000 kg $CO_2$ eq. throughout the lifetime of the vehicle, which is an incredibly high amount compared to the zero emissions of the EV or the 10 to 14 kg $CO_2$ eq. of the FCV caused by the release of $H_2O$.

Once analyzed separately, the results can be combined together to obtain the total GHG emissions produced in all steps of the life cycle of each of the different technologies.

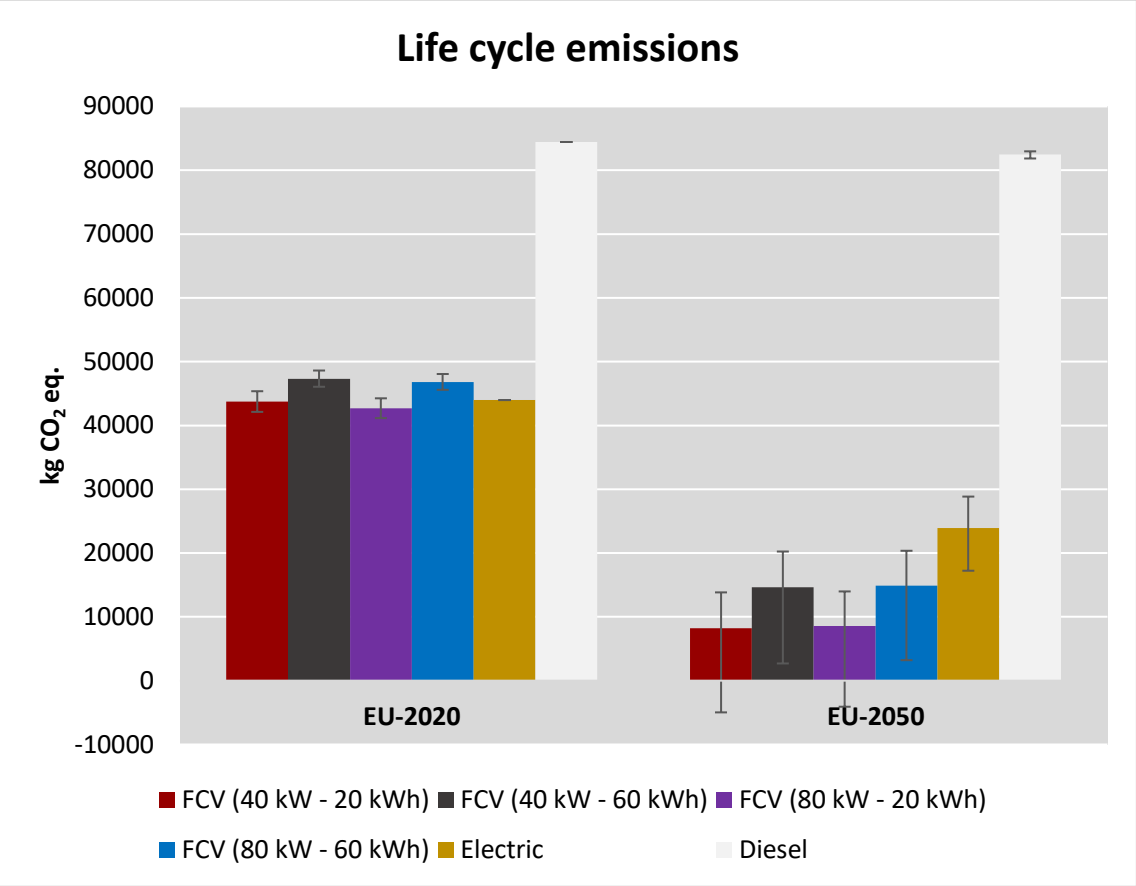


Figure 4.46: Life Cycle Emissions for all Vehicles

Figure 4.47 gives a complete picture of the environmental impact of all vehicles in terms of emissions. Clearly, the GHG emissions during its operation makes the diesel vehicle the one with the largest carbon footprint. As the values of this part of the cycle do not change with time, it is seen how this type of vehicle will see a very small reduction in terms of emissions throughout the years. The other vehicles, for their part, present lower $CO_2$ emissions in every scenario, with this difference becoming even bigger when energy mixes become greener. When comparing the different FCVs architectures to the BEV, similar GHG emissions are seen for the current scenario. However, due to the reduction in emissions in $H_2$ production, FCVs show the potential of becoming the least polluting of all the considered LCVs, to the point where, for the most optimistic scenarios, the life cycle of those with small batteries could reach net-zero emissions by the year 2050.

Figures 4.48 and 4.49 show a segmentation of the emissions for each vehicle in the closest and furthest away scenarios are presented next, proving the statements already mentioned. Clearly, the operation cycle places the diesel vehicle as the most pollutant vehicle in terms of global warming impact, while fuel production and batteries in FCVs and BEVs cause the differences in emissions between these types of LCVs.

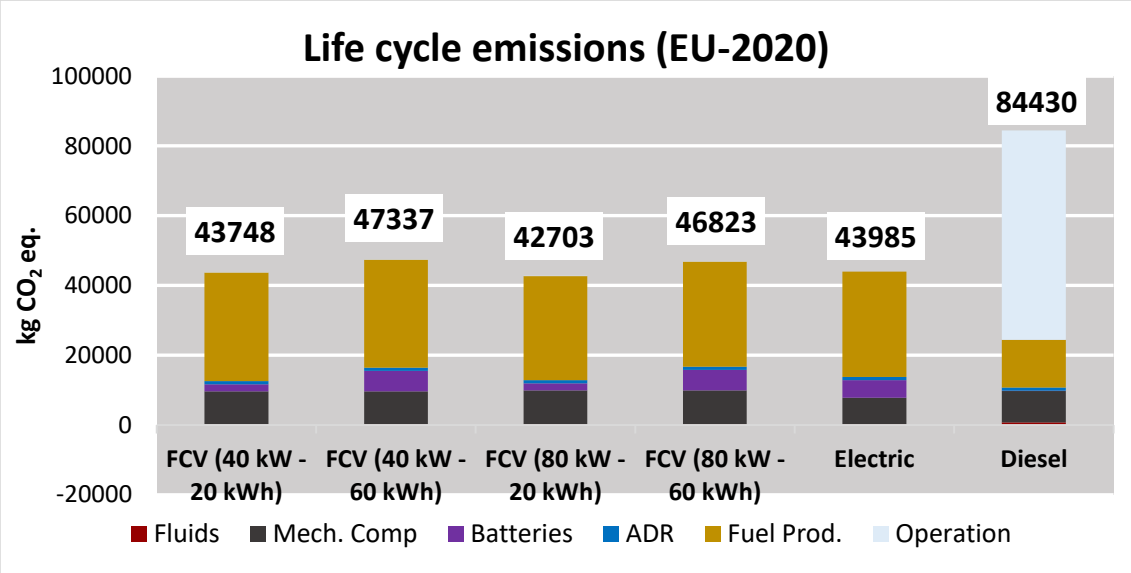


Figure 4.47: Segmented Life Cycle Emissions for all Vehicles in EU-2020 Scenario

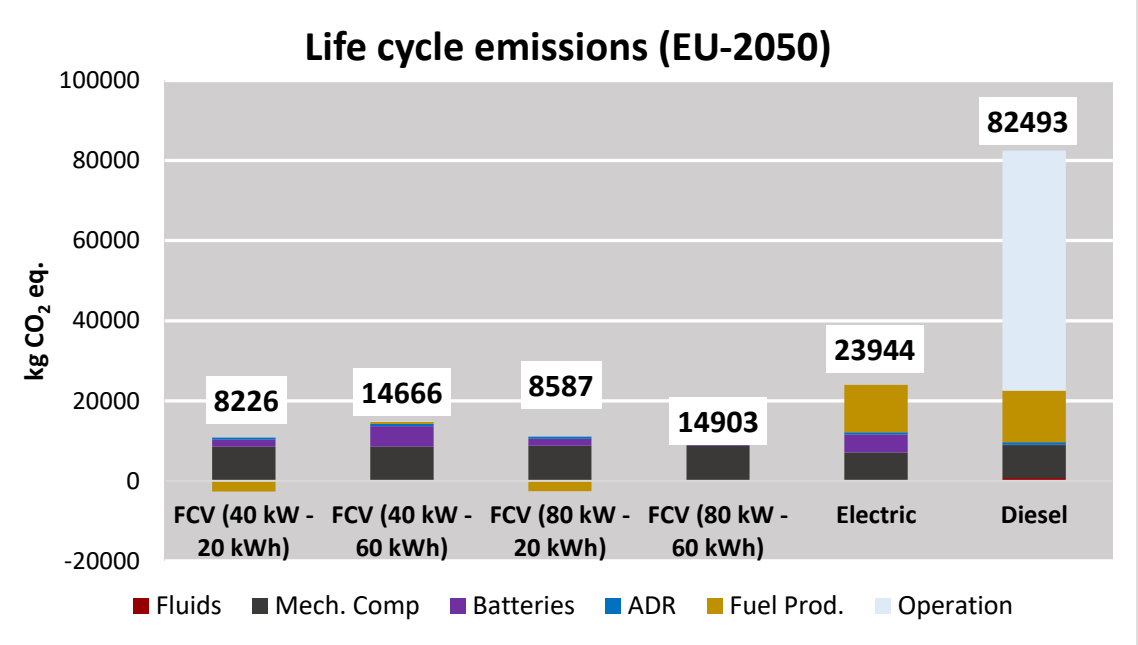


Figure 4.48: Segmented Life Cycle Emissions for all Vehicles in EU-2050 Scenario

Combining all this information, a payload versus emissions graph can be produced, representing visually the different vehicles as well as the evolution in their emissions in the future:

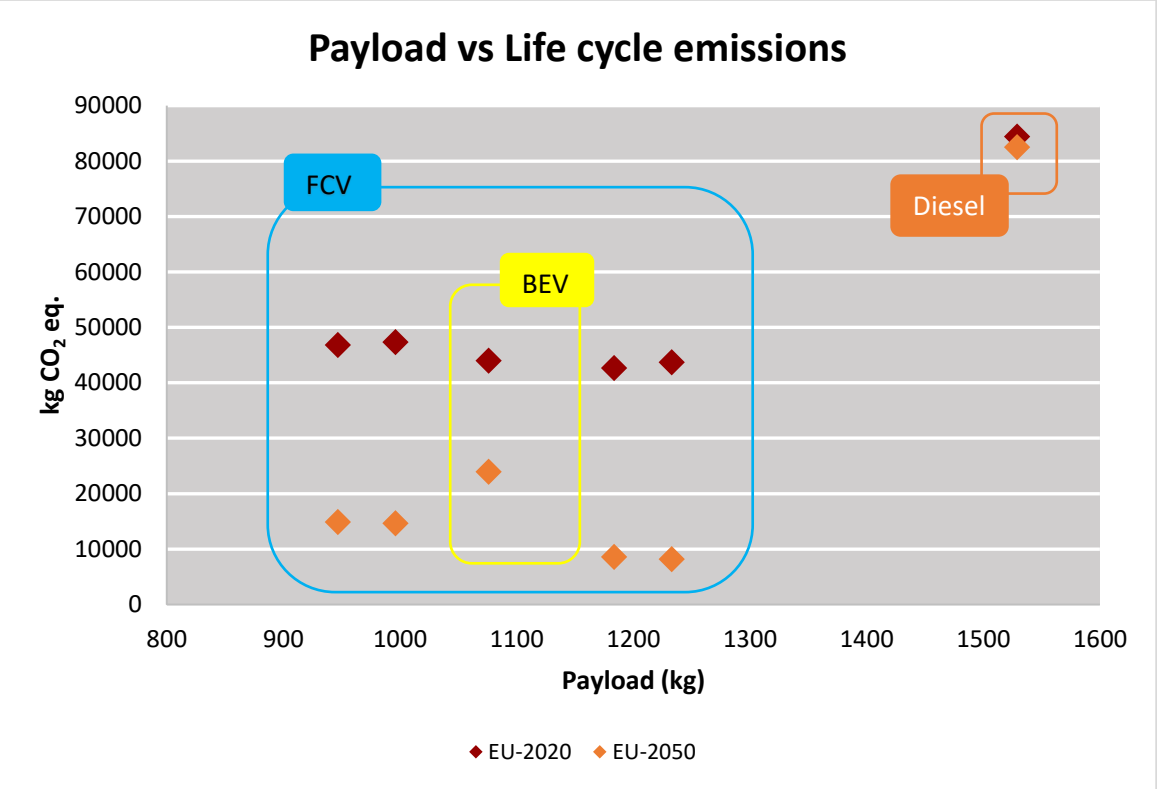


Figure 4.49: Payload and Emissions Comparison for all Vehicles in 2020 and 2050

This graph, again, reflects the previous conclusions. By using a diesel engine, with a low mass that translates into a higher payload, the largest number of emissions will be produced, with a minor reduction of them with the years. The BEV, represented by the points close the 1100 kg payload value, shows lesser emissions than the ICEV, with a noticeable reduction of them throughout the years. Finally, the FCVs, which are represented by the remaining points, show the potential of being the less pollutant vehicles in terms of GHGs, especially if small batteries are considered. In the year 2020, the 40 kW – 20 kWh FCV reduces GHG emissions by 48.2% when compared to the diesel vehicle and by 0.6% when compared to the BEV. In the year 2050, this change becomes even larger, as the formerly mention FCV has the potential of producing 90.0% less emissions than a diesel LCV and 65.7% less emissions than a BEV.

Therefore, it is concluded that FCVs are one of the most promising technologies for the decarbonization of the transportation sector due to their low GHG emissions and their decent performance when compared to current commercial vehicles. If performance is to be optimized, the vehicle should include a large $H_2$ tank, a large battery, and a medium-to-large FC stack, as well as a blended energy management strategy. If environmental impact is to be reduced, the ideal size of the components should be of a small battery and a medium-to-large FC stack, resulting in lower life cycle emissions than electric or diesel LCVs.

# CHAPTER 5: CONCLUSIONS

In this section of this BSc thesis, the conclusions drawn throughout this document are recapped, providing the complete operation and environmental analysis to obtain the ideal architecture for an FC LCV.

The first part of this study focuses on the sizing of the components of an LCV using a CD + CS energy management strategy. The components varied were the FC, from 40 kW to 100 kW maximum stack powers, the electric battery, with energy contents from 20.5 kWh to 60.3 kWh, and the $H_2$ tank, with capacities of 3 kg and 5 kg. When analyzing the results provided by the simulations, it is determined that, in terms of performance, the biggest battery (60 kWh) and $H_2$ tank (5 kg) are optimal, as the larger amount of energy onboard provides a far greater range in exchange for a small increase in consumption. As for the FC, due to the decrease in current density getting smaller each time stack power increases, an intermediate model (60 kW or 80 kW), both lighter than the 100 kW FC, will be sufficient to achieve an optimal performance. With an 80 kW – 60.3 kWh – 5 kg $H_2$ tank architecture, the FCV can travel 490 km without refueling with an energy consumption of 0.43 kWh/km.

Next, the system is optimized, changing the energy management strategy without varying any of the components of the vehicle. Here, by blending the operation of the FC and the battery, it is determined that the CB mode increases range and decreases consumption when comparing this strategy to the standard CD + CS approach. More specifically, it is detected that targeting the maximum number of cycles where the battery and FC and operate together will optimize the performance of the vehicle. By using a blended control strategy, the FCV increases its range by an average of 5.2% and reduces its consumption by 5.0%.

Finally, the environmental impact of the vehicle is evaluated, considering all processes in the vehicle life cycle in different scenarios and focusing on a light (40 kW – 20.5 kWh), heavy (80 kW – 60.3 kWh), and intermediate architectures (40 kW – 60.3 kWh, 80 kW – 20.5 kWh). First, the fuel production is analyzed, evaluating the emissions caused by the production of both $H_2$ and electricity. Through this, it is determined that vehicles with less powerful FCs will produce more well-to-tank emissions for the present scenarios due to their higher $H_2$ consumption and the large number of emissions associated to their lower efficiencies. However, for future scenarios where the production of electricity produces more emissions than that of $H_2$, vehicles with a 60.3 kWh result in a larger amount of well-to-tank emissions due to their large electricity storage capacity. Next, from the vehicle manufacturing data, it is concluded that battery production is the part of the cycle that causes the differences in GHG emissions between the considered architectures. Because of this, vehicles with a 20.5 kWh battery have the smallest footprint. Additionally, as $H_2O$ is the only product emitted from the FCV, it is seen how the operation cycle can be neglected. Therefore, when considering all the stages of the cycle, it is determined that an architecture with a small battery and a medium-to-large FC stack will have a small

environmental impact while maintaining a competent operation, reducing life cycle emissions by 8.8% in 2020 and by 42.4% in 2050 when compared to a large FC stack and large battery LCV. Finally, by evaluating the impact of BEVs and diesel LCVs, it is demonstrated that FCVs have the potential of the reducing the environmental footprint of both of these vehicles, producing 48.2% and 0.6% less GHG emissions than diesel and BEVs in 2020 respectively, and reducing these values to 90.0% and 65.7% in 2050.

In conclusion, all of the data drawn from this study proves that FCVs and $H_2$ can play a decisive role in decarbonizing transport and helping the European Union achieve its environmental goals.

# CHAPTER 6: FUTURE WORK

This BSc thesis has produced an accurate analysis of the behavior of a set of LCV architectures from performance and environmental points of view. From the information obtained, a set of new studies can be produced to complement the findings of this document.

First, a degradation analysis of the FC and the battery could be implemented in the simulations. Due to the limited length of the document, the degradation of these components of the vehicle is out of the scope of this project. Studying this phenomenon would be useful to understand the change in the behavior of the FC and the battery as they degrade, while also reflecting on the life cycle emissions of the vehicle if replacements of these units are needed.

Additionally, an analysis of the change in the behavior of the vehicle could be made when restricting the variation of current density. Again, due to the large amount of time required per simulation, this is not evaluated for this project. For the simulations in this study, a variation of 0.1 $A/cm^2s$ is allowed. The reduction of this parameter to values like 0.01 or 0.001 $A/cm^2s$ will result in a higher $H_2$ consumption in exchange for a less aggressive degradation of the fuel cell. Therefore, by combining the rate of change of the current density and a degradation model for the FC stack, an attractive study can be produced to find an optimal solution.

Another similar study to this could be made by varying the FC itself. In the case of this LCV, the behavior of the cell is based on a proton exchange membrane, as its low operating temperature, fast start and low maintenance make it ideal for transportation. However, the implementation of a different type of electrolyte could be studied. For instance, an alkaline or solid oxide fuel cells could be considered, which has a higher efficiency than a standard proton exchange membrane. If some of its deficiencies can be solved, like its higher temperature of operation, a study could be made to compare it to the already simulated LCVs.

Furthermore, when focusing on the LCA part of this study, other types of system outputs could be studied. For this project, GHG emissions are the main focus, but other types of emissions, like NOx, could be evaluated in the future. Also, this study could be extended by considering energy mixes from other parts of the world. For instance, by analyzing the energy mixes in large vehicle manufacturing nations like China or the United States, the emissions produced throughout the life cycle of each of the vehicles could be compared for each of the considered countries.

It would also be interesting to interpret the results of the simulations for specific applications. For this BSc thesis, driving cycles start with the $H_2$ tank and the battery fully loaded, and the vehicle is operated until both of the energy sources are consumed. However, this could not be the case for a real-life application. For instance, if the FC LCV is used in for a delivery service in urban areas, it is likely that the battery and the tank will not be fully discharged after every use. Therefore, a study for a series of different cases can be made to optimize a series of parameters like energy efficiency, user commodity or cost of the operation.

Furthermore, a total cost of ownership analysis of the FC LCV could be carried out, which would be especially interesting if it were to be compared with the economic cost of electric and ICE vehicles. Due to the novelty of $H_2$ and FCs, FCVs are currently much more expensive than other conventional vehicles. By complementing the LCA in this project with a financial viewpoint, the current and future status of FC LCVs could be evaluated to determine whether or not this technology could someday be affordable and therefore be able to represent a large part of the LCV fleet in Europe.

Finally, the data obtained through the GT-Suite and MATLAB model could be validated with an experimental, real driving cycle, to evaluate the precision of the model. However, this is unfeasible for this project due to the economic requirements of the experimental campaign.

# REFERENCES

[1]: IEA. (2022). CO2 Emissions in 2022: Latest trends and the role of clean energy policies. https://www.iea.org/reports/co2-emissions-in-2022

[2]: European Commission. (2018). A Clean Planet for all: A European strategic long-term vision for a prosperous, modern, competitive and climate-neutral economy. https://ec.europa.eu/clima/sites/clima/files/strategies/0370_communication_en_0.pdf

[3]: Fuel Cells and Hydrogen 2 Joint Undertaking, (2019). Hydrogen roadmap Europe : a sustainable pathway for the European energy transition, Publications Office. https://data.europa.eu/doi/10.2843/341510

[4]: ZESTAs. (n.d.). Technologies. https://zestas.org/technologies/

[5]: U.S. Department of Energy, Office of Energy Efficiency & Renewable Energy. (n.d.). Energy Efficiency & Renewable Energy. https://www.energy.gov/eere/office-energy-efficiency-renewable-energy

[6]: Desantes J.M., Novella R., Pla B. & Lopez-Juarez M. (2022). A modeling framework for predicting the effect of the operating conditions and component sizing on fuel cell degradation and performance for automotive applications. Applied Energy 317 119137. https://doi.org/10.1016/j.apenergy.2022.119137

[7]: Xu L., Ouyang M., Li J., Yang F., Languang L. & Jianfeng H. (2013). Optimal sizing of plug-in fuel cell electric vehicles using models of vehicle performance and system cost. Applied Energy 103 477-4987. https://doi.org/10.1016/j.apenergy.2012.10.010

[8]: Hu Z., Li J., Xu L., Song Z., Fang C., Ouyang M., et al. (2016). Multi-objective energy management optimization and parameter sizing for proton exchange membrane hybrid fuel cell vehicles. Energy Conversion and Management 129 108-121. http://dx.doi.org/10.1016/j.enconman.2016.09.082

[9]: Wu X., Hu X., Yin X., Peng Y. & Pickert V. (2019). Convex programming improved online power management in a renge extended fuel cell electric truck. J Power Sources 2020; 476:228642. https://doi.org/10.1016/j.jpowsour.2020.228642

[10]: Shojaeefard M.H., Mollajafari M., Pishe N.E. & Mousavi S.M. (2023). Plug-in fuel cell vehicle performance and battery sizing optimization based on reduced fuel cell energy consumption and waste heat. Sustainable Energy Technologies and Assessments 56 103099. https://doi.org/10.1016/j.seta.2023.103099

[11]: Molina S., Novella R., Pla B. & Lopez-Juarez M. (2021). Optimization and sizing of a fuel cell range extender vehicle for passenger car applications in driving cycle conditions. Applied Energy 285 116469. https://doi.org/10.1016/j.apenergy.2021.116469

[12]: Feroldi D. & Carignano M. (2016). Sizing for fuel cell/supercapacitor hybrid vehicles based on stochastic driving cycles. Applied Energy 183 645 - 658. https://doi.org/10.1016/j.apenergy.2016.09.008

[13]: European Automobile Manufacturers Association (ACEA). (2023). Vehicles in use Europe - 2023 edition. https://www.acea.auto/publication/report-vehicles-in-use-europe-2023/

[14]: European Commission, Joint Research Centre. (n.d.). Life Cycle Assessment (LCA). https://eplca.jrc.ec.europa.eu/lifecycleassessment.html

[15]: Corbo P., Migliardini F. & Veneri O. (2008). Experimental analysis of a 20 kWe PEM fuel cell system in dynamic conditions representative of automotive applications. Energy Conversion and Management 49 2688-2697. https://doi.org/10.1016/j.enconman.2008.04.001

[16]: Corbo P., Migliardini F. & Veneri O. (2007). Experimental analysis and management issues of a hydrogen fuel cell system for stationary and mobile application. Energy Conversion and Management 48 2365-2374. https://doi.org/10.1016/j.enconman.2007.03.009

[17]: Desantes J.M., Novella R., Pla B. & Lopez-Juarez M. (2021). Impact of fuel cell range extender powertrain design on greenhouse gases and NOX emissions in automotive applications. Applied Energy 302 117526. https://doi.org/10.1016/j.apenergy.2021.117526

[18]: Luján J.M., Guardiola C., Pla B., Reig A. (2016). Cost of ownership-efficient hybrid electric vehicle powertrain sizing for multi-scenario driving cycles. Proceeding of the Institution of Mechanical Engineers, Part D. 230(3):382–94. https://doi.org/10.1177/0954407015586333

[19]: Hyvia. (n.d.). Master Van H2-TECH. https://www.hyvia.eu/en/vehicle/master-van-h2-tech/

[20]: U.S. Department of Energy. (2019). Automotive fuel cell target status report. https://www.hydrogen.energy.gov/pdfs/20005-automotive-fuel-cell-targets-status.pdf

[21]: International Council on Clean Transportation. (n.d.). Worldwide Harmonized Light Vehicles Test Procedure (WLTP). Transport Policy. https://www.transportpolicy.net/standard/international-light-duty-worldwide-harmonized-light-vehicles-test-procedure-wltp/

[22]: CML - Department of Industrial Ecology. (2016). CML-IA Characterisation Factors. Universiteit Leiden. https://www.universiteitleiden.nl/en/research/research-output/science/cml-ia-characterisation-factors#downloads

[23]: Zhao Y., Tatari O. (2015). A hybrid life cycle assessment of the vehicle-to-grid application in light duty commercial fleet. Energy 93 1277-1286 https://doi.org/10.1016/j.energy.2015.10.019

[24]: Safarian S. (2023). Environmental and energy impact of battery electric and conventional vehicles: A study in Sweden under recycling scenarios. Fuel Comumunications 14 100083 https://doi.org/10.1016/j.jfueco.2022.100083

[25]: IPCC, Climate Change. (2014). Tech. rep., Cambridge; (2015). https://www.cambridge.org/core/product/identifier/CBO9781139177245A012/type/book_part

[26]: BP. (2020). BP Energy Outlook 2020 Edition. https://www.bp.com/content/dam/bp/business-sites/en/global/corporate/pdfs/energy-economics/energy-outlook/bp-energy-outlook-2020.pdf

[27]: European Biogas Association. (2021). Market state and trends in renewable and low-carbon gases in Europe. https://www.europeanbiogas.eu/gas-for-climate-market-state-and-trends-report-2021/#:~:text=The%20report%20Market%20state%20and%20trends%20in%20renewable,chain%20of%20biomethane%20and%20green%20and%20blue%20hydrogen.

[28]: IEA. (2021). An introduction to biogas and biomethane. Outlook for biogas and biomethane: Prospects for organic growth. https://www.iea.org/reports/outlook-for-biogas-and-biomethane-prospects-for-organic-growth/an-introduction-to-biogas-and-biomethane

[29]: BP. (2023). BP Energy Outlook 2023 Edition. https://www.bp.com/content/dam/bp/business-sites/en/global/corporate/pdfs/energy-economics/energy-outlook/bp-energy-outlook-2023.pdf

[30]: Sherwood S.C., Dixit V., Salomez C. (2018). The global warming potential of near-surface emitted water vapour. Environmental Research Letters 13 104006. https://doi.org/10.1088/1748-9326/aae018

[31]: Renault. (n.d.). Renault Master Z.E. eléctrico. https://empresas.renault.es/electricos/master-electrico.html

[32]: Auto-Data.net. (n.d.). Renault Master III Fase III 2019 2.3 ENERGY dCi (180 Hp) L2H2 Furgón. Retrieved May 11, 2023, from https://www.auto-data.net/es/renault-master-iii-phase-iii-2019-panel-van-2.3-energy-dci-180hp-l2h2-40042

[33]: Apostolaki-Iosifidou E., Codani P., Kempton W. (2017). Measurement of power loss during electric vehicle charging and discharging. Energy 127 730-742. https://doi.org/10.1016/j.energy.2017.03.015

# DOCUMENT II:

# BUDGET

# BUDGET INDEX

1. Introduction ..... 77
2. Time distribution ..... 77
3. Labour costs ..... 78
4. Equipment costs ..... 79
5. Total costs ..... 80

## 1. INTRODUCTION

The following chapter has the objective of evaluating the costs throughout the complete duration of the project. In order to do so accurately, the cost of the human resources, the equipment and the operation are evaluated considering the amount of time invested in this BSc thesis.

## 2. TIME DISTRIBUTION

The totality of this project can be divided into two main branches. The first took place between the months of February and July of the year 2022. During this phase, the initial research on the operation of FCVs was made as well as the establishments of the different sizes and energy use strategies, the launch of the majority of simulations, and the analysis of the different architectures. The data obtained was analyzed with the co-tutor of this project in meetings that took place between two to three times per month with a duration of one hour per meeting. This first period represents the totality of the simulation time spent for this project, which is detailed in Table 14:

| Simulation | Number of architectures | Simulations per architecture | Average time per simulation | Time |
|---|---|---|---|---|
| CD + CS | 24 | 1 | 6 h | 144 h |
| CB | 9 | 4 | 4 h | 144 h |
| Electric | 1 | 2 | 1 h | 2 h |
| Total | | | | 290 h |

Table 14: Simulation Time Distribution

Meetings and development were paused during the summer and the first term of the 2022/2023 academic year. The project was then resumed in February 2023 and continued until the month May. During these months, the LCA section of this study was elaborated and the report was written. Meetings to debrief the work made happened twice a month for one hour per meeting. Table 15 summarizes the total time distribution and estimates the amount of time invested in the project.

| Assignment | Dedicated time |
|---|---|
| Simulation | 290 h |
| Research and calculations | 200 h |
| Meetings | 23 h |
| Report writing | 150 h |
| Total | 663 h |

Table 15: Total Time Distribution

**3. LABOUR COSTS**

The labour costs include the time worked in the project by all the people involved, which includes the PhD professor, the PhD assistant, and the graduate industrial engineer. To do so, the hours worked per day, the working days throughout the year and the average salary of each of the people involved is estimated.

The time worked by the people involved is based on the working calendar in Valencia. Considering a year with 365 days, 48 two-day weekends, 30 vacation days and 14 regional and national holidays, the total time estimated of work is of 225 days per year. Considering a full-time 8 hour per day position, it is estimated that a total of 1800 hours is worked every year.

To obtain an approximation of the salary of each of the participants of the project, remuneration tables published on the website of Universitat Politècnica de València are used and detailed as follows:

· PhD professor: annual retribution of 47 114.20 €, which results in 26.17 €/h

· PhD assistant: annual retribution of 30 000.00 €, which results in 16.67 €/h

· Graduate engineer: annual retribution of 17 100.00 €, which results in 9.50 €/h

Knowing the hourly cost of each worker, estimating the amount of hours invested in this project by each one of them, and including a 33% of the salary for social security payments, the total labour costs are calculated:

| Subject | Dedicated time | Cost | Cost w/ social security | Total cost |
|---|---|---|---|---|
| PhD professor | 15 h | 26.17 €/h | 34.81 €/h | 552.18 € |
| PhD assistant | 63 h | 16.67 €/h | 22.17 €/h | 1 396.50 € |
| Graduate engineer | 373 h | 9.50 €/h | 12.64 €/h | 4 712.86 € |
| Total | | | | 6 631.54 € |

Table 16: Labour Costs Distribution

## 4. EQUIPMENT COSTS

The totality of this project was made using simulation tools and other applications. In this section, the cost of the licences as well as the equipment used is evaluated. Costs are evaluated per year, considering the total 8760 hours in a year to calculate the cost for this specific BSc thesis:

- GT-Suite: annual cost of an educational license of 3 000 €, resulting in 0.34 €/h.
- MATLAB: annual cost a university license of 250 €, resulting in 0.03 €/h.
- Microsoft Office: annual cost of personal license of 69 €, resulting in 0.01 €/h.
- GaBi: annual cost of 3 500 €, resulting in 0.40 €/h.
- Laptop: HP 15s-fq5061ns, with a cost of 999 € and a repayment time of 6 years, resulting in 0.02 €/h.

Considering the time dedicated with each if the mentioned tools, the total cost is calculated:

| License | Dedicated time | Cost | Total cost |
|---|---|---|---|
| GT-Suite | 290 h | 0.34 €/h | 99.32 € |
| MATLAB | 252 h | 0.03 €/h | 7.19 € |
| Microsoft Office | 320 h | 0.01 €/h | 2.52 € |
| GREET | 100 h | --- | --- |
| GaBi | 10 h | 0.40 €/h | 4.00 € |
| Equipment | | | |
| Laptop | 663 h | 0.02 €/h | 12.60 € |
| Total | | | 125.62 € |

Table 17: Licences and Equipment Costs

## 5. TOTAL COSTS

Finally, by considering all the costs that are previously presented, a total budget for the project is obtained. To do so, overhead costs of 15% and industrial benefits of 6% are considered. These overhead costs include a series of services that can be quantified for the project, like the personnel involved in the maintenance of servers, licences or the building where this project was completed, as well as other services like light and electricity to power the computer. Furthermore, value added taxes (VAT, or IVA in Spanish) of 21% are considered. The complete cost segmentation of the project can be seen in Table 18.

| Description | Cost |
|---|---|
| Labour costs | 6 631.54 € |
| Equipment costs | 125.52 € |
| Material budget | 6 757.16 € |
| Overhead costs (15%) | 1 013.57 € |
| Industrial benefits (6%) | 405.43 € |
| Operating budget | 8 176.17 € |
| VAT (21%) | 1 716.99 € |
| Overall budget | 9 893.16 € |

Table 18: Summary of the total Cost of the Project

Finally, the total cost of the project is of nine thousand, eight hundred and ninety-three euros with sixteen cents.

# DOCUMENT III:

# ANNEX

| Sustainable Development Goals | High | Medium | Low | Not applicable |
|---|---|---|---|---|
| 1. No poverty | | | | x |
| 2. Zero hunger | | | | x |
| 3. Good health and well-being | | x | | |
| 4. Quality Education | | | | x |
| 5. Gender Equality | | | | x |
| 6. Clean water and sanitation | | | | x |
| 7. Affordable and clean energy | x | | | |
| 8. Decent work and economic growth | | | | x |
| 9. Industry, innovation, and infrastructure | | x | | |
| 10. Reduced inequalities | | | | x |
| 11. Sustainable cities and communities | | x | | |
| 12. Responsible consumption and production | x | | | |
| 13. Climate action | x | | | |
| 14. Life below water | | | | x |
| 15. Life on land | | | x | |
| 16. Peace, justice and strong institutions | | | | x |
| 17. Partnerships for the goals | | | | x |

Table 19: European Union Sustainable Development Goals